NASA CR 66345

LAUNCH VEHICLE OPTIMIZATION STUDY

FINAL REPORT

NASA CR 66345

CONTRACT NAS 1-6395

LOCKHEED MISSILES & SPACE COMPANY
A Group Division of Lockheed Aircraft Corporation
Sunnyvale, California

March 1967

FOREWORD

This report was prepared by the Advanced Flight Mechanics Department; Navigation, Guidance and Control, Lockheed Missiles & Space Company, Sunnyvale, California. It presents the final documentation of the work completed for the NASA Langley Research Center under Contract NAS 1-6395.

The study was planned and conducted by D. I. Kepler. Mr. H. N. Stone was responsible for the operation and modification of the optimization program, the development of the simplified hill climber routine, and a major portion of the data analysis. Valuable assistance was provided by R. E. Willwerth and B. W. Silver of Advanced Flight Mechanics and by R. C. Rosenbaum of the LMSC Aerospace Sciences Laboratory. The vehicle structural weight formulations and the associated weight constants used in this investigation were obtained from an analysis made by John D. Bird of the NASA Langley Research Center.

ABSTRACT

A dual-loop gradient optimization method is described which was developed for the solution of design synthesis problems on large multiple stage liquid propellant launch vehicles. The complete formulation of the system optimization equations is presented.

The procedure was mechanized in a digital computer program that incorporates an advanced version of the PRESTO trajectory optimization routine. This program was applied to a series of model liquid launch vehicle design problems using radically simplified equations for the relationships between the design and the jettison weights. The results from those problems are described in detail.

A convergence study was conducted to investigate problems encountered with the system optimization computer program. The gradient optimization problem was reduced to a problem in two controls and a high speed computer routine was used to investigate the behavior of various gain selection and non-linear approaches. Representative results are presented for these convergence studies.

Brief convergence studies were also completed using the system optimization computer program. The results are presented from a systematic study of the influence of optimization gains on the program behavior. Results are included from two experimental cases run with a modified parabolic fit routine developed to accommodate some of the second order influences.

Most of the gain selection and non-linear techniques investigated demonstrated substantial improvements in convergence on selected problems. None of the techniques demonstrated consistently superior behavior on all problems over that of the original gradient routine.

The basic problem remains. The current system optimization routine does not consistently reach solutions within the number of iterations or with the accuracy of modern gradient trajectory optimization programs. Some new approaches are therefore suggested that offer the promise of the consistent behavior so necessary for practical optimization routines.

TABLE OF CONTENTS

TERMINOLOGY

A_e	Nozzle exit area
A_t	Nozzle throat area
C^*	Propellant characteristic velocity
C_E	Motor weight coefficient
C_{F_v}	Vacuum thrust coefficient
C_S	Interstage weight coefficient
C_T	Tank weight coefficient
D	Determinant
$d\psi$	Constraint changes
e_i	Exchange ratio parameters
f	Payload
g	Acceleration due to gravity
g_o	Conversion constant for mass to weight
I_{sp_v}	Vacuum specific impulse

J	Jettison weight
K_f	Gradient coefficient
K_w	Gradient coefficient
m	Mass
m_f	Final mass
m_j	Jettison mass
m_p	Propellant mass
$\dot{m}$	Time derivative of mass
N	Step size
P	Propellant load
p	Chamber pressure or atmospheric pressure
q	Dynamic pressure
$\dot{q}$	Time derivative of q
$\ddot{q}$	Time derivative of $\dot{q}$
q_{max}	Maximum dynamic pressure
R_ϕ	Mass partials with respect to system variables
R_ψ	Constraint partials with respect to system variables

r	Radial coordinate from Earth center
r_f	Final value of radial coordinate from Earth center
S_F	Gradient derivative sum
S_{FW}	Gradient derivative sum
S_W	Gradient derivative sum
S_Y	Constraint partials with respect to program inputs, Y
S_ψ	Constraint partials with respect to adjustable parameters
T_v	Vacuum thrust
t	Burn time
t_f	Final integration limit
t_i	Initial integration limit
t_o	Launch time integration limit
V	Velocity
W	Launch weight
W	Weighting factor matrix for control variables
W_{PL}	Load supported by interstage
X_i	P_i, p_i, t_i or ϵ_i

X	Program inputs with distributed effects (I_{sp}, T_v, A_e)
Y	Program inputs without distributed effects (J, t)
Y	Weighting factor matrix for adjustable parameters
γ	Flight-path angle
δm_o	Variation in launch mass
$\delta\tau$	Variations in adjustable parameters
ϵ	Nozzle expansion ratio
η_i	Gain factors used for system loop
η	Angle of attack in pitch plane
θ	Angle between payoff and constraint vectors
Λ_ϕ	Control derivatives evaluated for mass
Λ_ψ	Control derivatives evaluated for constraints
λ_x	Adjoint variables
ρ	Mass density of atmosphere

Section 1.0

INTRODUCTION

The nature of the launch system performance problem changes as the design departs more radically from existing components. At one extreme a series of existing components are assembled and performance is determined by simulating the behavior of those components in a prescribed environment. The variables that may be adjusted to satisfy the mission constraints are almost completely divorced from the component design and system arrangement. Maximum performance is achieved by varying the control history to produce maximum payload with fixed mission constraints or to maximize some mission parameters with fixed payload. At the other extreme all component and system variables and the control history are free. Maximum performance is achieved by varying both the design variables and the control history to satisfy the mission requirements with the lightest or lowest cost system, or to maximize the payload within selected weight or cost constraints. One problem involves optimization of control with fixed system characteristics. The other includes optimization of both the system characteristics and the control with some sizing parameters fixed. In its most general form it embodies the complete synthesis of a launch system that in some sense delivers maximum performance.

The work described in this report considers a category of optimization problems that is between these extremes. Many of the launch system characteristics are fixed so that the synthesis problem is reduced to one that includes only selected variables. The influence of some variables such as

the number of stages, the specific impulse of the propellants used, and the structural efficiency are evaluated by trial and error. Others, however, such as stage propellant capacities and thrust levels, are included directly in the optimization process along with the control history.

A gradient technique is used to solve this reduced launch system optimization problem. The approach closely parallels that used in the PRESTO[1] and PRESTO II[2] computer programs developed by LMSC for the NASA Langley Research Center during 1964 and 1965. The procedure was first applied by LMSC to design optimization problems for large multi-stage solid propellant launch vehicles carrying payloads to low altitude earth orbits. This early work considered both maximum performance and minimum cost problems. The digital computer programs developed for that purpose successfully determined the combination of up to sixteen design variables together with the attitude program that produced maximum payload or minimum cost.

The operation of these programs proved somewhat difficult. Convergence problems were frequently encountered and multiple passes were required to achieve acceptable solutions. The programs were also slow, requiring about .5 hr. UNIVAC 1107 time per run. It was consequently expensive to experiment with the optimization gain and step size selection techniques required to resolve these convergence difficulties.

During 1966 two events occurred that carried the promise of circumventing the difficulties associated with these early programs. The PRESTO II computer program which offered about a factor of five increase in speed for control program optimization was completed. New UNIVAC 1108 computers were introduced that provided an additional factor of five speed improvement with only a moderate cost increase. The potential was thereby created for at least an order of magnitude reduction in the computer costs for solving launch system optimization problems. It was then possible to economically experiment with the convergence problems that plagued the earlier programs.

In early 1966 LMSC proposed[3] to NASA Langley Research Center a low level, 9-month study with the following objectives.

1) Adapt the solid propellant launch vehicle optimization program to a simpler, liquid propellant launch vehicle problem.

2) Incorporate the new PRESTO II control program optimization routine.

3) Run a matrix of mission-vehicle optimization problems to determine the sensitivity of performance to the design variables and to identify convergence problems.

4) Define the program changes required to include a dynamic pressure constraint during the optimization.

Work was initiated on this study in June 1966 under Contract NAS 1-6395.

The results from the study are presented in this report which includes a conceptual description of the optimization program logic, the derivation of the optimization and dynamic pressure constraint relationships, and results from the optimization and convergence studies.

---

[1] PRESTO- Program for Rapid Earth-to-Space Trajectory Optimization, NASA Contractor Report NASA CR-158, Februrary 1965.

[2] PRESTO II- A Digital Computer Program for Trajectory Optimization, NASA CR-686, February 1967.

[3] Launch Vehicle Optimization Study, Technical Proposal, LMSC 894437, February 1966.

Section 2.0
ANALYTICAL APPROACH

2.1 Optimization Concept

A gradient optimization procedure is used to determine the combination of launch system parameters that produces maximum payload and simultaneously satisfies the mission and sizing constraints. The approach is somewhat unusual in that the trajectory optimization process has been separated from the system optimization process. The operation is outlined in Figure 2-1.

Nominal system characteristics are defined by selecting a set of numerical values for the design variables that must be optimized. In this discussion these variables will be called the system controls. The design equations are next used to define the input parameters necessary to simulate the ascent trajectory. The trajectory control history is now optimized using the PRESTO or PRESTO II gradient optimization routines to satisfy the mission constraints and to determine maximum payload for the selected nominal system controls.

Exchange ratios are then computed that define the derivative of payload with respect to each trajectory program input under the condition that the mission constraints remain satisfied. These exchange ratios are combined with propulsion derivatives and numerically formed jettison weight partials to produce the optimization partials that will be used for optimization of the system controls. The optimization partials are the derivatives of final payload and launch weight with respect to each system control.

System control changes are now computed to produce selected changes in launch weight and payload using a steepest descent computation. These changes are added to the original system controls selected for the nominal vehicle and the design equations are re-entered to produce a new nominal. The entire process is then repeated until a specified minimum payload improvement can no longer be achieved without violating the launch weight or mission constraints.

LAUNCH VEHICLE OPTIMIZATION FLOW DIAGRAM
MODIFIED FOR HIGH SPEED OPERATION

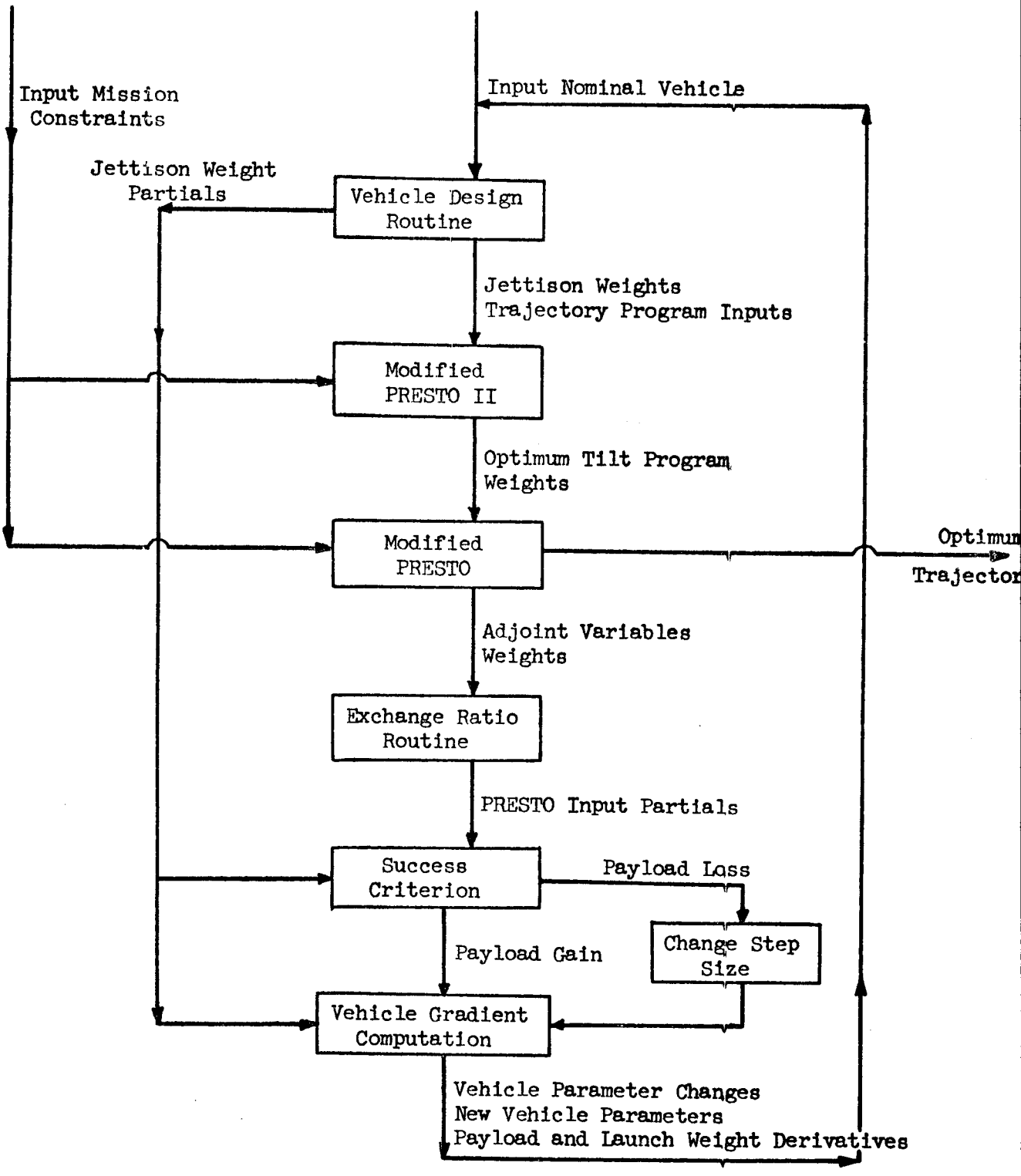

This optimization concept involves two gradient optimization loops, one for the system controls and one for the trajectory controls. The trajectory loop operates inside the system loop and a complete trajectory optimization is required for each system loop iteration. Information is fed between the two loops in the form of exchange ratios and the launch and burnout weights for each iteration. A direct output is available from the trajectory loop in the form of the intermediate trajectory iterations and the final optimized trajectory for each vehicle iteration.

The dual loop concept can be considered an intermediate step between a direct simultaneous optimization of both the trajectory and the launch vehicle and a technique where the vehicle adjustments are determined separately and then tested on the trajectory optimization program. It carries the advantage of the latter in that a complete design, its maximum payload and ascent trajectory are available at each iteration. It has the disadvantage of substantially increased run times since the number of trajectories computed is equal to the product of the inner and outer loop iterations.

The dual loop approach was selected both for expediency in producing an operating optimization program and to keep the system and trajectory influences separated so that we could take advantage of the feel that had already been established for the trajectory optimization and system optimization processes. The concept proved particularly useful in that it appears to be more easily understood by those familiar with previous system optimization techniques. It also provides the intermediate output necessary to convince a customer that a systematic procedure has been completed that converges toward an optimum system.

For the future some questions remain about the approach for an ultimate system synthesis program. The direct simultaneous optimization of both the system and the trajectory obviously offers the potential for the shortest run times. The dual loop approach may, as discussed in Section 3, offer some

advantages when significant nonlinearities are encountered in the system characteristics. The convergence problems that will be encountered with the simultaneous approach are as yet unknown and should be explored further.

2.2 Optimization Formulation

The arrangement selected for the optimization equations was based on the requirements of earlier solid propellant vehicle optimization studies. The system design parameters that proved most convenient for this work were the propellant loads (P), the chamber pressures (p), the burn times (t), and nozzle expansion ratios (ϵ) for each stage. In order to minimize the number of program modifications required for this study, this set of design parameters has been retained. However, the chamber pressure and nozzle expansion ratios remain fixed at the nominal input values for each case considered, since the weight equations used for the liquid propellant launch vehicles do not reflect the influence of changes in these parameters. The design parameters or system controls then become the propellant loads and burn times for each stage. The following equations relate the system controls to other parameters of interest, such as vacuum thrust and specific impulse.

$$T_v = C_{F_v} p A_t \qquad \text{where} \quad C_{F_v} = f(\epsilon)$$

$$I_{sp_v} = \frac{C_{F_v} C^*}{g_o} = -\frac{T_v}{g_o \dot{m}} = \frac{T_v t}{g_o m_p} = \frac{T_v t}{P} \tag{2-1}$$

$$T_v = \frac{C_{F_v} C^*}{g_o} \frac{P}{t}$$

$$A_e = \frac{\epsilon T_v}{C_{F_v} p} = \frac{\epsilon C^*}{g_o} \frac{P}{pt}$$

The optimization problem is formulated for the system controls by writing the following equation in payload (f) and launch weight (W) with changes in the system controls. In this case the launch weight represents

$$\delta f = \sum_i \frac{\partial f}{\partial X_i} \delta X_i \tag{2-2}$$

$$\delta W = \sum_i \frac{\partial W}{\partial X_i} \delta X_i \tag{2-3}$$

a constraint on the system design during optimization and is used to prevent the size of the system from increasing without limit as payload improvements are sought. The steepest descent solution to these equations is defined by the following,

$$\frac{\delta X_i}{\eta_i} = K_f \frac{\partial f}{\partial X_i} + K_W \frac{\partial W}{\partial X_i} \qquad (\eta_i = \text{gains})$$

which asserts that we will move each of the system controls in proportion to its effect on both the payoff and the constraint. When this solution is substituted into the previous equations, the following expression is derived for the control changes necessary to achieve specified changes in the payoff and constraint.

$$\frac{\delta X_i}{\eta_i} = \frac{\begin{vmatrix} \delta f & S_{FW} \\ \delta W & S_W \end{vmatrix}}{D} \frac{\partial f}{\partial X_i} + \frac{\begin{vmatrix} S_F & \delta f \\ S_{FW} & \delta W \end{vmatrix}}{D} \frac{\partial W}{\partial X_i} \tag{2-4}$$

where

$$S_F = \sum_i \left(\frac{\partial f}{\partial X_i}\right)^2 \eta_i$$

$$S_{FW} = \sum_i \frac{\partial f}{\partial X_i} \frac{\delta W}{\partial X_i} \eta_i$$

$$S_w = \sum_i \left(\frac{\partial W}{\partial X_i}\right)^2 \eta_i$$

$$D = \begin{vmatrix} S_F & S_{FW} \\ S_{FW} & S_W \end{vmatrix}$$

It is interesting that Eq. (2-4) can be rearranged as follows:

$$\frac{\delta X_i}{\eta_i} = \frac{\begin{vmatrix} \frac{\partial f}{\partial X_i} & S_{FW} \\ \frac{\partial W}{\partial X_i} & S_W \end{vmatrix}}{D} \delta f + \frac{\begin{vmatrix} S_F & \frac{\partial f}{\partial X_i} \\ S_{FW} & \frac{\partial W}{\partial X_i} \end{vmatrix}}{D} \delta W$$

Notice that this form of the expression is directly comparable with that used in the trajectory program where we have separated the influences of the constraint and payoff. In this case the multiplier of the payload improvement corresponds to the mass row of the B matrix in the trajectory program and the multiplier of the launch weight change corresponds to the remaining elements of the B matrix in the trajectory program.

The optimization procedure followed to determine the best combination of system controls is remarkably similar to that used in the PRESTO trajectory program. System control changes are computed for selected payload improvements and simultaneous launch weight adjustments using Eq. (2-4). These changes are then added to input nominal values and the new design is tested to determine whether the desired performance improvement was achieved. The results of this test determine the course of action to be followed for the next iteration.

The first step in the solution for the system control changes is to establish the changes in payload and launch weight for Eq. (2-4). The approach used in the system optimization loop is again similar to that used in the PRESTO trajectory optimization loop. The solution to Eq. (2-2) and (2-3) is

rearranged in the form

$$\frac{\partial f}{\partial X_i} = \frac{\dfrac{\delta X_i}{\eta_i} - \left[\dfrac{S_F \delta W - S_{FW} \delta f}{D}\right] \dfrac{\partial W}{\partial X_i}}{\left[\dfrac{S_W \delta f - S_{FW} \delta W}{D}\right]}$$

and substituted back into the expression for the change in payload. The resulting equation is

$$\delta f = \left[\frac{D}{S_W \delta f - S_{FW} \delta W}\right] \sum_i \frac{\delta X_i^2}{\eta_i} - \left[\frac{S_F \delta W - S_{FW} \delta f}{S_W \delta f - S_{FW} \delta W}\right] \delta W \qquad (2\text{-}5)$$

This manipulation has rearranged the expression to combine the control changes so that the initial step size estimate can reflect our feel for the nature of the control changes rather than our guess at the payload improvement. It could be used directly in this form by solving the quadratic for payload improvement as a function of the combined control changes and constraint adjustment. Problems can arise, however, if the constraint adjustment is of such magnitude that the estimated control changes are inadequate to satisfy that requirement alone. Mathematically, this situation causes imaginary numbers in the expression for payload improvement. We have, therefore, resorted to a procedure where the constraint changes are separated as follows: Eq. (2-5) is first solved for the case of fixed constraints by zeroing the constraint change terms; this gives the following relationship between the payload change and the control changes.

$$\delta f = \sqrt{\frac{D}{S_W} \sum_i \frac{\delta X_i^2}{\eta_i}} = N \sqrt{\frac{D}{S_W}} \qquad (2\text{-}6)$$

The multiplier of the control changes in this expression is the gradient of the payload under the condition that the constraint remains fixed, as such

it will approach zero as the optimum combination of system controls is approached. A second solution is added to Eq. (2-6) to accommodate the constraint adjustment. This solution is developed by solving Eq. (2-3) as though we were concerned with constraint changes only. The steepest descent solution to Eq. (2-3) then becomes

$$\frac{\delta X_i}{\eta_i} = \frac{\delta W}{S_W} \frac{\partial W}{\partial X_i} \tag{2-7}$$

and substituting this into Eq. (2-2), we have

$$\delta f = \frac{S_{FW}}{S_W} \delta W \tag{2-8}$$

This expression relates payload to the constraint adjustment under the condition that the constraint adjustment is achieved with a minimum of sum square control change. The procedure is essential to the understanding of the performance exchange ratio formulations that will be developed later. Adding this result to Eq. (2-6), we have

$$\delta f = N \sqrt{\frac{D}{S_W}} + \frac{S_{FW}}{S_W} \delta W \tag{2-9}$$

The basic expressions have now been defined for the system optimization loop. In the optimization program the sequence begins with a launch weight correction run using Eq. (2-7) to define the system control changes. Eq. (2-9) is then used to estimate the payload improvement for the first system optimization iteration. The technique from this point differs from the PRESTO approach in that we continue to use Eq. (2-9) at each iteration to estimate the payload improvement for the next iteration. The result is a constant step size operation rather than the expanding step size operation of the PRESTO program. After an unsuccessful case, the step size is halved by halving the quantity N from

Eq. (2-9) and the process is continued until the payload increment computed from Eq. (2-9) becomes less than a pre-selected minimum.

In order to help with the evaluation of the convergence process, one additional set of optimization parameters is computed. These parameters are designated the optimization derivatives and represent the derivatives of payload with respect to the system controls under the condition that the constraint (launch weight) is held fixed by a minimum sum square adjustment in the remaining controls. Algebraically, this is written

$$\left.\frac{\partial f}{\partial X_i}\right|_W = \frac{\partial f}{\partial X_i} + \frac{\partial W}{\partial X_i}\left.\frac{\partial f}{\partial W}\right|_{X_i}$$

The new term in this expression is $\left.\frac{\partial f}{\partial W}\right|_{X_i}$ which is formed by dropping the derivatives related to the control from each sum used in the equation. Thus,

$$\left.\frac{\partial f}{\partial X_i}\right|_W = \frac{\partial f}{\partial X_i} - \frac{\partial W}{\partial X_i}\left[\frac{S_{FW} - \frac{\partial f}{\partial X_i}\frac{\partial W}{\partial X_i}\eta_i}{S_W - \left(\frac{\partial W}{\partial X_i}\right)^2 \eta_i}\right] \qquad (2\text{-}10)$$

This is the expression used to compute the optimization derivatives which will approach zero as the procedure approaches the optimum combination of system controls. This completes the derivation of the relationships used for optimization.

2.3 Exchange Ratio Formulation

The key to the approach used for the system parameter optimization program lies in the derivatives that link the inner and outer loops of the optimization process; that is, the performance exchange ratios. These quantities are defined as the derivatives of final mass with respect to each

of the trajectory program inputs, under the condition that the mission constraints remain satisfied. They are computed following a trajectory optimization sequence before the final guided run is initiated.

The assumption used is that the trajectory control history is readjusted in a minimum integral square sense to maintain the constraints as the program input varies. While this at first glance seems rather arbitrary, it is important to recognize that if an optimum trajectory has been obtained before the exchange ratios are computed, then the assumption used for the control readjustment is unimportant. This is true because any departure from the optimum control history produces no first order change in the final weight.

The description of the exchange ratio formulation is developed in the following paragraphs, first for a simplified problem that is used to illustrate the procedure. The results are then expanded to the form of the complete expressions used in the optimization program. Although only the fixed final stage or variable launch weight option of the trajectory program is used by the system optimization program, exchange ratios will for completeness be derived for both the variable and fixed final stage options. This is consistent with the history of their original development and might therefore help to clarify the approach.

2.3.1 Simplified Formulation

Consider first a single-stage vehicle operating outside of the atmosphere. Exchange ratios for specific impulse and initial weight will be evaluated since they are representative of the two types of parameters to be treated. The distinction is that weight change will occur at a point in the trajectory while the specific impulse change is distributed over a region of the trajectory. This formulation is developed for a two-dimensional trajectory which satisfies a constraint on radius at the end of the trajectory. The equations of motion

of the trajectory program inputs, under the condition that the mission constraints remain satisfied. They are computed following a trajectory optimization sequence before the final guided run is initiated.

The assumption used is that the trajectory control history is readjusted in a minimum integral square sense to maintain the constraints as the program input varies. While this at first glance seems rather arbitrary, it is important to recognize that if an optimum trajectory has been obtained before the exchange ratios are computed, then the assumption used for the control readjustment is unimportant. This is true because any departure from the optimum control history produces no first order change in the final weight.

The description of the exchange ratio formulation is developed in the following paragraphs, first for a simplified problem that is used to illustrate the procedure. The results are then expanded to the form of the complete expressions used in the optimization program. Although only the fixed final stage or variable launch weight option of the trajectory program is used by the system optimization program, exchange ratios will for completeness be derived for both the variable and fixed final stage options. This is consistent with the history of their original development and might therefore help to clarify the approach.

2.3.1 Simplified Formulation

Consider first a single-stage vehicle operating outside of the atmosphere. Exchange ratios for specific impulse and initial weight will be evaluated since they are representative of the two types of parameters to be treated. The distinction is that weight change will occur at a point in the trajectory while the specific impulse change is distributed over a region of the trajectory. This formulation is developed for a two-dimensional trajectory which satisfies a constraint on radius at the end of the trajectory. The equations of motion

and mass flow rate can be written as

$$F = \dot{V} = \frac{T_v}{m} \cos \eta - g \sin \gamma$$

$$G = \dot{\gamma} = \frac{T_v}{mV} \sin \eta + \left(\frac{V}{r} - \frac{g}{V} \right) \cos \gamma$$

$$H = \dot{r} = V \sin \gamma$$

$$I = \dot{m} = - \frac{T_v}{g_o \, I_{sp_v}}$$

where η is the angle between the velocity and thrust vectors, and the definitions of the remaining variables are given in the terminology list, p. iv.

Assume that a nominal trajectory meeting terminal conditions has been determined. One is interested in finding the influence of changes in the vehicle parameters on payload, assuming that the angle of attack is adjusted so that the terminal constraints are still satisfied.

The adjoint differential equations, with the partial derivatives evaluated along the nominal trajectory, are

$$\frac{d\lambda_V}{dt} = - \frac{\partial G}{\partial V} \lambda_\gamma - \frac{\partial H}{\partial V} \lambda_r$$

$$\frac{d\lambda_\gamma}{dt} = - \frac{\partial F}{\partial \gamma} \lambda_V - \frac{\partial G}{\partial \gamma} \lambda_\gamma - \frac{\partial H}{\partial \gamma} \lambda_r$$

$$\frac{d\lambda_r}{dt} = - \frac{\partial F}{\partial r} \lambda_V - \frac{\partial G}{\partial r} \lambda_\gamma$$

$$\frac{d\lambda_m}{dt} = - \frac{\partial F}{\partial m} \lambda_V - \frac{\partial G}{\partial m} \lambda_\gamma$$

Their solution has the following property:

$$\left[\lambda_V \delta V + \lambda_\gamma \delta\gamma + \lambda_r \delta r + \lambda_m \delta m\right]_{t=t_f} = \left[\lambda_V \delta V + \lambda_\gamma \delta\gamma + \lambda_r \delta r + \lambda_m \delta m\right]_{t=t_o}$$

$$- \int_{t_f}^{t_o} \left(\lambda_v \frac{\partial F}{\partial \eta} + \lambda_\gamma \frac{\partial G}{\partial \eta}\right) \delta\eta \, dt - \int_{t_f}^{t_o} \lambda_m \frac{\partial I}{\partial I_{sp_v}} \delta I_{sp_v} dt \qquad (2\text{-}11)$$

The initial conditions for these adjoint equations are specified at the time the stopping parameter is reached, t_f. They are functions only of the terminal constraints and the stopping parameter. One separate solution of the adjoint equations is required for each terminal constraint and one for the payoff function, mass.

At the initial time, t_o, the perturbations δV, $\delta\gamma$, and δr are zero. Furthermore, δI_{sp_v} is constant. Assume radius to be the only terminal constraint and let the second subscripts ϕ and ψ indicate that the adjoint equations are solved using the initial conditions associated with mass and radius, respectively.

Using Eq. (2-11) and assuming we are on the nominal trajectory at t_o, the expressions for terminal deviations in mass and radius are

$$\delta m_f = \lambda_{m\phi} \delta m_o + \int_{t_f}^{t_o} \Lambda_\phi \delta\eta \, dt - R_\phi \delta I_{sp_v}$$

$$\delta r_f = \lambda_{m\psi} \delta m_o + \int_{t_f}^{t_o} \Lambda_\psi \delta\eta \, dt - R_\psi \delta I_{sp_v} \qquad (2\text{-}12)$$

where

$$A = -\lambda_v \frac{\partial F}{\partial \eta} - \lambda_\gamma \frac{\partial G}{\partial \eta}$$

and

$$R = \int_{t_f}^{t_o} \lambda_m \frac{\partial I}{\partial I_{sp_v}} \, dt$$

and

$$\lambda_{mf} = \lambda_{rf} = 1.0.$$

We have assumed a nominal trajectory that meets terminal conditions, i.e., $\delta r_f = 0$. In order to maintain this condition in the presence of perturbations in initial mass and specific impulse, it will be necessary to adjust the angle of attack, η. The minimum change in η that will enable the terminal conditions to be met is found by setting $\delta\eta = C\Lambda_\psi$. Substituting $\delta\eta$ in Eq. (2-12) gives

$$\begin{aligned} \delta m_f &= \lambda_{m\phi} \, \delta m_o - R_\phi \, \delta I_{sp_v} + C I_{\psi\phi} \\ \delta r_f &= \lambda_{m\psi} \, \delta m_o - R_\psi \, \delta I_{sp_v} + C I_{\psi\psi} \end{aligned} \qquad (2\text{-}13)$$

where

$$I_{\psi\phi} = \int_{t_f}^{t_o} \Lambda_\psi \, \Lambda_\phi \, dt$$

and $I_{\psi\psi}$, correspondingly. Solving for C, with the condition that $\delta r_f = 0$, one obtains $\delta\eta$

$$\delta\eta = \frac{-\lambda_{m\psi}\,\delta m_o + R_\psi\,\delta I_{sp_v}}{I_{\psi\psi}}\,\Lambda_\psi$$

To determine the influence of these perturbations on final mass, substitute for $\delta\eta$ in Eq. (2-12)

$$\delta m_f = (\lambda_{m\phi} - U\lambda_{m\psi})\,\delta m_o - (R_\phi - UR_\psi)\,\delta I_{sp_v} \qquad (2\text{-}14)$$

where

$$U = \frac{I_{\psi\phi}}{I_{\psi\psi}}$$

The coefficients of δm_o and of δI_{sp_v} in Eq. (2-14) give the influence of these perturbations on final mass, assuming the angle of attack is adjusted to meet terminal conditions. They are the exchange ratios for m_ϕ and I_{sp_v}.

2.3.2 Expanded Formulation

Moving now to the more general form of the exchange ratio equations and adopting the terminology used for the PRESTO program, the expresssions for changes in the terminal constraints may be written.

$$d\psi = \int_{t_f}^{t_i} \Lambda_\psi\,\delta\alpha\,dt + S_\psi\,\delta\tau + \int_{t_f}^{t_i} \Lambda_{X\psi}\,\delta X\,dt + S_{Y\psi}\,\delta Y \qquad (2\text{-}15)$$

where

$$\Lambda_X = \begin{bmatrix} \Lambda_{X1_1} & \Lambda_{X2_1} & \cdot & \cdot & \cdot & \Lambda_{XN} \\ \Lambda_{X1_2} & \Lambda_{X2_2} & \cdot & \cdot & \cdot & \cdot \\ \cdot & \cdot & \cdot & \cdot & \cdot & \cdot \\ \cdot & \cdot & \cdot & \cdot & \cdot & \cdot \\ \cdot & \cdot & \cdot & \cdot & \cdot & \cdot \\ \Lambda_{X1_{jc}} & \Lambda_{X2_{jc}} & \cdot & \cdot & \cdot & \Lambda_{XN_{jc}} \end{bmatrix}$$

representing the time derivatives of the partials of final mass and each constraint with respect to the program inputs X1, X2 . . . XN, that have distributed effects. $\Lambda_{X\psi}$ contains all but the first row of Λ_X.

Where

$$S_Y = \begin{bmatrix} S_{Y1_1} & S_{Y2_1} & \cdot & \cdot & S_{YN_1} \\ S_{Y1_2} & S_{Y2_2} & \cdot & \cdot & \cdot \\ S_{Y1_3} & \cdot & \cdot & \cdot & \cdot \\ \cdot & \cdot & \cdot & \cdot & \cdot \\ \cdot & \cdot & \cdot & \cdot & \cdot \\ S_{Y1_{jc}} & \cdot & \cdot & \cdot & S_{YN_{jc}} \end{bmatrix}$$

representing the partials of final mass and each constraint with respect to the program inputs Y1, Y2 . . . YN, that have no distributed effects. $S_{Y\psi}$ contains all but the first row of S_Y. The elements of Λ_X are formed in an analagous manner to those of Λ using

$$\Lambda_X = \lambda G$$

where

$$G = \begin{bmatrix} \frac{\partial F}{\partial X1} & \frac{\partial F}{\partial X2} & \cdot & \cdot & \cdot & \frac{\partial F}{\partial XN} \\ \frac{\partial G}{\partial X1} & \frac{\partial G}{\partial X2} & \cdot & \cdot & \cdot & \cdot \\ \frac{\partial I}{\partial X1} & \cdot & \cdot & \cdot & \cdot & \cdot \\ \frac{\partial K}{\partial X1} & \cdot & \cdot & \cdot & \cdot & \cdot \\ \frac{\partial \dot{m}}{\partial X1} & \cdot & \cdot & \cdot & \cdot & \cdot \\ \frac{\partial H}{\partial X1} & \cdot & \cdot & \cdot & \cdot & \cdot \\ \frac{\partial J}{\partial X1} & \frac{\partial J}{\partial X2} & \cdot & \cdot & \cdot & \frac{\partial J}{\partial XN} \end{bmatrix}$$

As in the previous example, Eq. (2-15) is solved by setting the control change proportional to its effect on the constraints. Using PRESTO terminology,

$$\delta\alpha = W^{-1}\Lambda_\psi^T C$$

and

$$\delta\tau = Y^{-1}S_\psi^T C$$

where C is an arbitrary array of proportionality constraints, and W and Y are the gains. Using these solutions, Eq. (2-15) becomes

$$d\psi = \left[\int_{t_f}^{t_i} \Lambda_\psi W^{-1} \Lambda_\psi^T dt + S_\psi Y^{-1} S_\psi^T\right] C + \int_{t_2}^{t_1} \Lambda_{X\psi}\, \delta X\, dt + S_{Y\psi}\, \delta Y$$

This is solved to eliminate C and determine the values of $\delta\alpha$ and $\delta\tau$ that correspond to $d\psi = 0$. Thus,

$$C = -\left[\int_{t_f}^{t_i} \Lambda_\psi W^{-1} \Lambda_\psi^T dt + S_\psi Y^{-1} S_\psi^T\right]^{-1} \left[\int_{t_2}^{t_1} \Lambda_{X\psi}\, \delta X\, dt + S_{Y\psi}\, \delta Y\right]$$

and

$$\delta\alpha = -W^{-1}\Lambda_\psi^T \left[\int_{t_f}^{t_i} \Lambda_\psi W^{-1} \Lambda_\psi^T dt + S_\psi Y^{-1} S_\psi^T\right]^{-1} \left[\int_{t_2}^{t_1} \Lambda_{X\psi}\, \delta X\, dt + S_{Y\psi}\, \delta Y\right]$$

$$\delta\tau = -Y^{-1}S_\psi^T \left[\int_{t_f}^{t_i} \Lambda_\psi W^{-1} \Lambda_\psi^T dt + S_\psi Y^{-1} S_\psi^T\right]^{-1} \left[\int_{t_2}^{t_1} \Lambda_{X\psi}\, \delta X\, dt + S_{Y\psi}\, \delta Y\right]$$

Now write the equation for the change in final mass,

$$\delta m = \int_{t_f}^{t_i} \Lambda_{\phi}\, \delta\alpha\, dt + S_{\phi}\, \delta\tau + \int_{t_2}^{t_1} \Lambda_{X\phi}\, \delta X\, dt + S_{Y\phi}\, \delta Y$$

Substituting for $\delta\alpha$ and $\delta\tau$

$$\delta m = -\left[\int_{t_f}^{t_i} \Lambda_{\phi} W^{-1} \Lambda_{\psi}^{T}\, dt + S_{\phi} Y^{-1} S_{\psi}^{T}\right] \left[\int_{t_f}^{t_i} \Lambda_{\psi}\, W^{-1} \Lambda_{\psi}^{T}\, dt + S_{\psi}\, Y^{-1} S_{\psi}^{T}\right]^{-1}$$

$$\left[\int_{t_2}^{t_1} \Lambda_{X\psi}\, \delta X\, dt + S_{Y\psi}\, \delta Y\right] + \int_{t_2}^{t_1} \Lambda_{X\phi}\, \delta X\, dt + S_{Y\phi}\, \delta Y$$

If we now assume that the distributed parameter changes δX are constant over the region considered and regroup the terms, the equation becomes

$$\delta m = (T_{\phi} - UT_{\psi})\, \delta Y + (R_{\phi} - UR_{\psi})\, \delta X \qquad (2\text{-}16)$$

where

$$R_{\phi} = \int_{t_2}^{t_1} \Lambda_{X\phi}\, dt \qquad T_{\phi} = S_{Y\phi}$$

$$R_{\psi} = \int_{t_2}^{t_1} \Lambda_{X\psi}\, dt \qquad T_{\psi} = S_{Y\psi}$$

$$U = \left[\int_{t_f}^{t_i} \Lambda_{\phi}\, W^{-1}\, \Lambda_{\psi}^{T}\, dt + S_{\phi}\, Y^{-1}\, S_{\psi}^{T}\right] \left[\int_{t_f}^{t_i} \Lambda_{\psi}\, W^{-1}\, \Lambda_{\psi}^{T}\, dt + S_{\psi}\, Y^{-1}\, S_{\psi}^{T}\right]^{-1}$$

This equation corresponds directly to Eq. (2-14) in the simplified example.

At this point we must define the variables for which exchange ratios are to be computed. These variables are

launch mass	m_o
stage jettison mass	m_j
stage burn time	t
stage vacuum specific impulse	I_{sp_v}
stage vacuum thrust	T_v
stage nozzle exit area	A_e

The first three variables have non-distributed effects and their exchange ratios will be of the type defined by vector T in Eq. (2-15). The last three parameters have distributed effects and their exchange ratios are defined by vector R. More specifically following the program terminology, we can write

$$\delta m_f = e_o \, \delta m_o + \sum_{\substack{\text{no. of} \\ \text{stages}}} (e_1 \, \delta I_{sp} + e_2 \, \delta T_v + e_3 \, \delta A_e + e_4 \, \delta m_j) + \sum_{\substack{\text{all but} \\ \text{the final stage}}} e_5 \, \delta t$$

where

$$\left.\begin{matrix} e_0 \\ e_4 \\ e_5 \end{matrix}\right\} \quad \text{correspond to} \quad \begin{cases} Y_1 \\ Y_2 \\ Y_3 \end{cases}$$

and

$$\left.\begin{matrix} e_1 \\ e_2 \\ e_3 \end{matrix}\right\} \quad \text{correspond to} \quad \begin{cases} X1 \\ X2 \\ X3 \end{cases}$$

Notice that the propellant mass is implied by this equation and may be obtained from the other variables using the relationship given in Eq. (2-1). Also, if

the launch weight is varied independently from the other parameters then the last stage burn time and propellant load must vary. This corresponds to the operation of the fixed launch mass option of the PRESTO program where the stopping condition determines the propellant and burn time for the final stage.

The partial derivatives may now be written for the matrix G.

$$\frac{\partial F}{\partial I_{sp_v}} = 0$$

$$\frac{\partial F}{\partial T_v} = \frac{1}{m} \cos \eta \cos x \ \text{sgn A}$$

$$\frac{\partial F}{\partial A_e} = - p \frac{\partial F}{\partial T_v}$$

$$\frac{\partial G}{\partial I_{sp_v}} = 0$$

$$\frac{\partial G}{\partial T_v} = \frac{1}{mV} \sin \eta \ \text{sgn A}$$

$$\frac{\partial G}{\partial A_e} = - p \frac{\partial G}{\partial T_v}$$

$$\frac{\partial H}{\partial I_{sp_v}} = 0$$

$$\frac{\partial H}{\partial T_v} = \frac{1}{mV} \frac{\cos \eta \sin x \ \text{sgn A}}{\cos \gamma}$$

$$\frac{\partial H}{\partial A_e} = - p \frac{\partial H}{\partial T_v}$$

$$\frac{\partial I}{\partial I_{sp_v}} = \frac{\partial I}{\partial T_v} = \frac{\partial I}{\partial A_e} = 0$$

$$\frac{\partial J}{\partial I_{sp_v}} = \frac{\partial J}{\partial T_v} = \frac{\partial J}{\partial A_e} = 0$$

$$\frac{\partial K}{\partial I_{sp_v}} = \frac{\partial K}{\partial T_v} = \frac{\partial K}{\partial A_e} = 0$$

$$\frac{\partial \dot{m}}{\partial I_{sp_v}} = \frac{T_v}{g_o I_{sp_v}^2}$$

$$\frac{\partial \dot{m}}{\partial T_v} = -\frac{1}{g_o I_{sp_v}}$$

$$\frac{\partial \dot{m}}{\partial A_e} = 0$$

Before e_i can be computed, the elements of matrix S_Y must be defined. By direct analogy with the simplified example S_{Y1} and S_{Y2} are the adjoint variables for mass evaluated at the time t_1 at which the mass change occurs. The remaining parameter in S_Y is the burn time, t. Examining conditions at the end of a stage

$$\frac{\partial \psi}{\partial t} = \frac{\partial \psi}{\partial x} \frac{\partial x}{\partial t} = \lambda \dot{x} = S_{Y3}$$

and the S_Y matrix is written

$$\begin{bmatrix} \lambda_{m_1}\big|_{t_o} & \lambda_{m_1}\big|_{t_1} & \\ \lambda_{m_2}\big|_{t_o} & \lambda_{m_2}\big|_{t_1} & \\ \vdots & \vdots & \lambda\dot{x} \\ \lambda_{m_{jc}}\big|_{t_o} & \lambda_{m_{jc}}\big|_{t_1} & \end{bmatrix}_{t_1}$$

2.3.3 Constant Launch Mass Mode

Exchange ratios in the constant launch mass mode of operation are computed first for the case of constant propellant mass.[1] This immediately implies a relationship between the remaining propulsion variables I_{sp_v}, T_v and t from Eq. (2-1). When computing the exchange ratios for each of these variables the other two variables are alternately held fixed. When the trajectory program operates in the constant launch mass mode, the exchange ratios with fixed propellant mass therefore become

$$\left.\frac{\partial m_f}{\partial I_{sp_v}}\right|_{T_v} = e_1 + e_5 \left.\frac{\partial t}{\partial I_{sp_v}}\right|_{T_v} \qquad \left.\frac{\partial m_f}{\partial I_{sp_v}}\right|_{t} = e_1 + e_2 \left.\frac{\partial T_v}{\partial I_{sp_v}}\right|_{t}$$

$$= e_1 + \frac{g_o \dot{m}_p}{T_v} e_5 \qquad = e_1 + \frac{g_o \dot{m}_p}{t} e_2$$

[1] i.e., in all but the final powered stage.

$$\left.\frac{\partial m_f}{\partial T_v}\right|_{I_{sp_v}} = e_2 + e_5 \left.\frac{\partial t}{\partial T_v}\right|_{I_{sp_v}} \qquad \left.\frac{\partial m_f}{\partial T_v}\right|_{t} = e_2 + e_1 \left.\frac{\partial I_{sp_v}}{\partial T_v}\right|_{t}$$

$$= e_2 - \frac{t}{T_v} e_5 \qquad = e_2 + \frac{t}{g_o \dot{m}_p} e_1$$

$$\left.\frac{\partial m_f}{\partial t}\right|_{T_v} = e_5 + e_1 \left.\frac{\partial I_{sp_v}}{\partial t}\right|_{T_v} \qquad \left.\frac{\partial m_f}{\partial t}\right|_{I_{sp_v}} = e_5 + e_2 \left.\frac{\partial T_v}{\partial t}\right|_{I_{sp_v}}$$

$$= e_5 + \frac{T_v}{g_o \dot{m}_p} e_1 \qquad = e_5 - \frac{T_v}{t} e_2$$

$$\frac{\partial m_f}{\partial m_o} = e_o$$

$$\frac{\partial m_f}{\partial A_e} = e_3$$

$$\frac{\partial m_f}{\partial m_j} = e_4$$

In the fixed launch mass mode of operation, the propellant and burn time for the final stage must vary in the manner defined by the stopping parameter. The exchange ratios for the propulsion parameters for this stage therefore carry a somewhat different interpretation. No burn time exchange ratio is defined and burn time and propellant mass are always dependent variables. In this case the

the final stage exchange ratios become

$$\frac{\partial m_f}{\partial I_{sp_v}} = e_1 \qquad \frac{\partial m_f}{\partial T_v} = e_2$$

$$\frac{\partial m_f}{\partial m_o} = e_o$$

$$\frac{\partial m_f}{\partial A_e} = e_3$$

$$\frac{\partial m_f}{\partial m_j} = -1$$

The basic information has already been developed to complete the exchange ratio set for the fixed launch mass mode of operation. Although no exchange ratios have been defined for propellant weight, these may be derived from those for I_{sp_v}, T_v and t using

$$\left.\frac{\partial m_f}{\partial m_p}\right|_{T_v,\, t} = e_1 \left.\frac{\partial I_{sp_v}}{\partial m_p}\right|_{T_v,\, t} = -\frac{I_{sp_v}}{m_p} e_1$$

$$\left.\frac{\partial m_f}{\partial m_p}\right|_{I_{sp_v},\, t} = e_2 \left.\frac{\partial T_v}{\partial m_p}\right|_{I_{sp_v},\, t} = \frac{g_o I_{sp_v}}{t} e_2$$

$$\left.\frac{\partial m_f}{\partial m_p}\right|_{I_{sp_v},\, T_v} = e_5 \left.\frac{\partial t}{\partial m_p}\right|_{I_{sp_v},\, T_v} = \frac{g_o I_{sp_v}}{T_v} e_5$$

The propellant mass exchange ratios are not defined for the last stage in this mode of operation. A complete summary of the exchange ratios for the fixed launch mass mode is presented in Table 2-1.

2.3.4 Fixed Final Stage Mode

When the trajectory program operates in the fixed final stage option where launch mass now becomes a dependent variable the constant propellant mass, exchange ratios derived in the previous section must be modified as follows

$$\left.\frac{\partial m_f}{\partial X,Y}\right|_{\substack{\text{fixed}\\ \text{final}\\ \text{stage}}} = \left.\frac{\partial m_f}{\partial X,Y}\right|_{m_o} + \frac{\partial m_o}{\partial X,Y} e_o$$

$$m_o = m_f + \sum(m_p + m_j)$$

$$\frac{\partial m_o}{\partial X,Y} = \left.\frac{\partial m_f}{\partial X,Y}\right|_{\substack{\text{fixed}\\ \text{final}\\ \text{stage}}} + \sum\left(\frac{\partial m_p}{\partial X,Y} + \frac{\partial m_j}{\partial X,Y}\right)$$

EXCHANGE RATIOS FOR FIXED LAUNCH MASS MODE

Independent Variable	Variables held Constant	Final Mass Partial	
		Lower Stages	Final Stage
I_{sp_v}	m_p, T_v	$e_1 + \frac{g_o m_p}{T_v} e_5$	e_1
	m_p, t	$e_1 + \frac{g_o m_p}{t} e_2$	-
T_v	m_p, I_{sp_v}	$e_2 - \frac{t}{T_v} e_5$	e_2
	m_p, t	$e_2 + \frac{t}{g_o m_p} e_1$	-
t	m_p, I_{sp_v}	$e_5 - \frac{T_v}{t} e_2$	-
	m_p, T_v	$e_5 + \frac{T_v}{g_o m_p} e_1$	-
m_o	-	e_o	e_o
A_e	-	e_3	e_3
m_j	-	e_4	-1
m_p	I_{sp_v}, T_v	$\frac{g_o I_{sp_v}}{T_v} e_5$	-
	T_v, t	$-\frac{I_{sp_v}}{m_p} e_1$	-
	I_{sp_v}, t	$\frac{g_o I_{sp_v}}{t} e_2$	-

thus

$$\left.\frac{\partial m_f}{\partial X,Y}\right|_{\substack{\text{fixed}\\ \text{final}\\ \text{stage}}} = \frac{1}{1 - e_o}\left[\left.\frac{\partial m_f}{\partial X,Y}\right|_{m_o} + \sum\left(\frac{\partial m_p}{\partial X,Y} + \frac{\partial m_j}{\partial X,Y}\right) e_o\right]$$

The jettison mass and propellant mass partials in this expression are zero unless the jettison mass or propellant mass are the dependent variables. In that case the partials are equal to one.

A complete set of exchange ratios is also now available for the final stage since it is possible to fix the burn time and propellant mass for that stage when the launch mass becomes the dependent variable. This stage remains unique, however, in that the burn time derivative e_5 does not enter the relationships. The effect of last stage burn time variations is already implied in the e_i defined for the fixed launch mass option. A complete summary of the fixed final stage exchange ratios is presented in Table 2-2. These are the exchange ratios used in the system optimization program.

2.4 Formulation of Optimization Partials

It is now a straightforward process to form the partial derivatives $\frac{\partial f}{\partial X_i}$ and $\frac{\partial W}{\partial X_i}$ that are used in the system optimization program. These derivatives are written for convenience in terms of the exchange ratios that have already

EXCHANGE RATIOS FOR FIXED FINAL STAGE MODE

$$e^* = \frac{1}{1-e_o}$$

Independent Variable	Variables held Constant	Final Mass Partial	
		Lower Stages	Final Stage
I_{sp_v}	m_p, T_v	$e^*\left(e_1 + \frac{g_o m_p}{T_v} e_5\right)$	$e^* e_1$
	m_p, t	$e^*\left(e_1 + \frac{g_o m_p}{t} e_2\right)$	$e^*\left(e_1 + \frac{g_o m_p}{t} e_2\right)$
T_v	m_p, I_{sp_v}	$e^*\left(e_2 - \frac{t}{T_v} e_5\right)$	$e^* e_2$
	m_p, t	$e^*\left(e_2 + \frac{t}{g_o m_p} e_1\right)$	$e^*\left(e_2 + \frac{t}{g_o m_p} e_1\right)$
t	m_p, I_{sp_v}	$e^*\left(e_5 - \frac{T_v}{t} e_2\right)$	$-e^* \frac{T_v}{t} e_2$
	m_p, T_v	$e^*\left(e_5 + \frac{T_v}{g_o m_p} e_1\right)$	$e^* \frac{T_v}{g_o m_p} e_1$
m_o	-	-	-
A_e	-	$e^* e_3$	$e^* e_3$
m_j	-	$e^* e_4$	-1
m_p	I_{sp_v}, T_v	$e^*\left(\frac{g_o I_{sp_v}}{T_v} e_5 + e_o\right)$	$e^* e_o$
	T_v, t	$e^*\left(-\frac{I_{sp_v}}{m_p} e_1 + e_o\right)$	$e^*\left(-\frac{I_{sp_v}}{m_p} e_1 + e_o\right)$
	I_{sp_v}, t	$e^*\left(\frac{g_o I_{sp_v}}{t} e_2 + e_o\right)$	$e^*\left(\frac{g_o I_{sp_v}}{t} e_2 + e_o\right)$

been derived and the propulsion and jettison weight partials.

$$\begin{bmatrix} \frac{\partial f}{\partial P} \\ \frac{\partial f}{\partial p} \\ \frac{\partial f}{\partial t} \\ \frac{\partial f}{\partial \epsilon} \end{bmatrix} = \begin{bmatrix} \frac{\partial P}{\partial P} & \frac{\partial T_v}{\partial P} & \frac{\partial t}{\partial P} & \frac{\partial A_e}{\partial P} \\ \frac{\partial P}{\partial p} & \frac{\partial T_v}{\partial p} & \frac{\partial t}{\partial p} & \frac{\partial A_e}{\partial p} \\ \frac{\partial P}{\partial t} & \frac{\partial T_v}{\partial t} & \frac{\partial t}{\partial t} & \frac{\partial A_e}{\partial t} \\ \frac{\partial P}{\partial \epsilon} & \frac{\partial T_v}{\partial \epsilon} & \frac{\partial t}{\partial \epsilon} & \frac{\partial A_e}{\partial \epsilon} \end{bmatrix} \begin{bmatrix} \frac{\partial f}{\partial P}\Big|_{T_v,t} \\ \frac{\partial f}{\partial T_v}\Big|_{P,t} \\ \frac{\partial f}{\partial t}\Big|_{P,T_v} \\ \frac{\partial f}{\partial A_e} \end{bmatrix} + \frac{\partial f}{\partial J} \begin{bmatrix} \frac{\partial J}{\partial P} \\ \frac{\partial J}{\partial p} \\ \frac{\partial J}{\partial t} \\ \frac{\partial J}{\partial \epsilon} \end{bmatrix}$$

or

$$\frac{\partial f}{\partial X_i} = \frac{\partial Pr}{\partial X_i} E + \frac{\partial f}{\partial J} \frac{\partial J}{\partial X_i} \qquad (2\text{-}17)$$

$$\frac{\partial W}{\partial X_i} = \begin{bmatrix} \frac{\partial W}{\partial P} \\ \frac{\partial W}{\partial p} \\ \\ \frac{\partial W}{\partial t} \\ \frac{\partial W}{\partial \epsilon} \end{bmatrix} = \frac{\partial f}{\partial X_i} + \begin{bmatrix} \frac{\partial J}{\partial P} + 1 \\ \frac{\partial J}{\partial p} \\ \\ \frac{\partial J}{\partial t} \\ \frac{\partial J}{\partial \epsilon} \end{bmatrix}$$

When the optimization partials $\frac{\partial f}{\partial X_i}$ and $\frac{\partial W}{\partial X_i}$ are formed, the remaining system controls are held constant and the rows in $\frac{\partial Pr}{\partial X_i}$ and $\frac{\partial J}{\partial X_i}$ reflect this. The partials used in these expressions will be defined in the following paragraphs.

The exchange ratios for the fixed final stage option derived in Section 2.3 can now be used for the elements of the matrix E and for $\frac{\partial f}{\partial J}$ appearing in Eq. (2-17) for $\frac{\partial f}{\partial X}$. Taking the terms from Table 2-2 the exchange ratio partials become

$$\left.\frac{\partial f}{\partial P}\right|_{T_v,t} = \left.\frac{\partial m_f}{\partial m_p}\right|_{T_v,t}$$

$$\left.\frac{\partial f}{\partial T_v}\right|_{P,t} = g_o \left.\frac{\partial m_f}{\partial T_v}\right|_{t}$$

$$\left.\frac{\partial f}{\partial t}\right|_{P,T_v} = g_o \left.\frac{\partial m_f}{\partial t}\right|_{T_v}$$

$$\frac{\partial f}{\partial A_e} = g_o \frac{\partial m_f}{\partial A_e}$$

$$\frac{\partial f}{\partial J} = \frac{\partial m_f}{\partial m_j}$$

The propulsion relationships given in Eq. (2-1) have already been used to develop some of the partials appearing in the matrix $\frac{\partial Pr}{\partial X_i}$. The remaining elements of this matrix are rather obvious and the complete matrix is given below.

$$\frac{\partial Pr}{\partial X_i} = \begin{bmatrix} 1 & \frac{T_v}{P} & 0 & \frac{A_e}{P} \\ 0 & 0 & 0 & -\frac{A_e}{P} \\ 0 & -\frac{T_v}{t} & 1 & -\frac{A_e}{t} \\ 0 & \frac{T_v}{C_{F_v}} \frac{\partial C_{F_v}}{\partial \epsilon} & 0 & \frac{A_e}{\epsilon} \end{bmatrix}$$

where T_v and A_e are defined by Eq. (2-1) and $\frac{\partial C_{F_v}}{\partial \epsilon}$ is a numerically determined derivative from Figure 2-2 which defines C_{F_v} as a function of ϵ.

The final derivatives to be evaluated are the jettison weight derivatives, $\frac{\partial J}{\partial X}$. Jettison weights are defined for the liquid propellant launch vehicle study by the following equation.[1]

$$J = C_T P + C_E T_v + C_S W_{PL}$$

where C_i are inputs and remain constant during a run and W_{PL} is the weight carried by the stage considered (i.e., nose load). Derivatives are formed numerically rather than algebraically so that the equations can readily be replaced by more complex relationships. For these operations, T_v is replaced using Eq. (2-1) so that the jettison weights are expressed directly in terms

[1] Suggested from an analysis made by J. D. Bird of NASA Langley Research Center.

FIGURE 2-2

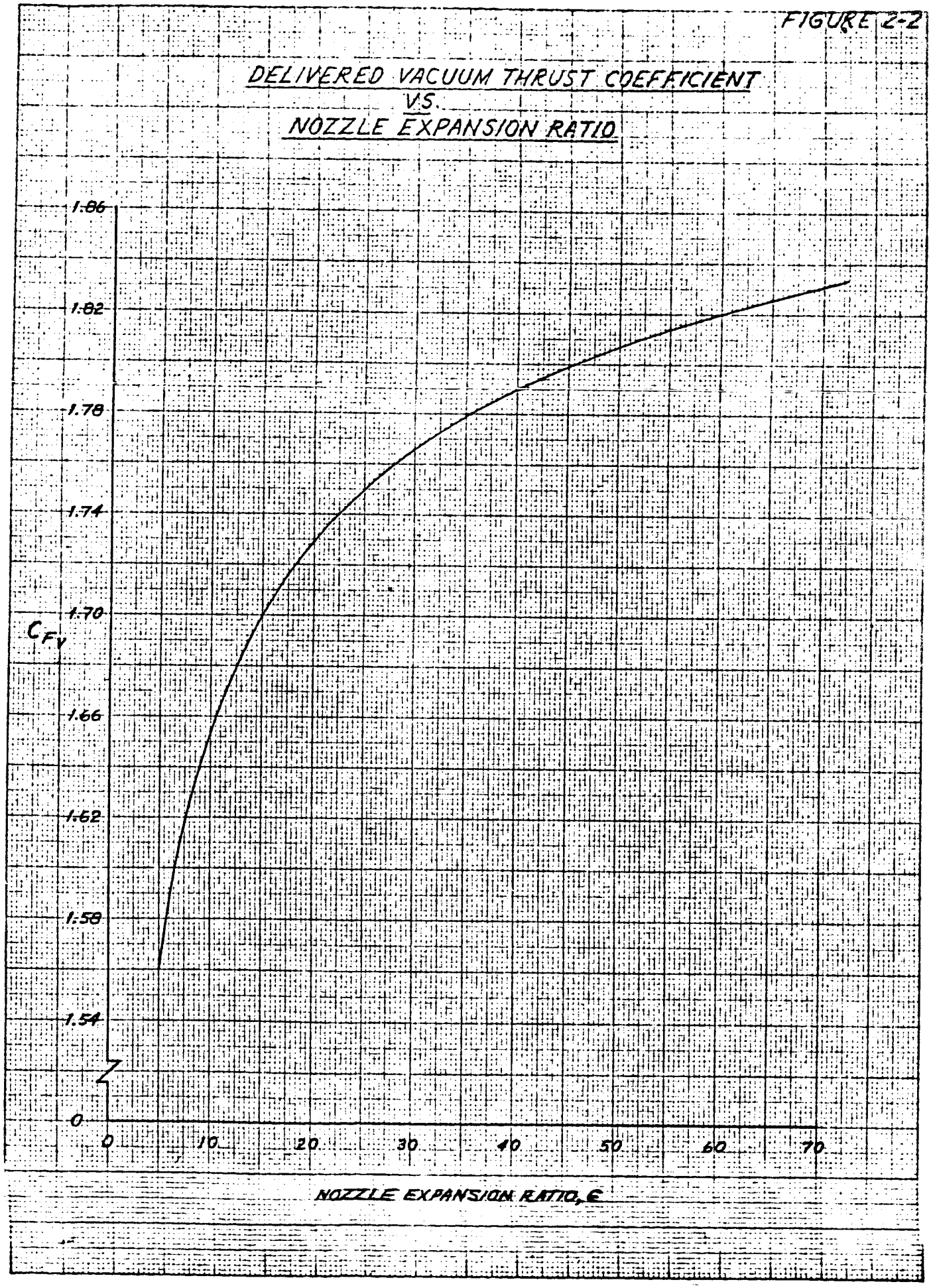
DELIVERED VACUUM THRUST COEFFICIENT
VS.
NOZZLE EXPANSION RATIO
1.86
1.82
1.78
1.74
1.70
1.66
1.62
1.58
1.54
C_{F_V}
0
0
10
20
30
40
50
60
70
NOZZLE EXPANSION RATIO, ε

of the system controls.

$$J = C_T P + C_E \frac{C_{F_v} C^* P}{g_o t} + C_S W_{PL}$$

Each stage in the system influences through W_{PL} the stages below it, creating a series of cross derivatives for jettison weight that define the interstage influences. In the system optimization program these influences are also defined numerically by differencing all of the stage jettison weights each time a system parameter is perturbed.

2.5 Dynamic Pressure Constraint Formulation

An important relationship has been ignored up to this point for the launch system optimization problems being considered. Usually the launch environment significantly influences the system design. This in turn influences performance indirectly through the jettison weights and directly through the geometry and its associated aerodynamic characteristics. In large low acceleration launch systems the weight to drag ratio is high and the major environmental feedback is through loads and heating to jettison weights. In small high acceleration systems the direct aerodynamic feedback is proportionately higher and may be as significant as the feedback through jettison weights.

It would not be very difficult to formulate optimization equations that would properly accommodate these effects. A problem arises however when it becomes necessary to define the partial derivatives that relate the launch environment to the jettison weights and the geometry to the aerodynamics. Usually these effects are established through a rather involved analytical or empirical procedure that is cumbersome for the problem at hand.

The problem can be solved crudely by constraining the launch environment during the optimization so that the jettison weight relationships properly reflect the situation. The environmental constraint can then be adjusted by a trial and error process and the system re-optimized with new jettison weight relationships that reflect those adjustments until the maximum payload is determined.

An alternate approach would be to ignore the environmental relationships during the optimization, use the resulting environment to define new weight relationships, use the new relationships to run a new optimization, etc. This method may be divergent and partly for that reason is not considered as desirable as the first approach. More importantly, however, it is a dead-end because the mechanism is not developed for accommodating environmental derivatives should they later become available.

A single environmental constraint that does reflect a major portion of the environmental feedback is the peak dynamic pressure. This parameter is therefore used in the following discussion where a formulation is developed to constrain peak dynamic pressure during the system optimization. The approach is general in that it is applicable to any environmental factor affecting the design, whether it be one that is encountered at some point along the trajectory or one that involves some cumulative effect that is a function of the trajectory history. The formulation has not been included in the optimization program at this writing so we have no practical experience with the behavior of the program with the dynamic pressure constraint included. This could be the subject of a future study.

For the present formulation the dynamic pressure constraint must reflect the ability of both the trajectory control program and the vehicle control program (i.e., the combination of design variables) to adjust peak dynamic pressure. Another way of stating this is that the vehicle design derivatives $\frac{\partial f}{\partial X_i}$ and $\frac{\partial W}{\partial X_i}$ must recognize the imposition of a constraint. Enough procrasti-

nation forces one to the easy method of accomplishing this. Treat the constraint in exactly the same fashion as the terminal trajectory constraints. Since design optimization studies practically do not require the use of all six terminal constraints provided for in the PRESTO trajectory routine, we will use one constraint for dynamic pressure. Logically, this means that a set of adjoint variables will be initialized using the first time point following peak dynamic pressure on the forward trajectories. The stopping parameter for this constraint becomes $\dot{q}$. It is interesting that the stopping condition is always $\dot{q} = 0$. Following the PRESTO formulation

$$\delta q = \delta q\Big|_{\substack{\text{time for} \\ q_{max}}} - \frac{\dot{q}}{\ddot{q}} \delta \dot{q}\Big|_{\substack{\text{time for} \\ q_{max}}} = \delta q\Big|_{\substack{\text{time for} \\ q_{max}}}$$

This relation says that to first order the peak dynamic pressure point will not shift on the time scale with changes in the trajectory controls and that initialization at $\dot{q} = 0$ is equivalent to initialization using the time on the forward trajectory for $\dot{q} = 0$. The initial conditions for the adjoint variables become

$$\lambda_r = \frac{V^2}{2} \frac{\partial \rho}{\partial r} \qquad \lambda_m = 0$$

$$\lambda_v = \rho V \qquad \lambda_\lambda = 0$$

$$\lambda_\gamma = 0 \qquad \lambda_\psi = 0$$

One additional precaution must be observed to avoid trouble when the PRESTO closed loop formulation is used beyond the q_{max} point. The q constraint miss must be set equal to zero in this region.

The introduction of this initialization logic and the incorporation of the constraint error in the $d\psi$ constraint miss list automatically imposes a peak dynamic pressure constraint during the trajectory shaping process. Furthermore, the exchange ratio formulation is such that the new constraint is also reflected in each derivative computed in the trajectory program. This in turn means that the constraint is properly reflected in each design derivative and the process is complete.

When the PRESTO II trajectory routine is in operation, the procedure is directly analogous to that used with PRESTO. One constraint is replaced with peak dynamic pressure. The derivatives $\frac{\partial q_{max}}{\partial \gamma}$ and $\frac{\partial q_{max}}{\partial m_i}$ required for K_S and L_S in the PRESTO II control equation

$$d\varepsilon = Z^{-1} K_S^T \left(K_S Z^{-1} K_S^T\right)^{-1} \left(d\psi\Big|_s - L_S\, dm_i\right)$$

are formed numerically during the development of the first stage table. Dynamic pressure is tested at each integration step to detect the first decrease. A parabolic fit is then used to find q_{max} and the value is stored. Differences in the stored q_{max} values are divided by the kick angle and launch mass perturbations to determine the derivatives. Only two derivatives are required because q_{max} is not affected by later control changes.

Finally, a few comments are in order on the extension of the simple dynamic pressure constraint to a more advanced program where the magnitude of q_{max} is to be optimized automatically. Consider the constraint magnitude as a design variable just like thrust and propellant load.

$$\frac{\partial f}{\partial q_{max}} = \left.\frac{\partial f}{\partial q_{max}}\right|_J + \frac{\partial J}{\partial q_{max}} \left.\frac{\partial f}{\partial J}\right|_{q_{max}}$$

and

$$\frac{\partial W}{\partial q_{max}} = \frac{\partial f}{\partial q_{max}} + \frac{\partial J}{\partial q_{max}}$$

The derivative $\left.\frac{\partial f}{\partial q_{max}}\right|_J$ will be available in the trajectory routine just like the derivative with respect to any other constraint. The derivative $\left.\frac{\partial f}{\partial J}\right|_{q_{max}}$ is an exchange ratio that will also be available. Thus, if $\frac{\partial J}{\partial q_{max}}$ were known, all the elements necessary to include q_{max} as a design variable are known and the optimization could proceed. The new dynamic pressure constraint will leave us but one short step away from a fully-automated program that can be developed as soon as the required structural information $\left(\frac{\partial J}{\partial q_{max}}\right)$ is available.

Section 3.0

OPTIMIZATION STUDY RESULTS

When a new optimization program is developed, it is necessary to conduct preliminary studies of typical optimization problems to gain experience in the application of the new program and to identify areas where the techniques require further improvement. In particular, for this study we are interested in the application of the system optimization program to multiple-stage liquid launch vehicle problems. When the study was planned, it was decided that this experience could be developed by applying the system optimization program to a selected number of specific optimization problems. In addition to the objective of testing the program performance on this type of problem, the final results themselves were of interest, since they would help to develop a proper feel for the important parameters to be considered.

As the study progressed it developed that we were somewhat frustrated in our first objective because the program formulated specifically for this study proved ineffective for many of the optimization problems considered. Some solutions moved into regions for which the approximations incorporated in the high-speed trajectory optimization routine were inappropriate. When this was recognized early in the study, we decided to resort to a previous program formulation that included the full PRESTO trajectory optimization routine; and the majority of the results discussed in this section were developed with that program. For the future the PRESTO II routine still carries a strong potential for this type of problem, although some of the approximations must be modified and considerable experience must be developed with the application of the PRESTO II trajectory routine to trajectory optimization problems of the type that will be encountered during the system optimization process. Extensive experience of this type had already been

developed with the full PRESTO program prior to its application to this problem and it was therefore possible to successfully complete most of the optimization case matrix without further modification.

In the following sections the actual vehicle-mission matrix used during the optimization study is described. The results for each case in the matrix are discussed in detail and interpreted in terms of their implications for liquid launch system design problems.

3.1 Launch Vehicle-Mission Matrix

A matrix of ten launch vehicle mission combinations was run on the system optimization program to determine the combination of system controls that produced maximum payload for a fixed launch weight. The complete matrix is defined in Table 3-1.

Two low altitude circular orbit missions were selected to permit investigation of the relationships between the ascent gravity loss and the stage thrust levels or burn times. Coast periods were not used during ascent to orbit because we wished to maximize the influence of the mission requirements on the launch system characteristics. Experience has shown that system characteristics are not as sensitive to orbit altitude when coasts are permitted. Furthermore, the systems will optimize with high dynamic pressure, short burn time trajectories that are not consistent with the current weight equations. Launch was assumed to be at 90 degrees azimuth from the Atlantic Missile Range. Both two- and three-stage systems have been included to provide for the information on the relationships between velocity losses and vehicle characteristics. The vehicle parameters that vary between the cases in this matrix are the jettison weight constants and the propulsion system specific impulse. In the case of the three-stage systems, the vehicle parameter variables for the matrix have been restricted

MISSION-VEHICLE MATRIX FOR LIQUID LAUNCH VEHICLE OPTIMIZATION STUDY

Case No.	Circular Orbit Mission Altitude (nautical miles)	Vacuum Specific Impulse (seconds)			Jettison Weight Factors		
		Stage 1	Stage 2	Stage 3	Tanks	Thrust	Interstage
1	100	300	425	425	.05	.02	.008
2	400	300	425	425	.05	.02	.008
3	100	425	425	425	.05	.02	.008
4	400	425	425	425	.05	.02	.008
5	100	425	425	---	.05	.02	.008
6	400	425	425	---	.05	.02	.008
7	100	425	425	425	.075 Stg1 .05 Stg2 .05 Stg3	.02	.008
8	100	425	425	425	.05 Stg1 .05 Stg2 .075 Stg3	.02	.008
9	100	425	425	425	.05	.03 Stg1 .02 Stg2 .02 Stg3	.008
10	100	425	425	425	.05	.02 Stg1 .02 Stg2 .03 Stg3	.008

to the first and third stages. It is felt that these variables will demonstrate the extremes of the effects associated with these parameters. It is also interesting to investigate the influences of engine weights on the optimum thrust levels. The last two cases in the matrix are designed to demonstrate this, again for stages one and three.

The design parameters or system controls that are permitted to vary during the optimization process are the stage propellant loads and burn times. The propulsion units were assumed to deliver a constant vacuum specific impulse and the engine performance variation with altitude was determined for the following fixed nozzle expansion ratios that remained constant during the optimization process. Under these assumptions the

Stage	Nozzle Expansion Ratio - ϵ	
	$I_{sp_v} = 300$	$I_{sp_v} = 425$
1	8.6	34.2
2	-	34.2
3	-	34.2

optimization of propellant loads and burn times is equivalent to the optimization of propellant loads and thrust levels. This is evident from the propulsion equations defined in Section 2. For all cases the system sizing constraint was a launch weight of 650,000 lbs. When the study was initiated, no additional vehicle constraints were considered although in the process of determining solutions for the first few cases in the matrix some trends were encountered that forced us to impose a constraint on the minimum burn time that would be permitted during first stage operation.

3.2 Discussion of Results

In the following sections the evaluation techniques used to determine the validity of the results produced by the optimization program are described and a detailed discussion is presented of the optimization history for each case in the vehicle mission matrix described in the previous section. In addition, an interpretation of the trends indicated by the final results obtained for each case is included.

3.2.1 Evaluation Techniques

With any gradient process, it seems to be difficult to determine when the procedure has converged to an acceptable result. For the constraints this represents no particular problem because the constraint miss is easily computed and is output at each iteration of the gradient procedure. For the payoff the evaluation is extremely difficult and there are good reasons why convergence may not be achieved on a typical optimization run.

The difficulties normally are traceable to three problem areas. First, the relationship between the step size and the non-linearity of the problem is important. With the present formulation, for example, it is easy to enter a situation where the vehicle variables will oscillate during the optimization process. Second, the weighting factors or gains (η_1) used in the vehicle gradient loop must be in the correct ratio to avoid a situation where some variables creep and others oscillate. Finally, the trajectory optimization process itself must be carefully examined to assure that adequate convergence has been achieved in the trajectory and exchange ratio loop.

In many cases the evaluation is based on judgment and experience with similar problems. It has been possible, however, to develop several indicators that have proved helpful in evaluating results from the system optimization

program.

Five types of parameters are particularly useful and their elements have been output at each step of the system optimization process.

1. The changes in payoff (the payload gain asked, δf) and the constraint (the change in launch weight, δW) from the previous iteration.

2. The changes in the vehicle variables (the burn times, t, and the propellant loads, P) from the previous iteration.

3. The optimization derivatives, $\left.\frac{\partial f}{\partial X_i}\right|_W$

4. The gradient deterimant, D.

5. The angle (θ) between the constraint gradient and the payoff gradient vectors.

All of these variables approach zero as the vehicle optimization process proceeds. The manner in which this occurs provides the important feel necessary for a proper assessment of the convergence. The trajectory and exchange ratio loop may be assessed from the normal trajectory program output that is also available at each step of the vehicle optimization process.

The first two types of parameters listed above are rather obvious and are normally available in most gradient problems. The payload gain asked is computed in the vehicle optimization program from Eq. (2-9). This computation is designed to produce a constant step size rather than the usual increasing step size associated with a fixed δf. As the optimum is approached the δf would therefore be expected to approach zero and is in fact used to terminate the optimization sequence for most cases considered in this study. This type of termination was used when the δf became less than two pounds.

The optimization derivatives are computed by the system optimization program for output only and we think they are an important evaluation aid. These parameters are the derivatives of the payoff with respect to the system controls under the condition that the constraint remains fixed. A gradient formed from these derivatives would be the gradient of the payoff along a surface for a constant value of the constraint. At the optimum each of these derivatives must approach zero unless the corresponding system control is constrained for some reason.

The determinant, D, is computed in the process of determining the proportionality constants (K_f and K_w) of the vehicle gradient process. The nature of the gradient solution is such that a singularity is encountered at the optimum. Mathematically, this is evidenced by the determinant approaching zero and this characteristic can be used to identify the approach of convergence in the vehicle gradient loop.

At the optimum the angle, θ, between the payoff gradient and constraint gradient vectors must also approach zero. This may be deduced by reasoning that the constraint gradient vector is perpendicular to the surface along which the constraint is satisfied. At the optimum the payoff gradient vector must also be perpendicular to the surface along which the constraint is satisfied, since further motion on the constraint surface will produce no improvement in the payoff. This angle can be computed rather easily from the following expression:

$$\cos\theta = \frac{S_{FW}}{\sqrt{S_F\, S_W}}$$

where S_{FW} is the dot product of the two vectors and the square root is the product of their magnitudes.

Some comments are in order regarding the interpretation of these parameters. It is important to recognize that the magnitudes of each parameter are functions of the input gain constants, η_i, δf is also a

function of the input value of the sum of the squares of the system control changes (N) and they establish the step size. Thus, in assessing the validity of the convergence the important thing to examine is the change that occurred in these parameters during a run rather than their magnitudes at the completion of a run. Typically, one or more orders of magnitude reduction in each parameter is realized. Some assessment of the magnitudes of the optimization derivatives can be accomplished by comparing the changes occurring in the vehicle variables with those occurring in the derivatives. If small variable changes reverse the sign of a derivative or greatly influence its magnitude, proximity to the optimum is indicated. A slowly changing derivative with large parameter changes indicates convergence has not been realized. The linearity of the system can be assessed by comparing the requested δf with that actually achieved on a particular iteration. When the actual and realized values are similar and the gain is achieved with relatively small system control changes, the run is usually far from convergence. If the sign of cos θ oscillates between iterations but the magnitude of the angle is close to zero, the program is operating back and forth along the constraint surface near the maximum payload.

3.2.2 Vehicle Mission Matrix Case Histories

In this section the details of each launch vehicle optimization run in the ten-case vehicle mission matrix will be discussed. The results are summarized in Tables 3-2 thru 3-11. For the most part the cases were completed in the order described and it is evident from the number of iterations required that we benefited from the experience gained from the earlier cases.

Before entering the discussion for each case, it must be understood that the results shown represent output from two different optimization programs. One program contains only the PRESTO trajectory formulation which

formed the basis for most of the cases run. The other program contained the high-speed PRESTO II formulation which was used at the beginning of the study until difficulities were encountered with the trajectory program approximations. In addition, four different types of system optimization program terminations have been used: (1) number of iterations; (2) total run time; (3) total output page count; (4) minimum δf. Each of these terminations was encountered frequently during this study.

Case 1

The iteration sequence for Case 1 is presented in Table 3-2. Ten computer passes were required to complete this case. The first pass was made with the PRESTO II version of the program. It was terminated on the number of iterations and exhibited gross changes in the system characteristics from the original nominal estimates.

It is evident that the original combination of system controls used was far from the optimum since the program was able to gain approximately the amount of payload asked at each iteration. This process was still continuing when the run terminated after thirteen iterations.

When the PRESTO II formulation became operational we resumed the computation of this case and the next six iterations shown were computed with the high-speed program. The system optimization trend continued as the routine consistently removed propellant from the low specific impulse first stage and maintained the first stage thrust with corresponding reductions in the burn time. This second pass actually terminated through a failure of the trajectory optimization program to complete the trajectory for the seventh iteration. The reason was that the entire combination of system controls had become radical during the optimization process as the program attempted to eliminate the low specific impulse stage.

Since we were already violating the vacuum assumption for second stage used with PRESTO II, it was decided to stop the process, return to the

eighth iteration of the first pass where the environment at second stage ignition seemed compatible with the PRESTO II assumptions, and constrain the first stage burn time in an attempt to prevent atmospheric operation of the second stage. When this case was re-submitted we again experienced difficulty because the program still attempted to remove first stage propellant with the burn time constraint imposed, and the resulting rapid change in launch thrust to weight ratio upset the trajectory optimization loop to the degree that the trajectory program failed to optimize properly on the first iteration.

At this point we modified the program so that the time for launch kick-over was re-computed at the beginning of each iteration to maintain a constant velocity at kick-over. The run was again submitted and the program continued to remove propellant from stage 1.

The first stage propellant loading was then constrained to produce an initial launch thrust to weight ratio minimum of about 1.25 and the run was re-submitted with the PRESTO II formulation. This run failed to gain payload. We were now operating in a region where there was little feel for the PRESTO II behavior and the program no longer achieved successful optimization runs during the trajectory shaping loop.

Rather than experiment further with PRESTO II we resorted to a series of three runs with the original PRESTO formulation and continued to constrain the first stage burn time and propellant load. These cases produced what appear to be a satisfactory optimum which is shown at the bottom of the first page of Table 3-2. However the first stage propellant optimization derivatives now showed a positive sign which indicated that the constraint on first stage propellant loading should be released. This was exactly the reverse of the situation with the PRESTO II operation. The difference is a reflection of the absence of atmospheric effects to degrade the thrust and introduce drag in the second stage in the PRESTO II formulation. The first stage propellant constraint was therefore removed and the case was

Table B-2 Case 1

Altitude = 100 N.M.	Stage 1 Isp = 300 Tank factor = .05 Thrust factor = .02				Stage 2 Isp = 425.5 Tank factor = .05 Thrust factor = .02				Stage 3 Isp = 425.5 Tank factor = .05 Thrust factor = .02				Vehicle Data				Payload loss on unsuccessful iterations (Failure payload miss)
	Propellant		Burn Time		Propellant		Burn Time		Propellant		Burn Time						
Iteration No.	Loading	Optim. Deriv.	Time	Optim. Deriv.	Loading	Optim. Deriv.	Time	Optim. Deriv.	Loading	Optim. Deriv.	Time	Optim. Deriv.	Current Payload	Current Launch wt.	Payload Gain Added	Current Perform.	
Nominal	367170	.0061713	110.0	-114.33	135086	.026657	239.0	-11.96	56215	-.11569	398.0	-10.94	34538	650000	—	.0068913	
2	365519	.010430	105.9	-106.64	141603	.025521	222.9	-35.73	48312	-.02446	394.1	-8.55	36534	649841	2226	.0055509	
3	362147	.016014	101.2	-91.28	149327	.024425	207.1	-26.29	41263	-.04813	390.3	-6.47	38091	649858	1820	.0026027	
4	355128	.019273	95.8	-80.58	159126	.019768	191.7	-17.22	35918	-.01162	386.5	-4.52	39263	649713	1373	.0014402	
5	343597	.023042	89.5	-68.76	169839	.016251	178.0	-9.65	34190	.01632	382.9	-3.50	40157	650052	1015	.0010106	
6	327657	.019410	83.0	-73.26	180398	.012066	168.9	-7.07	37097	.01956	379.6	-3.37	40979	650128	839	.000966	
7	313261	.021021	75.8	-63.09	188468	.013666	162.0	-4.97	40678	.02146	376.3	-3.98	41761	650154	810	.000852	
8	296601	.020825	69.3	-54.02	198273	.014126	156.8	-4.18	41886	.01798	372.1	-3.90	42489	650141	754	.000719	
9	278596	.018984	63.1	-56.46	209412	.012161	152.0	-3.31	49180	.01779	367.7	-3.77	43175	650168	689	.000678	
10	261735	.021328	56.9	-41.01	219391	.011949	148.1	-2.16	53145	.01949	363.2	-3.97	43819	650243	662	.000591	
11	241382	.018642	51.2	-45.60	232679	.012377	145.4	-2.08	47836	.01551	358.1	-3.50	44419	650141	607	.000533	
12	222741	.017796	45.1	-43.26	244454	.011401	142.6	-.67	61805	.01481	353.3	-3.31	44785	650317	578	.000482	
13	203945	.020242	38.9	-21.76	256454	.014797	141.6	-.83	65837	.01598	348.5	-3.30	45514	650443	529	.000432	
Continue count of iterations using program with PRESTO II formulation																	
Nominal	201625	.215711	38.147	-77.83	254934	.036656	141.75	1.15	65620	.018997	348.54	-2.31	17115	647270	—	.00244	
2	177286	.050199	33.967	-62.07	271766	.040707	142.49	2.73	67955	.025285	347.01	-1.53	50786	650130	1232	.00264	
3	156517	.050902	30.128	-53.92	290010	.041238	144.22	5.02	70959	.027542	346.07	-1.16	52176	650260	1237	.00268	
4	133300	.038924	26.786	-63.28	308817	.028910	147.41	9.94	74259	.019208	345.34	-1.17	53439	650054	1243	.00189	
5	112650	.035588	22.049	-21.84	325080	.029970	155.02	3.48	77056	.015207	344.44	-1.02	54304	650341	1038	.00131	
6	89938	.022009	20.049	-89.19	346357	.009736	158.33	19.00	79796	.0048846	343.46	-1.04	55276	650001	819	.00193	
Second stage in atmosphere, re-input with first-stage burn time constrained to 69.26 sec. (see iteration 8 above)																	
Nominal	295806	.031291	69.26	—	197872	.034087	156.81	.455	91808	.024612	372.12	-3.84	44516	649936	—	.00107	
As above, but hold time re-calculated for each iteration to allow for rapidly lowering initial thrust-to-weight ratio																	
Nominal	295792	.031567	69.26	—	197861	.032851	156.81	-6.49	91806	.016617	372.12	-3.09	43828	650068	—	.00111	
2	271708	.029968	69.26	—	215484	.027171	150.85	-2.21	87678	.020161	369.28	-3.30	44613	649978	870	.000810	
3	247325	.023456	69.26	—	238514	.021082	149.17	-1.11	51759	.016380	365.73	-2.62	45349	650019	794	.000494	
4	222991	.024084	69.26	—	258471	.021733	146.95	2.88	56006	.0159496	362.11	-2.12	46047	650146	579	.000538	
5	198993	.011280	69.26	—	278095	.010644	150.74	4.98	60583	.0082031	359.31	-2.10	46573	647870	597	.000152	
Second stage in atmosphere, re-input to PRESTO II formulation with fixed time (69.26 sec) and fixed payload (215525 lb.) to get value of $\dot{h}$																	Val. of $\dot{h}$ 1.25
Nominal	215525	—	69.26	—	264112	.0001323	146.95	5.24	57472	.0045569	362.11	-2.08	46285	650167	—	.0000143	-622, -359, -141, -60, -28, -15, -35
As above, but re-input to PRESTO formulation with fixed launch hold time.																	
Nominal	215525	—	69.26	—	267032	.0016969	146.71	.936	57992	.017862	362.09	-2.80	42569	649988	—	.0000260	
2	215525	—	69.26	—	256674	.0082455	150.05	-12.18	68753	.015638	352.03	-3.27	42619	649843	223	.0000817	-69
3	215525	—	69.26	—	258103	.0008474	137.76	1.44	66078	.0057002	348.70	-3.06	42694	649937	201	.0000707	
4	215525	—	69.26	—	255322	.0038056	142.70	-5.52	69410	.0022828	338.09	-2.37	42712	649977	61	.0000194	
Continuation of above, due to above termination from excess stage count																	
Nominal	215525	—	69.26	—	255322	.0032859	142.70	-5.74	69410	.0069091	338.09	-2.56	42711	649978	—	.0000195	-12
2	215525	—	69.26	—	255897	.0010786	136.77	.93	68198	.0016113	335.43	-1.62	42732	649998	49	.0000165	
3	215525	—	69.26	—	255250	.0015130	140.06	-2.83	69172	.0013111	329.60	-1.39	42737	649997	14	.0000186	-5
Continuation of above, due to above termination from excess stage count																	
Nominal	215525	—	69.26	—	255515	.0013480	137.13	.24	68588	.0014922	328.14	-.95	42677	650079	—	.0000056	-3, -3

Table 3-1 (Cont'd) Case 1

Altitude = 100 N.M.

	Stage 1 (I_{sp} = 300, Tank factor=.05, Thrust factor=.02)				Stage 2 (I_{sp} = 425.5, Tank factor=.05, Thrust factor=.02)				Stage 3 (I_{sp} = 425.5, Tank factor=.05, Thrust factor=.02)				Vehicle Data				Payload loss on unsuccessful iterations		
	Propellant		Burn Time		Propellant		Burn Time		Propellant		Burn Time								
	Loading	Optim. Deriv.	Time	Optim. Deriv.	Loading	Optim. Deriv.	Time	Optim. Deriv.	Loading	Optim. Deriv.	Time	Optim. Deriv.	Current Payload	Current Launch Wt.	Payload Gain Asked	Current Deferral			
Recue at last series	with	first	stage	propellant	first	since	above	cases	showed	positive	stage	one step	Plant	Optimization	decrease				
Nominal	255525	.033002	69.26	—	255515	.030980	137.13	2.46	68588	.021030	328.14	-.82	42677	650029	—	.00105			
2	218459	.027979	69.26	—	252879	.027872	137.43	1.35	68109	.017247	328.04	-.86	42765	649989	98	.000671			
3	221451	.025751	69.26	—	250273	.023005	137.63	1.35	67623	.015535	327.91	-1.18	42839	649971	85	.000570			
4	229442	.019423	69.26	—	247661	.017355	137.81	-2.65	67149	.012626	327.72	-.83	42910	649992	78	.000328			
5	227436	.021820	69.26	—	245073	.019489	137.89	.58	66642	.013698	327.55	-1.02	42971	650004	59	.000411			
6	230424	.019460	69.26	—	242471	.011027	137.95	.19	66149	.008516	327.35	-.57	43026	649984	65	.000135			
7	233436	.015803	69.26	—	239924	.012423	138.01	-.33	65613	.008958	327.16	-.80	43074	650014	39	.000167			
8	236418	.013119	69.26	—	237333	.011838	137.91	.15	65108	.0081032	326.92	-.92	43118	650003	41	.000151			
Continuation of above set	with	which	was	stopped	due to	excess	slope	count											
Nominal	236418	.013080	69.26	—	237333	.011783	137.91	-.0055	65108	.0113128	326.92	-.77	43115	650008	—	.000149			
2	228401	.0058271	69.26	—	226956	.0053190	137.90	-.156	63130	.0035959	325.91	-.73	43256	649982	158	.0000305			
3	260315	.0004110	69.26	—	216620	.0005820	137.47	.575	61289	.0007579	323.91	-1.05	43307	649977	73	.00000207	-16		
4	261995	-.0023729	69.26	—	214462	.0027881	140.54	-2.52	62004	.0020231	318.29	-.73	43327	649986	10	.0000152	-4		
5	260221	.0015870	69.26	—	216367	.0015338	138.05	.0113	61628	.0006204[illegible]	317.57	.18	43313	649992	13	.0000229	-6, -1		

completed with two additional passes with the full PRESTO trajectory optimization routine.

Before leaving this case it is interesting to examine the situation at the point before the first stage burn time constraint was imposed. This corresponds to the sixth iteration shown for pass two. On this trajectory the maximum dynamic pressure encountered was 11,152 lbs/sq. ft at a flight time of approximately 102 seconds, well into stage 2 operations. Even at Stage 3 ignition the dynamic pressure was 250 lbs/sq ft. The velocity contribution from first stage under these conditions was 764 ft/sec and staging occurred subsonically at an altitude of 3,850 feet. Thus, although this case apparently produced the maximum payload, 55,276 pounds, it is obvious that the result is fictitious because the structural equations certainly do not reflect the environment actually experienced, and the second stage drag and thrust losses are not included.

Case 2

This case, summarized in Table 3-3, was started with approximately the same combination of launch system parameters that was used to start Case 1. The full PRESTO trajectory routine was used from the beginning because we anticipated from our experience with Case 1 that the optimization would tend to eliminate the low specific impulse first stage. By the end of the second pass it was apparent that we were again encountering a severe environment at second stage ignition and therefore the burn time constraint used on the previous case was imposed.

When the computation was resumed, oscillations were encountered in several of the system parameters and the run had to be re-submitted after the first pass with adjusted optimization gains to achieve satisfactory convergence. These last two passes have been selected to illustrate the convergence process. Figure 3-1 shows a summary of the history of the optimization derivatives for this case, beginning with the third pass.

Table 3-3 Case 2

Payload loss on unsuccessful iterations (Failure payload miss)

Altitude = 400 p.m.	Stage 1 Isp = 300 Tank factor = .05 Thrust factor = .02				Stage 2 Isp = 425.5 Tank factor = .05 Thrust factor = .02				Stage 3 Isp = 425.5 Tank factor = .05 Thrust factor = .02				Vehicle Data					
	Propellant		Burn Time		Propellant		Burn Time		Propellant		Burn Time							
Iteration No.	Loading	Optim. Deriv.	Time	Optim. Deriv.	Loading	Optim. Deriv.	Time	Optim. Deriv.	Loading	Optim. Deriv.	Time	Optim. Deriv.	Current Payload	Current Launch Wt.	Payload Gain Asked	Current Determ.		
Nominal	371312	.021470	109.95	-105.01	140130	.0063740	238.90	-33.148	55966	-.15007	398.03	16.655	24969	619999	2711	.00717		
2	376663	.012272	106.33	-90.101	141645	.0051882	227.46	-21.222	46081	-.073348	403.78	19.091	26926	619630	2317	.00347		
3	381283	.0064627	101.86	-73.770	143496	.0014205	216.92	-9.4170	37301	-.022345	413.26	21.334	28151	619689	1626	.00126		
4	381846	.0020067	95.784	-64.751	144390	.0011832	209.15	-4.2116	33845	.019117	430.86	21.188	29009	650016	984	.00103		
5	375670	-.0093058	90.134	-60.358	145136	.0088696	205.29	-8.7316	37252	-.0052873	450.56	18.594	29810	650055	872	.000929		
6	368952	.014970	84.323	-49.082	151030	.0085857	196.86	-5.5865	35725	.017582	468.52	18.727	30614	650093	826	.000854		
7	357526	.014255	79.348	-45.890	157039	.0133410	191.18	-9.3232	39078	.0040034	487.56	16.428	31378	650076	782	.000792		
Continuation of above series (Macro formulation, which was cut off for max. pages																		
Nominal	357526	.014702	79.348	-46.325	157039	.0132580	191.18	-9.2727	39078	.0038293	487.56	16.560	31326	650135	—	.000797		
2	346279	.016727	74.169	-40.365	166698	.011022	181.38	-6.3538	38309	.016072	505.07	16.157	32043	650115	750	.000736		
3	332442	.014473	70.025	-43.095	175106	.012660	174.36	-8.5424	41644	.0011751	523.26	14.672	32747	650095	717	.000689		
4	320080	.017347	65.101	-30.372	185155	.011164	164.56	-4.8819	41385	.015647	540.11	14.500	33398	650155	692	.000600		
5	304070	.015268	61.365	-30.206	195566	.014265	158.53	-6.9410	45021	-.0019895	558.05	12.077	34009	650069	638	.000518		
6	288983	.015265	57.347	-27.223	208823	.010487	149.25	-1.3724	44515	.014524	574.21	11.782	34556	650143	594	.000432		
7	272344	.012406	53.362	-30.158	219580	.012169	147.24	-4.7554	48545	.0066586	591.58	9.2007	35054	650069	534	.000378		
8	257958	.014271	48.619	-20.202	233072	.0072350	139.71	3.4343	46546	.018170	606.18	7.3833	35472	650220	500	.000356		
9	240736	.0108816	45.327	-23.354	243732	.013168	145.36	-6.6633	52184	.018198	621.63	6.0179	35821	619937	473	.000379		
													(Second stage in atmosphere)					
Continuation starting at #3 above except stg. 1 burn time fixed at 69.26 sec. (Macro formulation)																		
Nominal	332442	.014132	69.26	—	175106	.014279	174.36	-8.6088	41644	.0032918	523.26	14.512	32707	650444	—	.000495		
2	318166	.012150	69.26	—	188432	.0072152	162.74	-5.1807	41563	.0120179	542.89	14.143	33218	650041	568	.000378		
3	304285	.0074704	69.26	—	198306	.0070418	154.72	-6.5285	45067	.0069144	564.81	11.716	33674	649997	514	.000276		
4	294319	.0070004	69.26	—	209662	.0025495	142.87	2.1908	42697	.019085	586.10	11.627	33996	650017	440	.000253		
5	284479	.0010771	69.26	—	213009	.0067459	147.03	-2.3173	49529	.035494	606.23	6.5138	34160	649725	419	.000431		
6	285791	.0065379	69.26	—	219876	.0034884	133.47	11.391	39252	.043535	617.72	10.275	34197	649642	565	.000673		
7	280316	.0034756	69.26	—	217144	.0054962	146.75	-9.6188	49316	.010882	629.73	4.5238	34316	649527	705	.000493		
8	284016	.0045897	69.26	—	222452	.0056772	133.64	11.823	38779	.043856	636.90	9.1071	34337	649567	614	.000668		
9	280319	.0034955	69.26	—	217946	.0056807	147.16	-10.207	48451	.041993	646.58	3.6710	34320	649516	707	.000519		
Continuation of above but with new gains ($t_2 \times 4$, $P_3 \times 0.5$, $t_3 \times 5$)																		
Nominal	282168	.0010788	69.26	—	220199	.0021920	140.55	.58189	43615	.010776	660.00	4.5090	34597	649791	—	.000131		
2	280286	.0023791	69.26	—	224189	.0011882	134.49	5.5006	40877	.0060375	719.08	1.1239	34801	649935	317	.000151	-168.	-41
3	281300	.0005552	69.26	—	224690	.0019085	147.78	3.5580	40520	.022576	723.13	.61674	34837	650011	83	.000113	-4	
4	281160	.0006351	69.26	—	225150	.0011864	142.81	.66291	39754	.011351	724.51	1.1584	34850	650006	35	.0000340		
5	281498	.0004429	69.26	—	225770	.0009705	144.82	.23321	38910	.0099611	726.95	1.1511	34868	650001	16	.0000177		
6	281774	.0005088	69.26	—	226336	.0005969	145.65	.53512	38092	.0069260	734.08	1.1586	34880	649997	14	.0000134		
7	282135	.0011909	69.26	—	226755	.0018738	147.82	.29376	37454	.0056817	740.00	1.0243	34894	650002	12	.0000119		
8	281227	.0010801	69.26	—	228148	.0002320	146.55	1.3301	36856	.0020798	745.56	1.0222	34900	649998	11	.0000145		
9	281973	.0004976	69.26	—	227992	.0031132	151.74	-2.0111	36657	.0086555	750.59	.87216	34907	650006	13	.0000307	-1	
10	281961	.0004776	69.26	—	228063	.0004343	149.00	.028618	36373	.0023320	752.06	.70760	34915	650008	9	.0000398	-1	

Figure 3-1

OPTIMIZATION DERIVATIVES - Case 2

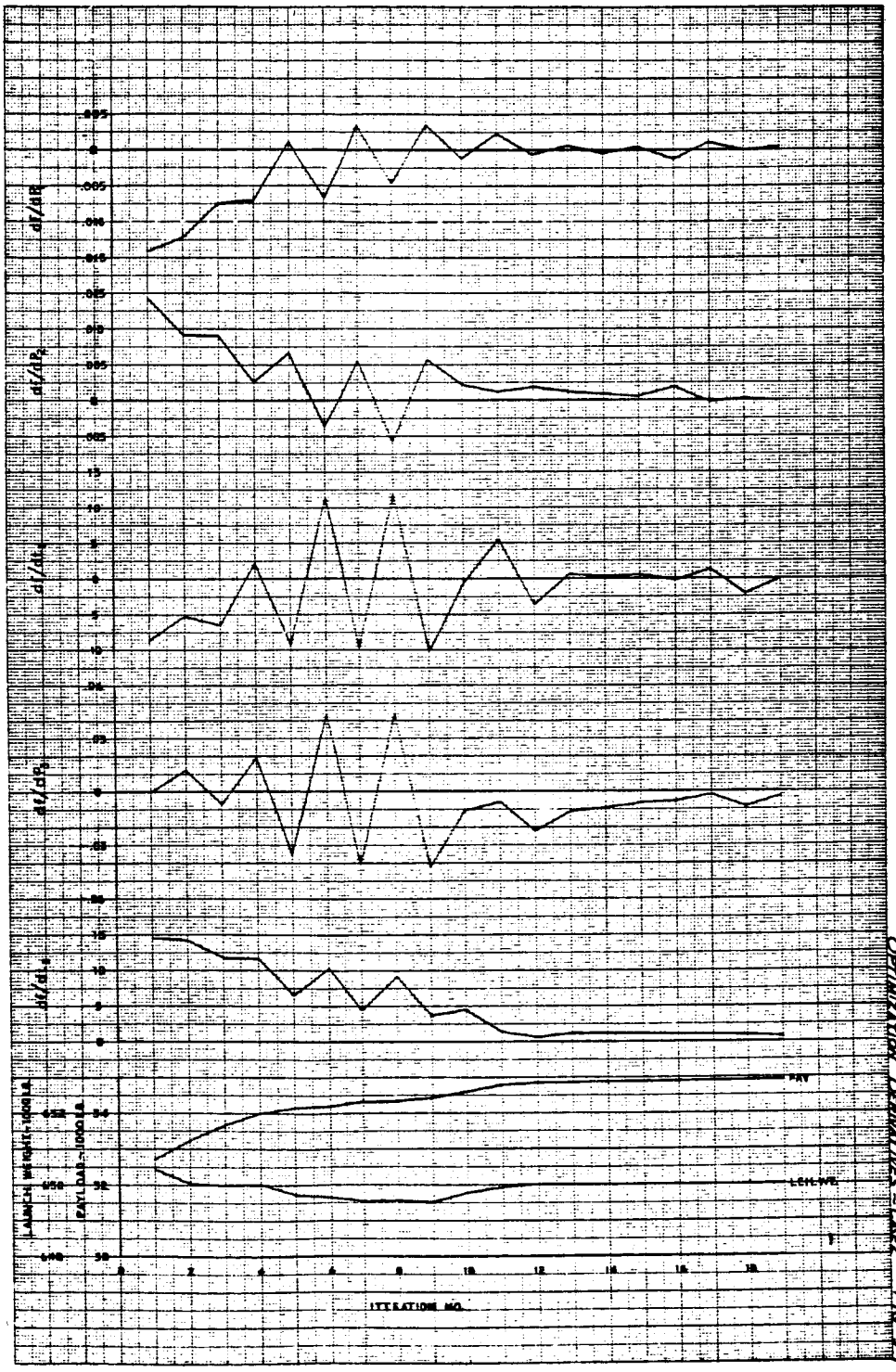

OPTIMIZATION DERIVATIVES - CASE 2

3-15

Recall that each of these derivatives approaches zero as the optimum combination of system parameters is approached. It is apparent that the gain change introduced half-way through the process considerably improved the situation and by the end of the run we had achieved at least an order of magnitude reduction in each of the optimization derivatives. The history of payload and launch weight during this process is shown in the lower curve of this figure.

Before the first stage burn time constraint was imposed, the optimization routine had reduced the first stage size to the point where the dynamic pressure at separation was 1670 lbs/sq ft. Separation was occurring at an altitude of 41,000 feet and a velocity of 2457 ft/sec. Both the first stage propellant load and burn time derivatives at these conditions indicated that the process would continue to reduce the staging velocity if the burn time constraint were not imposed.

Case 3

This case was started with the PRESTO II formulation because, with equal specific impulse for each stage, the vacuum trajectory approximations in the upper stages were expected to be adequate. The result shown in Table 3-4 from the first pass was deceiving. After a review of the evaluation criteria it was decided that the run had developed properly. Each of the optimization derivatives had reduced by close to an order of magnitude. The sensitivities of the derivatives to changes in the system parameters indicated that only minor parameter changes would drive the derivatives to zero.

It was when we later compared the optimum system parameters with the remaining cases that this result became suspicious. The run was later re-submitted with the full PRESTO formulation and new gains. On the second pass propellant was transferred from the first stage to the third stage and a substantial reduction in each of the stage burn times was introduced. None

Altitude = 100 n.m.

	Stage 1 Isp = 425.5 Tank factor = .05 Thrust factor = .02				Stage 2 Isp = 425.5 Tank factor = .05 Thrust factor = .02				Stage 3 Isp = 425.5 Tank factor = .05 Thrust factor = .02				Vehicle Data				Table 3-4 Case 3
	Propellant		Burn Time		Propellant		Burn Time		Propellant		Burn Time						Payload loss on unsuccessful iterations
Iteration No.	Loading	Optim. Deriv.	Time	Optim. Deriv.	Loading	Optim. Deriv.	Time	Optim. Deriv.	Loading	Optim. Deriv.	Time	Optim. Deriv.	Current Payload	Current Launch Wt.	Payload Gain Asked	Current Determ	(Failure payload miss)
Nominal	364167	.021984	110.04	-18.809	123644	.0002580	239.06	-29.295	45357	-.11081	398.01	-8.0946	53893	650064	1306	.00422	
2	371540	.012386	107.71	-28.945	123715	.0054576	225.07	-19.577	35277	.082862	394.14	-5.2107	55216	649672	1668	.00216	-
3	377628	.0055642	105.78	-13.045	126344	.0037146	211.96	-8.4227	24760	.040549	390.65	-1.2603	55937	649537	1225	.000484	-213
4	380549	.0013465	104.85	-6.6691	128239	.0000195	205.99	-1.9491	19338	.0044667	389.76	.14938	55981	649508	303	.0000146	-142, -37, -64, -36, -62
Continue with adaptive scheme but using program with PRESTO formulation and new gains ($t_1 \times 5$, $t_2 \times 4$, $P_3 \times 0.5$, $t_3 \times 5$)																	
Nominal	380818	.0023117	104.84	-1.6086	128350	.0021953	205.98	-2.0633	19349	.023897	389.76	-1.8932	55603	650000	—	.000123	
2	379687	.0035577	103.24	-.93607	127288	.0005975	200.22	-1.4189	20966	.023612	383.15	-1.8071	55656	650003	72	.0000962	
3	377714	.0030440	102.88	-1.8235	127254	.0001692	195.74	-1.5665	22771	.019164	376.01	-1.9921	55714	650002	63	.0000817	
4	375881	.0031219	102.11	-1.0299	127154	.0001054	190.38	-1.0750	24363	.019373	367.88	2.0495	55766	650006	58	.0000767	
5	373934	.0028833	101.66	.039482	127217	.0002469	186.57	-.92076	26025	.018168	358.40	-1.8888	55829	650015	56	.0000653	
6	371979	.0019883	101.64	-2.1997	127377	.0005956	183.04	-.88188	27714	.014644	349.34	-1.7804	55883	650028	51	.0000572	
7	370458	.0024720	100.49	.47916	126928	.0004407	179.22	-.42913	29253	.015116	339.68	-1.5773	55922	650008	45	.0000439	
8	368411	.0012643	100.27	-3.4591	127284	.0011636	177.21	.99174	30971	.011268	330.43	-1.5351	55968	650006	42	.0000417	
9	367326	.0025316	98.709	2.7203	126313	.0012448	172.44	.47194	32285	.014370	321.20	-.97417	55986	650009	41	.0000375	
10	365061	.0034959	100.42	-9.7408	127404	.0032804	174.84	-1.8586	34054	.0039372	315.01	-1.1925	56021	649907	39	.0000892	-18
11	365168	.0012505	98.436	-3.5005	126470	.0007347	171.78	-.50263	34211	.0086361	312.56	-.92080	56022	649976	31	.0000229	-.4
12	364810	.0015888	97.733	-1.6938	126263	.0000189	170.96	-.15387	34552	.0089906	310.68	-.68233	56023	649998	8	.0000145	
13	364238	.0016783	97.306	-.88842	126270	.0002776	170.65	-.22424	34995	.0088530	308.94	-.61190	56026	650001	6	.0000128	
14	363599	.0015864	97.067	-1.0961	126375	.0002522	170.16	-.31634	35462	.0079083	307.28	-.60837	56031	650001	6	.0000114	
15	362947	.0014897	96.756	-.58970	126475	.0003000	169.43	-.22655	35905	.0077269	305.52	-.50453	56035	650002	5	.0000957	

of the evaluation criterion indicated that this was possible after the first pass.

Case 4

The first three passes for this case, shown in Table 3-5, used the PRESTO II formulation. An examination of the PRESTO II trajectory output revealed that major trajectory control adjustments were being introduced on the final guided run. This indicated that the PRESTO II trajectory approximation was inadequate in the latter part of the ascent trajectory. Rather than experiment with the trajectory program inputs, we decided to proceed with the PRESTO formulation and three additional passes were completed. After the first pass an optimization gain change was introduced to reduce oscillations that were developing in some system controls. The last pass was initiated with a reduced step size because we were still experiencing difficulties with these oscillations.

Case 5

This case, shown in Table 3-6, was completed in a single pass on PRESTO II. The convergence was deemed satisfactory although the second stage burn time derivative indicates that there may be some room for payload improvement through a reduction in the second stage burn time.

Case 6

Results for this case are summarized in Table 3-7. The nominal system parameter combination is similar to that used for Case 5. When this case was started we had decided to continue with the full PRESTO trajectory optimization routine rather than experiment further with the PRESTO II routine.

On the first pass for Case 6 oscillations were encountered in both the first and second stage propellant loads. This is characteristic of a

Altitude = 400 n.m.

Iteration No.	Stage 1 Isp = 425.5 Tank factor = .05 Thrust factor = .02				Stage 2 Isp = 425.5 Tank factor = .05 Thrust factor = .02				Stage 3 Isp = 425.5 Tank factor = .05 Thrust factor = .02				Vehicle Data				Table 4-5 Case 4
	Propellant		Burn Time		Propellant		Burn Time		Propellant		Burn Time		Current Payload	Current Launch Wt.	Payload Gain Asked	Current Peterm	Payload loss on unsuccessful iterations (Failure payload miss)
	Loading	Optim. Deriv.	Time	Optim. Deriv.	Loading	Optim. Deriv.	Time	Optim. Deriv.	Loading	Optim. Deriv.	Time	Optim. Deriv.					
Nominal	365237	.059425	110.02	-68.134	224181	.039953	239.02	-9.8225	54847	.097588	397.99	19.483	41689	649998	—	.00493	
2	382614	.040404	107.09	-45.746	111840	.032538	234.78	1.0641	46829	.045019	406.41	20.819	43281	649818	1851	.00323	
3	400665	.017431	104.15	-14.586	96967	.018912	235.46	7.7791	41360	.0016516	419.81	20.503	44253	649819	1256	.000880	
4	413425	.005051O	102.65	-7.5278	83253	.0004314	243.45	2.6334	41050	.0014227	440.88	15.220	44715	649711	791	.000416	
5	419000	.002445	101.52	1.7325	83781	.0010866	247.10	8.7312	34204	.032325	463.71	12.140	45110	649922	555	.000469	-46
6	415870	.0021428	101.80	-.8998	83338	.0046088	252.57	.0025380	37796	.025000	473.86	12.847	45196	649656	341	.000345	
* 7	416177	.0031369	101.73	1.3960	86926	.0006917	252.57	1.6497	33924	.0140466	484.45	15.145	45413	650011	269	.000317	
9	415089	.0028569	101.70	1.5019	89727	.0028481	255.37	1.6906	32019	.0125034	507.25	15.004	45674	650018	248	.000428	
10	414057	.0003089	101.76	- - -	88984	.0017567	257.10	- - -	33756	.0066628	512.80	- - -	45701	649877	135	.000206	-0.3
Continue run-out of above with ASTO II formulation. Above job terminated by max. stages																	
Nominal	414057	.0003183O	101.76	-.68742	88984	.0018763	257.10	.45845	33756	.0066440	512.80	12.826	45578	649946	—	.000204	
2	413964	.0007809	101.72	-.16559	89703	.0012147	257.35	.86610	33088	.0013763	519.67	12.967	45652	649973	98	.000200	
3	413586	.0004402	101.71	.60363	90167	.0012781	257.81	.2968	32946	.0038743	526.70	12.721	45722	649983	93	.000194	
4	413421	.0002270	101.68	-.15271	90665	.0013610	257.98	.31449	32546	.0021685	533.67	12.584	45779	649982	92	.000188	
5	413061	.0004504	101.67	-.19881	91204	.0008228	258.15	.062279	32319	.0022162	540.71	12.605	45846	649975	91	.000188	
6	412893	.0003747	101.64	-.21136	91544	.0011857	258.12	-.20708	32087	.0025994	547.76	12.363	45900	649982	91	.000182	
7	412598	.0007597	101.63	-.28051	92061	.0012101	258.00	-.30298	31810	.0022719	554.78	12.249	45965	649991	89	.000178	
8	412289	.0000413	101.62	-1.1580	92551	.0007136	257.83	-.23582	31565	.0024028	561.80	12.853	46035	649963	88	.000196	
9	412315	.0004435	101.55	-.32182	92209	.0020674	257.64	-1.2686	31815	.0068448	568.84	11.877	46056	649957	94	.000180	
10	412159	.0017048	101.54	.60626	93047	.0014075	256.92	-.30953	31080	.0007238	575.63	12.082	46121	650015	91	.000174	
11	411939	.0024327	101.58	-2.9813	93620	.0007797	256.74	-.97119	31180	.0007578	582.65	12.448	46187	649945	85	.000185	
Continue run-out of above with ASTO II formulation. Above job terminated on max. stages in fact																	
Nominal	411459	.0021183	101.58	-3.1280	93620	.0005141	256.74	-1.3841	31180	.0026415	582.65	12.321	46181	649976	—	.000183	
2	412149	.0027547	101.23	2.1861	93232	.0027837	255.17	-.43582	30620	.0010143	596.59	11.900	46260	650032	183	.000175	
3	410968	.0010872	101.18	-3.3485	95427	.0008641	254.67	-2.1008	30841	.0089547	610.10	11.322	46376	649942	172	.000175	
4	410617	.0043113	101.09	-.47882	96216	.0035637	252.23	2.2409	28886	.031119	623.53	13.452	46551	650029	177	.000442	-491, -114, -123
5	410287	.0073683	101.10	6.5273	95984	.0008476	252.44	1.9120	29428	.028375	624.76	12.271	46860	649704	33	.000396	
* 8 From high sequence																	
Continue above series with new guess and with BKSTO accumulation ($t_2 \times 5$, $t_2 \times 4$, $P_3 \times 0.5$, $t_3 \times 5$)	411271	.0011209	101.84	1.6202	86562	.0051676	256.44	-1.2454	36123	.025341	497.05	11.862	45469	649794	239	.000317	
Nominal	410287	.0045369	101.10	-2.7914	95984	.0081724	252.44	-2.2286	29438	.039694	624.76	1.8335	46626	649772	—	.000752	
2	408649	.0070667	100.33	6.2701	99195	.0053081	231.92	-3.1386	27288	.012236	638.20	7.2725	46886	649917	378	.000401	
3	409915	.0041879	100.80	-2.6316	102024	.0041893	222.36	-4.6072	28194	.0033215	665.90	6.1597	47151	650014	267	.000342	
4	402136	.0059937	99.729	-1.8061	101420	.0035996	207.15	-2.4935	27878	.0079491	691.33	6.2496	47372	650019	241	.000282	
5	398672	.0042469	98.919	-1.2954	106686	.0044896	198.08	-3.4002	28580	.0070484	719.79	4.9302	47577	650007	218	.000220	
6	395581	.0049587	98.260	9.1398	109897	.0053678	189.03	-1.5022	27873	.011521	745.26	5.2313	47741	650016	193	.000247	
7	392154	.0014757	102.66	-6.1154	113515	.0029048	183.45	-3.7578	28964	.026587	770.79	3.1012	47839	649936	204	.000222	
8	393106	.0034792	99.559	6.6629	113737	.0010181	168.04	4.5854	26313	.032528	786.70	5.2114	47901	649963	200	.000404	
9	391246	.0015678	102.06	-4.6832	114283	.0023078	182.00	-5.0119	28717	.044424	806.56	1.5850	47950	649809	265	.000364	
10	392228	.0025546	100.20	5.5122	115610	.0052844	165.94	5.9360	25278	.035960	812.92	4.8226	47988	649859	265	.000437	
11	390976	.0020600	102.19	-4.5114	115379	.0021903	181.86	-4.9191	27836	.044818	830.59	1.2047	48023	649792	284	.000380	
12	392219	.0024623	100.94	5.7905	116619	.0009540	166.43	5.6578	24265	.038924	835.32	4.4895	48060	649845	272	.000457	

Table 3-5 (cont'd) Case 4

Altitude = 400 n.m.	Stage 1 I_{sp} = 425.5 Tank factor = .05 Thrust factor = .02				Stage 2 I_{sp} = 425.5 Tank factor = .05 Thrust factor = .02				Stage 3 I_{sp} = 425.5 Tank factor = .05 Thrust factor = .02				Vehicle Data				Payload loss on unsuccessful iterations
	Propellant		Burn Time		Propellant		Burn Time		Propellant		Burn Time						
	Loading	Optim. Deriv.	Time	Optim. Deriv.	Loading	Optim. Deriv.	Time	Optim. Deriv.	Loading	Optim. Deriv.	Time	Optim. Deriv.	Current Payload	Current Launch Wt.	Payload Gain Desired	Current Determ	
13	391050	.0013768	102.98	-4.2288	116186	.0019473	182.63	-4.8294	26972	.046829	851.42	1.0563	48081	649773	291	.000373	
14	392489	.0023787	100.82	5.6371	117310	.0013320	167.33	5.6996	23365	.040744	855.60	4.2213	48119	649845	271	.000460	
Continue above series with θ_1 changed ... ($\theta_2 \times 0.5$, $P_3 \times 0.5$)																	
Nominal	391770	.0000078716	101.65	.44494	116748	.0008946	174.98	-.16662	25169	.012108	854.00	2.1714	48126	649878	—	.0000361	
2	391822	.0006494	102.20	.79703	118333	.0005648	174.14	1.3054	23661	.002260	881.48	2.4396	48209	649991	89	.0000392	
3	392804	.0006382	103.16	-1.7146	117362	.0014605	180.47	-2.6529	23981	.010083	911.07	.71972	48244	649954	83	.000112	
4	393548	.0005092	101.89	4.2951	118808	.0005276	172.87	1.9065	21100	.032639	916.23	2.9589	48262	649898	143	.000169	
5	393193	.0019339	104.77	-5.0230	118415	.0003013	183.16	-2.8967	22977	.043239	933.51	.57488	48276	649858	179	.000141	
6	394952	.0014947	101.59	7.1694	118183	.0010738	175.76	3.8969	20256	.030117	937.18	2.7017	48308	649934	168	.000158	
7	393749	.0027382	105.87	-7.2145	119090	.0014826	185.17	-2.9927	22048	.044202	953.51	.39246	48312	649870	171	.000163	
8	396029	.0021206	101.63	8.1445	117917	.0018179	178.07	3.7526	19462	.031986	955.89	2.5627	48342	649952	179	.000171	
9	394365	.0030767	106.48	-7.8825	119379	.0017156	186.79	-2.9797	21293	.047691	970.74	.30907	48343	649873	176	.000187	
Restart above series with θ_1 & N halved																	
Nominal	391770	.0000078716	101.65	.44494	116748	.0008946	174.98	-.16662	25169	.012108	854.00	2.1714	48126	649878	—	.0000361	
2	391828	.0003535	101.92	.55847	117556	.0002099	174.56	.60642	24416	.0067583	867.74	2.3192	48173	649996	49	.0000347	
3	392170	.0004983	102.28	.14246	117743	.0004088	176.12	.220948	23986	.013187	882.70	1.8851	48211	649997	39	.0000304	
4	392641	.0004128	102.38	1.0402	118130	.0001281	176.06	.89544	23071	.0041785	875.68	2.1236	48242	649994	37	.0000295	
5	393039	.0007637	103.09	-.47182	118254	.0001566	178.57	.28443	22803	.015486	910.53	1.5375	48276	649994	36	.0000275	
6	393796	.0001370	102.76	2.0647	118411	.0001950	177.74	1.4249	21699	.0025545	921.65	2.0883	48303	649996	35	.0000326	
7	393923	.0011560	104.11	-1.7738	118581	.0001390	181.53	.89738	21867	.021472	935.53	1.1518	48325	649980	38	.0000374	-35
8	394417	.0004566	103.57	.72148	118524	.0000897	180.42	.48774	21211	.0055843	939.10	1.6700	48341	649992	21	.0000187	
9	394695	.0005576	103.88	.34237	118581	.0000811	181.27	.38626	20969	.0069625	946.43	1.6291	48354	649996	15	.0000185	

Altitude = 100 n.m.

Stage 1 I_{sp} = 425.5, Tank factor = .05, Thrust factor = .02

Stage 2 I_{sp} = 425.5, Tank factor = .05, Thrust factor = .02

Table 3-6 Case 5

Payload loss on unsuccessful iterations (Failure payload miss)

Iteration No.	Stage 1 Propellant Loading	Stage 1 Propellant Optim. Deriv.	Stage 1 Burn Time Time	Stage 1 Burn Time Optim. Deriv.	Stage 2 Propellant Loading	Stage 2 Propellant Optim. Deriv.	Stage 2 Burn Time Time	Stage 2 Burn Time Optim. Deriv.	Vehicle Data: Current Payload	Current Launch Wt.	Payload Gain Asked	Current Determ.
Nominal	427399	.0021995	128.40	16.559	109222	.0026611	350.00	-2.2629	54133	650299	—	.0000356
2	434255	.022437	120.16	12.795	100096	.023595	349.19	-1.7540	54190	650092	134	.0004100
3	412135	.018192	122.07	23.104	122863	.018158	349.06	-4.3362	54204	649951	525	.0003305
4	431832	.020523	118.19	14.021	101683	.020700	348.69	-1.7454	54262	649655	518	.0003342
5	421051	.0005813	119.27	-3.3430	113039	.0004507	348.62	-2.8449	54303	649603	263	.0000188
6	417200	.0012120	115.63	-.34949	116499	.0011849	347.06	-2.6021	54366	650089	54	.0000146

Payload loss on unsuccessful iterations (Failure payload miss)
-117, -26, -98, -104

Altitude = 400 N.M. | Stage 1 Isp = 425.5 Tank factor = .05 Thrust factor = .02 | Stage 2 Isp = 425.5 Tank factor = .05 Thrust factor = .02 | Vehicle Data | Table 3-7 Case 6

Payload loss on unsuccessful iterations (Failure payload miss)

Iteration No.	Stage 1 Propellant Loading	Stage 1 Propellant Optim. Deriv.	Stage 1 Burn Time	Stage 1 Burn Time Optim. Deriv.	Stage 2 Propellant Loading	Stage 2 Propellant Optim. Deriv.	Stage 2 Burn Time	Stage 2 Burn Time Optim. Deriv.	Current Payload	Current Launch Wt.	Payload Gain Assist	Current Determ.
Nominal	439192	.069444	128.28	-20.762	116921	.064576	357.51	74.675	32427	649998	—	.00328
2	459534	.0052388	127.25	5.0835	94255	.0053409	359.37	73.941	33379	649303	1611	.000303
3	465595	.012937	126.09	12.419	88441	.012777	365.15	71.180	33788	649937	524	.000391
4	453327	.027943	129.89	-4.1257	101009	.026919	370.63	68.552	34070	649723	554	.000749
5	471578	.031040	129.42	14.001	81643	.034239	374.21	67.553	34255	649399	781	.00107
6	451852	.031538	130.65	-7.9748	101962	.031232	377.19	65.093	34485	649280	744	.000707
Continue above	series	but hold	second-stage	propellant	gain							
Nominal	461760	.0023178	129.80	-.69873	91800	.0027030	385.00	62.606	35259	650159	—	.000172
2	463925	.0042840	129.66	1.2192	89575	.0038769	391.28	60.260	35637	649989	390	.000163
3	460031	.0065395	129.91	-1.0279	92813	.0069559	397.49	57.536	36010	649853	388	.000162
4	465222	.012463	129.08	2.7279	86959	.012093	403.46	56.112	36331	649742	387	.000190
5	455961	.017833	129.60	-1.9412	96329	.017655	408.84	52.819	36607	649847	421	.000233
6	467544	.022406	128.75	8.2791	83905	.022397	413.40	52.906	36827	649755	472	.000304
7	454314	.023209	130.00	-3.2928	97602	.022846	417.41	49.436	37027	649655	543	.000296
8	467692	.023131	128.73	7.8368	83340	.023132	421.20	50.132	37224	649674	542	.000303
9	454044	.024007	129.91	-9.2355	97530	.023609	425.01	46.688	37402	649633	547	.000299
10	467808	.023476	128.50	7.6973	82848	.023472	428.58	47.917	37579	649653	546	.000300
11	453878	.023701	129.67	-9.6834	97354	.023320	432.24	44.444	37743	649620	545	.000286
Continue above	series	but multiply	both burn-time	gains	by .5							
Nominal	460850	.0022459	129.00	-5.7824	70.00	.0041946	440.00	42.869	38175	650198	—	.000427
2	461845	.0062812	125.32	.86886	87579	.0052502	453.18	39.717	38741	650000	610	.000363
3	458365	.0060749	125.92	-5.8914	90845	.0083315	467.67	34.873	39270	649752	572	.000308
4	461781	.0096569	121.49	9.5905	85692	.011992	480.91	32.572	39702	649973	530	.000326
5	456301	.018204	128.52	-5.4529	92871	.022640	492.97	27.266	40027	649828	542	.000443
6	465168	.021178	118.84	14.080	81142	.025364	501.61	28.576	40230	649832	640	.000493
7	454904	.021824	127.25	-6.121	93553	.026318	510.24	23.158	40474	649726	673	.000471
8	465249	.021071	117.43	16.267	80310	.026083	517.36	25.104	40620	649774	669	.000492
9	455051	.023712	127.15	-7.053	93113	.028356	524.96	19.834	40813	649736	676	.000492
10	465997	.022660	116.99	17.439	79133	.028180	530.93	22.516	40912	649782	682	.000521
11	455228	.024514	127.13	-7.592	92583	.029266	537.55	17.316	41070	649702	698	.000498
12	466588	.022777	116.70	18.211	78235	.028604	542.73	20.166	41143	649717	689	.000519
13	455840	.025554	127.31	-8.232	91930	.030393	548.69	15.087	41275	649703	697	.000516
Continue above	series	but multiply	both burn-time	gains	by 2							
Nominal	461200	.0052447	122.00	2.2725	85080	.0043924	560.00	14.918	41563	650012	—	.000113
2	466613	.0014337	127.63	3.6485	80531	.0006533?	578.87	12.365	41833	649981	315	.0000808
3	464886	.0030465	116.93	12.097	79737	.010422	597.35	10.121	41990	650171	269	.000209
Continue above	series	but multiply	1st stage	burn-time	gain	by	0.3					
Nominal	464886	.0073156	116.93	12.078	79737	.0093929	597.35	10.033	41995	650172	—	.000114
2	461259	.012429	121.45	.89224	84521	.011989	603.65	7.7824	42074	650052	153	.0000802
3	468224	.0084253	121.85	5.1635	77186	.0091923	609.47	8.6071	42131	649915	130	.0000701
4	463042	.014792	124.31	3.8491	83170	.014485	616.35	6.0003	42181	649929	131	.0000955

-14

Altitude = 400 N.M.

	Stage 1 I_{sp}=425.5 Tank factor=.05 Thrust factor=.02				Stage 2 I_{sp}=425.5 Tank factor=.05 Thrust factor=.02				Vehicle Data				Table 3-7 Cont'd Case 6 Continued
	Propellant		Burn Time		Propellant		Burn Time						
	Loading	Optim. Deriv.	Time	Optim. Deriv.	Loading	Optim. Deriv.	Time	Optim. Deriv.	Current Payload	Current Launch Wt.	Payload Gain Assed	Current Determ.	Payload loss on unsuccessful iterations
5	470387	.012041	122.74	5.2417	75079	.012832	620.46	7.4711	42207	649891	151	.0000908	
6	463849	.014699	124.93	4.5853	82404	.015081	625.70	4.8308	42245	649896	150	.0000976	
7	471385	.013073	123.08	5.3327	74072	.013892	628.97	6.5438	42260	649882	155	.0000954	
8	464451	.015087	125.26	4.8929	81814	.015495	633.46	3.9040	42290	649884	154	.0000992	
9	472122	.014106	123.30	5.5507	73327	.014972	636.08	5.9113	42298	649875	157	.000104	
10	464933	.015390	125.48	6.0481	81331	.015805	639.97	3.1612	42322	649872	161	.000101	
11	472701	.014317	123.47	5.6497	72741	.015206	642.07	5.2260	42327	649871	159	.000103	
12	465383	.015590	125.69	5.1934	80896	.016015	645.52	2.5573	42346	649868	161	.000102	
13	473202	.014696	123.64	5.7059	72245	.015600	647.21	4.6767	42348	649867	160	.000105	
14	465761	.015878	125.86	5.3203	80527	.016309	650.27	1.9834	42364	649864	162	.000105	
15	473624	.014853	123.78	5.7934	71827	.015774	651.56	4.2711	42365	649864	163	.000106	
Continue above	series but halve 2nd stage propellant gain and double 2nd stage burn-time gain												
Nominal	469700	.0013119	124.82	3.0431	76177	.0010538	652.00	2.9807					
2	470944	.0051740	128.57	3.9186	75808	.0069926	664.32	1.4225	42391	649915	—	.0000949	
3	473067	.0035892	126.58	1.9979	73132	.0030268	666.75	1.9373	42426	649991	54	.0000139	-21
4	470984	.0022394	124.99	3.3891	74935	.0012160	671.89	.98853	42435	649992	30	.0000574	
5	472556	.0026016	128.26	1.6562	74054	.0031211	675.09	.69251	42444	649999	19	.0000389	
6	473636	.0020965	127.31	3.2378	72713	.0011328	676.91	.96956	42449	649996	16	.0000276	-4
7	472865	.0017865	125.69	.93684	73142	.0015238	678.04	.80018	42451	649999	7	.0000357	
8	471713	.0017489	124.87	.81745	74147	.0020285	680.40	.26162	42452	650005	7	.0000117	
									42453	650001	4	.0000949	-5

ridge-type situation where the quantities producing the major payload increases are the slowly increasing burn times. The second stage propellant load gain was reduced but the run continued to oscillate. Both burn time gains were then increased and we encountered an oscillation in the first stage burn time. Two more gain adjustments were required before satisfactory convergence was achieved. Notice that the total change in second stage burn time was about 320 seconds during the entire optimization sequence. This radical increase in burn time is consistent with the increase in mission altitude.

Case 7

Three passes with the full PRESTO trajectory optimization routine were required to complete this case which is summarized in Table 3-8. The nominal system characteristics used were similar to those determined by the first pass for Case 3 since it was not apparent that Case 3 had not properly converged at the time Case 7 was initiated. A large oscillation in the second stage burn time was encountered and the run was re-submitted with the burn time gain reduced. A second gain adjustment was required before the convergence was considered satisfactory.

Case 8

This case shown in Table 3-9, was also started with nominal system parameters close to those determined by the first pass in Case 3. Only two passes were required and no gain adjustments were considered necessary to achieve satisfactory convergence. The first pass terminated on maximum computer time and the case was simply resubmitted to complete the run.

Case 9

This case, shown in Table 3-10, was completed in two passes, again starting from nominal system characteristics corresponding to the first pass

Altitude = 100 N.M.

	Stage 1 (I_{sp}=425.5, Tank factor=.075, Thrust factor=.02)				Stage 2 (I_{sp}=425.6, Tank factor=.05, Thrust factor=.02)				Stage 3 (I_{sp}=426.5, Tank factor=.05, Thrust factor=.02)				Vehicle Data				Table 3-8 Case 7
	Propellant		Burn Time		Propellant		Burn Time		Propellant		Burn Time						Payload loss on unsuccessful iterations (Failure payload miss)
Iteration No.	Loading	Optim. Deriv.	Time	Optim. Deriv.	Loading	Optim. Deriv.	Time	Optim. Deriv.	Loading	Optim. Deriv.	Time	Optim. Deriv.	Current Payload	Current Launch Wt.	Payload Gain Asked	Current Returns	
Nominal	380589	-.021119	104.85	-3.1581	122500	.014170	196.80	1.0672	18455	.050810	372.00	.93144	53172	649613	—	.000564	
2	361400	-.010411	102.78	-2.7747	135567	.0060194	202.41	-6.0098	24945	.013619	365.86	-2.2607	53626	649773	642	.000328	
3	349179	-.0064592	95.272	-1.7395	142887	.0004072	160.92	9.5828	27233	.054237	346.33	-.36225	53760	650224	483	.000813	
4	344130	-.0044483	94.330	-15.268	143148	.0021337	203.25	11.185	33034	-.0034500	344.33	3.2154	53833	649720	704	.000849	
5	339529	-.0076578	86.179	15.018	144840	.0063580	154.94	10.433	32048	.050755	326.94	.016545	53889	650080	765	.00103	
Continue above series with gain on 2nd stage burn time halved																	
Nominal	341830	-.0076799	80.255	-.16933	143994	.0049134	179.10	1.7068	32541	.019580	335.64	-1.6414	54018	649886	—	.000101	
2	325361	-.0021894	89.989	-6.550	154861	.0094161	168.39	-.51091	38508	.0078092	309.87	-.19963	54147	649939	265	.000494	-390, -9
3	325898	-.0036205	85.329	.94948	152492	.0011236	168.02	.031926	38778	.015881	309.52	-.34770	54191	649985	142	.0000348	
4	323127	-.0024331	85.958	-7.493	153563	.0048993	168.11	-.6980	40855	.0054030	307.18	-.61406	54213	649981	39	.000215	-13
5	323087	-.0030299	83.628	1.5984	152626	.0017822	167.19	1.0592	40997	.011399	306.34	-.50058	54219	649996	47	.0000264	
6	321489	-.0008318	84.235	-2.902	153600	.0033606	165.55	.97388	41853	.0068250	304.25	-.18335	54228	649992	17	.000119	
Continue above series but halve 1st and 2nd burn-time gains																	
Nominal	321489	-.00020219	84.235	-2.445	153600	.0027868	165.55	.95522	41853	.0071330	304.25	-.37864	54225	649992	—	.0000607	
2	321562	-.0016522	82.667	5.5712	152603	.0002673	165.06	.62285	42205	.0086584	303.29	-.20519	54228	650004	25	.0000202	
3	320581	-.0024154	81.447	3.5039	152936	.0009154	164.96	.77959	42948	.0083619	302.38	-.31558	54229	650005	14	.0000138	
4	318850	-.0022029	80.785	-1.7960	153123	.0009008	163.63	.79965	43815	.0075554	300.69	-.22817	54233	650000	11	.0000108	
5	317068	-.0015784	80.248	3.9677	153890	.0003204	162.66	.84051	44702	.0060661	299.32	-.10729	54238	650001	10	.00000886	-2, -1, -.7

Table 3-9 Case 8

Altitude = 100 N.M.

Iteration No.	Stage 1 Isp = 425.5 Tank factor = .05 Thrust factor = .02 Propellant Loading	Propellant Optim. Deriv.	Burn Time	Burn Time Optim. Deriv.	Stage 2 Isp = 425.5 Tank factor = .05 Thrust factor = .02 Propellant Loading	Propellant Optim. Deriv.	Burn Time	Burn Time Optim. Deriv.	Stage 3 Isp = 425.5 Tank factor = .075 Thrust factor = .02 Propellant Loading	Propellant Optim. Deriv.	Burn Time	Burn Time Optim. Deriv.	Vehicle Data Current Payload	Current Launch Wt.	Payload Gain Assumed	Current Determ.	Payload loss on unsuccessful iterations (Failure payload miss)
Nominal	380819	.00011618	104.85	4.8701	128851	.00010866	205.98	1.9407	19349	.0019671	389.76	1.7534	55127	650020	—	.0000513	-383, +56
2	380707	.00270110	102.24	4.5182	127538	.0017941	197.61	1.3607	19144	.0114506	380.30	1.2201	55130	650000	46	.0000575	
3	378960	.00056489	104.52	5.8834	128808	.0018626	203.17	1.9335	20528	.0012291	379.07	1.7053	55157	649983	49	.0000578	-3
4	379166	.00092782	103.04	1.0148	128153	.00067138	199.23	.27435	20518	.0054551	369.73	1.2676	55162	649990	25	.0000142	
5	378502	.00105407	102.52	.72085	128107	.00023912	198.11	.21448	21061	.0053411	363.21	1.2539	55171	650001	13	.0000133	
Continuation of above series with no changes (above series stopped because of poor nominal trajectory for AREST)																	
Nominal	378502	.00112779	102.52	.11207	128107	.00025582	198.11	.26499	21061	.0058674	363.21	1.3420	55172	650003	—	.0000154	
2	377720	.00071978	102.47	.81168	128281	.00010186	197.07	.19602	21621	.0045309	356.60	1.1790	55181	649999	12	.0000114	
3	377140	.00083000	102.00	.18346	128200	.00007998	196.17	.11502	22125	.0050342	349.83	1.0035	55190	650001	11	.0000097	
4	376395	.00055953	101.89	.68411	128270	.00012163	195.58	.24896	22748	.0036441	343.41	.90115	55199	650001	10	.0000079	
5	375821	.00086691	101.40	.22062	128147	.00020181	194.13	.056530	23263	.0046392	336.84	.84216	55204	650001	8	.0000695	
6	374987	.00023866	101.56	1.3909	128352	.00048408	193.79	.39968	23923	.0026990	330.64	.78394	55212	649998	8	.0000657	-3, -.4, -1.7

Altitude = 100 n.m. | Stage 1 (I_{sp} = 425.5, Tank factor = .05, Thrust factor = .02) | Stage 2 (I_{sp} = 425.5, Tank factor = .05, Thrust factor = .02) | Stage 3 (I_{sp} = 425.5, Tank factor = .05, Thrust factor = .02) | Vehicle Data | Table 3-10 Case 9

Iteration No.	Propellant Loading	Propellant Optim. Deriv.	Burn Time	Burn Time Optim. Deriv.	Propellant Loading	Propellant Optim. Deriv.	Burn Time	Burn Time Optim. Deriv.	Propellant Loading	Propellant Optim. Deriv.	Burn Time	Burn Time Optim. Deriv.	Current Payload	Current Launch Wt.	Payload Gain Asked	Current Determ.	Payload loss on unsuccessful iterations (failure payload miss)
Nominal	380589	.026871	104.85	32.859	149050	.026469	191.10	2.8820	17827	.071854	360.00	.54268	51662	699674	—	.00195	
2	377355	.021483	107.72	19.836	122441	.019252	193.16	.71483	19080	.056839	359.51	.28859	51970	650021	308	.000988	
3	373562	.016335	110.17	7.4025	125819	.012483	193.94	.95703	20462	.043111	358.52	1.0175	52165	650011	197	.000435	
4	369261	.011281	111.54	6.3081	129119	.0099191	192.53	-1.9039	22038	.035348	356.60	.89108	52279	649986	132	.000305	
5	365121	.0080306	112.94	10.297	132252	.0078467	189.11	-2.2301	23580	.025989	354.37	-1.0059	52345	649961	112	.000193	
6	362010	.0086547	110.07	-5.3655	132995	.0035617	184.07	-1.4010	25005	.027393	351.53	-1.1641	52416	650027	92	.000153	
7	358183	.0079534	108.40	-4.4218	134585	.0034026	180.49	-1.2749	26697	.024955	347.89	-1.2286	52478	650004	76	.000128	
8	354350	.0065141	106.88	-7.6435	136256	.0015591	176.94	-1.0405	28384	.021915	343.60	-1.2052	52537	650006	71	.000118	
9	351106	.0071031	104.18	-2.2890	137046	.0035473	173.94	-.73376	29917	.021966	339.26	-1.1906	52583	650021	69	.0000948	
10	347100	.0051758	103.27	-3.2872	139077	.0023256	171.56	-.87082	31651	.018750	334.42	-1.0822	52636	650002	60	.0000729	
11	343397	.0049961	101.77	-2.3738	140602	.0019999	168.26	-.47211	33341	.017570	329.39	-.99298	52679	650011	54	.0000573	
12	339779	.0041690	100.55	-2.6029	142080	.0014434	166.28	.69363	35128	.014568	324.19	-.82938	52718	650006	47	.0000435	
13	336307	.0036106	99.019	-1.0904	143310	.0014800	162.94	-.13307	36833	.013966	318.77	-.65110	52749	650014	41	.0000326	
14	332803	.0028494	98.270	-1.9879	144778	.0010015	162.20	.92853	38738	.0095623	314.19	-.49962	52814	650041	34	.0000214	
15	329395	.0019265	97.017	-.057614	145992	.0006756?	155.80	1.2277	40339	.012009	309.88	-.095498	52823	650013	25	.0000265	-.2
16	328361	.0019841	97.039	-2.1050	146362	.0003839?	159.60	-1.3167	41244	.0055174	309.51	.37889	52831	649979	16	.0000174	
Continuation of Nominal	above series with one gains change ($t_2 \times 0.5$)																
	328361	.0019839	97.039	-2.1333	146362	.0004203?	159.60	-1.3021	41244	.0056391	309.51	.37058	52822	650007	—	.0000130	
2	326923	.0019658	95.884	.47278	146691	.0010763	156.72	-.17045	41851	.0077502	307.46	.19624	52827	650015	11	.00000962	
3	325172	.0010369	96.182	-2.9597	147671	.0004658	156.28	.55417	42821	.0047658	306.19	.18081	52828	649989	8	.00000955	
4	324256	.0019383	94.310	2.9027	147246	.0019508	154.85	.17989	43421	.0065961	305.02	.14411	52832	650030	11	.0000143	-4
5	323520	.0011555	95.061	.42363	147975	.0003779	154.66	.31927	43760	.0048253	304.64	.010245	52832	650005	5	.00000369	
6	322689	.0010251	94.896	.45450	148253	.0003849	153.99	.33013	44249	.0042913	304.69	.030773	52833	650001	3	.00000302	
7	321877	.0008560?	94.590	.76585	148502	.0001375?	153.23	.24416	44729	.0036670	304.52	.10371	52833	650001	3	.00000245	
8	321123	.0008846	94.111	.070402	148627	.0004520?	152.61	.22071	45185	.0033090	303.85	.067229	52834	650004	2	.00000186	

Table 3-11 Case 10

Payload loss on unsuccessful iterations (Failure payload miss)

.. Altitude = 100 n.mi.

Iteration No.	Stage 1 Propellant Loading	Stage 1 Propellant Optim. Deriv.	Stage 1 Burn Time (Iyy = 425.5, Tank factor = .05, Thrust factor = .02) Time	Stage 1 Burn Time Optim. Deriv.	Stage 2 Propellant Loading	Stage 2 Propellant Optim. Deriv.	Stage 2 Burn Time (Iyy = 425.5, Tank factor = .05, Thrust factor = .02) Time	Stage 2 Burn Time Optim. Deriv.	Stage 3 Propellant Loading	Stage 3 Propellant Optim. Deriv.	Stage 3 Burn Time (Iyy = 425.5, Tank factor = .05, Thrust factor = .02) Time	Stage 3 Burn Time Optim. Deriv.	Vehicle Data: Current Payload	Current Launch Wt.	Payload Gain Asked	Current Peteren.	Payload loss on unsuccessful iterations (Failure payload miss)
Nominal	380819	.00066568	102.85	-1.1631	128351	.0014630	205.99	-2.0336	19349	.013221	389.76	-1.3241	55391	650000	—	.0000305	
2	378266	.00415172	102.14	-1.0444	127722	.0053389	194.66	-1.9413	26484	.0096085	382.38	-2.5278	55430	649930	144	.0000681	-1
3	372918	.00233515	101.95	-1.0946	129596	.0008429	185.42	.030245	24743	.0080687	377.65	-1.3749	55490	649949	110	.0000101	
4	371823	.00098254	101.42	-2.3597	126788	.0016755	185.56	-3.2238	28540	.0065846	370.97	-2.0482	55504	649976	86	.0000248	
5	369732	.00024497	100.69	1.1801	130373	.0015094	175.56	2.5062	26560	.013501	369.62	-.88137	55512	649976	67	.0000303	
6	369269	.00010016	101.02	-3.9578	127461	.0008485	182.60	-3.3538	30230	.0091887	362.14	-1.8937	55525	649988	73	.0000294	-16
7	369381	.00054387	100.86	-.73883	128299	.0002498	177.82	-.43865	28962	.0018300	359.45	-1.3652	55539	649963	38	.0000301	
8	367728	.00022404	100.13	-1.3381	129059	.0004501	175.87	.044795	29753	.0011286	353.37	-1.0155	55552	650007	15	.0000172	-3
Continue above but increase Δt burn-time gains ($t_1 \times 5$, $t_2 \times 4$, $t_3 \times 5$)																	
Nominal	368182	.00071675	99.737	.11582	128144	.0005176	175.74	.23773	30075	.0012931	350.38	-1.0518	55551	650000	—	.0000746	
2	367463	.00013320	99.818	.80769	128653	.0003949	174.39	.39468	30253	.0029761	342.90	.69953	55561	650002	9	.0000519	-.1
3	367389	.00043814	99.478	.15476	128420	.0001420	175.73	.20295	30499	.0016364	339.92	.66834	55561	650000	4	.0000329	
4	367058	.00026396	99.396	.36515	128526	.0001532	174.86	.17551	30669	.0022698	336.33	.47558	55564	650001	3	.0000221	-.3

from Case 3. A gain change was then introduced to accelerate the optimization process because the routine seemed to be creeping through a series of successful iterations that were achieving payload gains approximately as requested.

Case 10

This case, shown in Table 3-11, was also initiated with nominal system parameters corresponding to those of Case 3. It was completed in two passes with the full PRESTO trajectory optimization routine. For the second pass the burn time gains were increased to speed up the convergence process, as the behavior seemed similar to that experienced on the first pass for Case 9.

3.2.3 Interpretation of Results

Two of the optimization indicators, the angle between the constraint and payoff gradients, θ and the Determinant, D, are shown in Table 3-12, where results from the nominal runs and the final optimized runs are compared. This table also includes the payloads for these cases and an additional parameter, the ideal velocity, that can be used to establish a feel for the relationship between the launch system characteristics and the trajectory.

For the first two cases it is evident that the trajectory and the system are closely related. The reduction in ideal velocity was near 2200 feet per second for Case 1 and almost 4000 feet per second for case 2. In Case 2 in particular the large velocity change was the result of a considerable extension in the total system burn time which permitted a more efficient ascent maneuver to the high altitude 400 nautical mile orbit.

Smaller velocity reductions are evident for Cases 5, 8 and 10. The large gain for Case 6 again was achieved through a major burn time increase

OPTIMIZATION INDICATORS

Case No.		Total Ideal Velocity ~ fps	Payload lb	Angle Between Constraint & Payoff Gradients ~ deg	Determinant
1	nominal	31,410	34,538	15.3	.006848
	final	29,240	43,313	1.6	.000002
2	nominal	35,010	24,969	39.3	.007170
	final	31,160	34,915	.9	.000004
3	nominal	29,255	53,893	16.4	.004220
	final	28,255	56,035	.8	.000009
4	nominal	32,230	41,689	23.3	.004930
	final	29,720	48,354	1.4	.000018
5	nominal	28,500	54,133	1.8	.000035
	final	28,330	54,366	.7	.000001
6	nominal	33,730	32,427	30.5	.003280
	final	30,570	42,453	.6	.000001
7	nominal	28,070	53,172	6.2	.000564
	final	28,280	54,238	.9	.000009
8	nominal	28,275	55,127	1.9	.000051
	final	28,230	55,212	.9	.000007
9	nominal	28,110	51,662	11.5	.001950
	final	28,420	52,834	.7	.000002
10	nominal	28,250	55,391	1.5	.000030
	final	28,240	55,564	.5	.000002

for the ascent to the high altitude orbit.

When jetison weight increases were introduced in Cases 7 and 9 the velocity losses in the optimum system were actually greater than those for the nominal. In these cases the solution tended to a less efficient trajectory in order to minimize the influence of the increased jettison weight.

Generally, however, these numbers indicate that it would be inappropriate to attempt to optimize a launch system with fixed ideal velocity requirements because the strong relationship between the system characteristics and the velocity losses is likely to overshadow many of the influences of the system optimization itself. Even for the optimum systems there is a considerable variation in total ideal velocity requirements although the major contributor to this appears to be the variation in first stage specific impulse. The variation in velocity requirements between the 100 nautical mile orbit cases is at least as great as that between 100 and 400 nautical mile missions.

The trajectory variables from the final shaped trajectories for each case are summarized in Table 3-13. It is interesting that the maximum dynamic pressure values encountered are significantly higher than those normally experienced by existing liquid propellant orbital launch vehicles. Current launch systems typically operate with peak dynamic pressure values ranging from 500 to 1000 lbs per square foot.

The first staging velocities for Cases 1 and 2 are extremely low even with the first stage burn time constrained to approximately 70 seconds. The staging dynamic pressure levels for these cases would be unacceptable for most liquid launch vehicle control systems although it is probably feasible to design control systems to accept this environment.

The increase in mission altitude between Cases 1 and 2 produced little effect on the atmospheric portion of the trajectory.

When the high specific impulse first stage was introduced in Cases 3 and 4 the staging environment for the optimum system was much more reasonable

SUMMARY OF TRAJECTORY CHARACTERISTICS

Case No.	Maximum Dynamic Pressure psf	Conditions at First Staging Point				Conditions at 2nd Staging Point		
		Altitude ft	Velocity ft/sec	Path Angle deg	Dyn.Press. psf	Altitude ft	Velocity ft/sec	Path Angle deg
1	1014	50,529	2,290	38.96	942	295,024	13,632	11.10
2	1168	59,067	2,801	38.82	925	526,524	16,888	21.38
3	1997	139,005	8,386	18.39	197	454,228	17,999	4.98
4	1915	182,885	9,844	21.38	53	820,619	20,466	12.27
5	1799	189,780	11,021	16.66	53	-	-	-
6	1617	354,340	14,178	29.96	0	-	-	-
7	2142	109,128	6,554	22.92	448	424,060	16,746	6.24
8	1950	146,173	8,919	17.08	166	465,726	19,713	3.85
9	1591	120,035	6,493	20.61	267	403,782	16,572	6.66
10	1959	140,797	8,556	17.47	190	448,719	18,733	4.68

Table 3-13

although the peak dynamic pressure values for these cases were nearly twice those for low specific impulse cases. These systems optimized at much higher launch thrust to weight ratios than those for Cases 1 and 2 and the first stage velocity addition became a significant portion of the total.

When the jettison weight increases were introduced in first stage in Cases 7 and 9 the first stage velocity contribution reduced substantially. Increasing atmospheric effects at the beginning of second stage were undoubtedly responsible for the increase in the ideal velocity requirements for these cases. When the third stage jetison weight was increased in Cases 8 and 10 only a minor increase in the first stage velocity contribution was evident. Most of the adjustment came through a substantial increase in the velocity contributed by the second stage for these cases and slight improvements were noted in the total ideal velocity requirements.

The system parameters and payloads determined for the optimized vehicles are summarized in Table 3-14. The mission altitude influence is apparent when cases 1 and 2 or cases 3 and 4 are compared. The primary effect of an increase in the mission altitude from 100 to 400 nm is a substantial increase in the burn time of the final stage. There is also a tendency to shift propellant from the upper stages to the first stage. Secondary influences are increases in the first stage thrust levels and second stage burn times. The large burn time increase helps to reduce the losses associated with a direct ascent to the 400 nm altitude. For a given stage the time can, of course, be extended by either reducing the thrust or increasing the amount of propellant. It is clear that the second alternative would not be as attractive because the launch weight is constrained. An increase in propellant in one stage therefore would mean a reduction in propellant in another stage and the net change in total burn time would be small. If the thrust is reduced to extend the burn time, it is also clear that this should occur in the upper stages where the flight path angles are lower and the rate of gravity loss is less. Even here the gravity loss may

SUMMARY OF RESULTS FROM OPTIMIZATION MATRIX

Case No.	Stage	Input Data: Mission Orbit Alt., ft.	Input Data: Vacuum Spec. Impulse, sec.	Input Data: Jettison Weight Factors: Tanks	Input Data: Jettison Weight Factors: Thrust	Input Data: Jettison Weight Factors: Inter-stg.	Results: Propellant lb	Results: Burn Time sec.	Results: Vacuum Thrust lb.	Results: Launch Weight lb.	Results: Payload Weight lb.*
1	1	100	300	.05	.02	.008	260221	69.26	1126656	649992	43313
	2	100	425				216367	138.05	666887		
	3		425				61628	317.57	82576		
2	1		300				281961	69.26	1220781	650008	34915
	2	400	425				228063	149.00	651285		
	3		425				36373	752.06	20580		
3	1		425				362947	96.755	1596182	650002	56035
	2	100	425				126475	169.43	317627		
	3		425				35905	305.52	50006		
4	1		425				394695	103.88	1616738	649996	48354
	2	400	425				118581	181.27	278352		
	3		425				20969	946.43	9428		
5	1	100	425				417200	115.63	1535271	650089	54366
	2		425				116499	347.06	142831		
6	1	400	425				471713	124.87	1607486	560001	42453
	2		425				74147	680.40	46371		
7	1		425	.075			317068	80.248	1681236	650001	54235
	2	100	425	.05			153890	162.66	402563		
	3		425	.05			44702	299.32	63548		
8	1		425	.05			374987	101.56	1571172	649998	55212
	2	100	425	.05			128352	193.79	281822		
	3		425	.075			23923	330.64	30787		
9	1		425	.05	.03		321123	94.111	1451917	650004	52834
	2	100	425	.05	.02		148627	152.61	414416		
	3		425	.05	.02		45185	303.85	63277		
10	1		425	.05	.02		367058	99.396	1571362	650001	55564
	2	100	425	.05	.02		128526	174.86	312753		
	3		425	.05	.03		30669	336.33	38802		

*Payloads are corrected to reflect value corresponding to 650,000 lbs. launch weight

Table 1

become excessive and propellant may therefore be moved to the lower stages. When the first stage burn time is constrained as in cases 1 and 2, this propellant shift must produce a thrust increase. Notice, however, that the thrust increase was also evident in case 4. The reason for this is not presently clear although the increase may be an attempt to reduce the gravity loss on a steepened first stage trajectory.

The influence of specific impulse in the first stage can be examined by comparing cases 1 and 3 or cases 2 and 4. The major changes associated with an increase in specific impulse are a shift in propellant to stage one and an increase in the stage one burn times. In fact when the first stage burn time constraint is not imposed on the low specific impulse stages the burn time is reduced until staging occurs well into the atmosphere. This, of course, violates the PRESTO II limitations. Even when the constraint was imposed on burn time the program removed propellant from first stage until staging was again occurring in the atmosphere and the launch thrust to weight ratio was extremely low. It was not until the complete PRESTO routine was used that the trend was reversed and more reasonable launch thrust to weight ratios were realized. If the burn time constraint were removed, it is likely that the program either would attempt to eliminate the first stage entirely or would require staging well into the atmosphere in a high dynamic pressure environment.

The comparison between cases 3 and 5 shows the influence of the number of stages. The major trends here are the increase in size of the first stage, the reduction in second stage thrust, and the reduction in total burn time for the vehicle. Notice that the payload of the two stage vehicle is only about 3% lower than that of the three stage vehicle. The compromise reached on the gravity loss is between the requirement for a reasonable thrust to weight ratio at the beginning of stage 2 and the proper burn time for direct ascent to 100 nm. Since the two stage system can have only one thrust level change, the second stage thrust to weight ratio is reduced but

the total burn time is also reduced.

The results from cases 7 thru 10 show the effect of changes in the inert weight factors. Case 3 will be used as the standard of comparison for each.

The increased first stage tank weight factor introduced in Case 7 reduced the optimum propellant loading and burn time for first stage. The propellant was moved to the upper stages to maintain the fixed launch weight constraint and a slight reduction in total burn time was experienced. Apparently the larger upper stages require a different gravity loss compromise that produces higher thrust levels and a shortening of the overall burn time. The net payload loss from case 3 is 1800 lb. which compares with an expected loss of nearly 2200 lb. for no reoptimization (the 2200 lb. estimate is derived from a procedure that uses the exchange ratio for first stage inert weight and the launch weight correction derivative).

Case 8 shows the influence of the third stage tank weight slope. A large reduction in third stage propellant load and a slight reduction in T/W accompanied this change. For the same reason as Case 7, the opposite trend (an increase) in total burn time is evident. The net payload loss is 823 lb. compared with an estimate of approximately 900 lb. for no reoptimization.

Cases 9 and 10 show the influence of the propulsion system weights. An increase in the first stage propulsion weight factor produced a reduction in both loading and burn time in Case 9. As expected, these changes also reduced the optimum thrust. Again, the associated increase in upper stage sizes resulted in a slight decrease in total burn time. In Case 9, the payload loss was 3201 lb. compared with 3810 lb expected without reoptimization. In Case 10, the third stage loading and thrust were significantly reduced by the increased propulsion weight factor. The total burn time increase with reduced upper stage size is again evident. The payload loss was 471 lb. compared with about 500 lb. expected without reoptimization.

Section 4.0
CONVERGENCE STUDY

The system optimization procedure discussed in the previous sections frequently encounters difficulty when there are strong interrelationships between the various system controls considered. These problems are readily apparent from the results presented in the previous sections and similar behavior was evident when the techniques were applied to optimization problems for large solid propellant boosters. The symptom is usually oscillation in some system controls while others slowly creep towards the optimum values.

Potentially, many different techniques are available which offer the possibility of resolving some of these difficulties. However, with the full optimization problem it becomes an expensive procedure to test the validity of the various schemes that might be used.

In this section an approach is developed for a simplified optimization program that can simulate the gradient process economically. Model problems are designed to present typical situations that produce problems similar to those encountered with the full vehicle optimization routine. A variety of modifications to the basic vehicle optimization routine are explored and tested on the simple program to compare the behavior with the original routine. Finally, a brief systematic gains study is described and one of the routines tested on the simplified program is demonstrated on the full system optimization program.

4.1 Simplified Hill Climber Routine

The process normally used by the launch system optimization program to define the payload and launch weight and the derivatives of those parameters

with respect to the system controls has been simulated with a simple analytical model. The optimization problem is reduced to one involving two control variables so that the payoff function may be conveniently represented as a hill that is readily described by a series of contour lines on a two-dimensional plot. The hill is defined analytically so that the payoff and its derivatives can rapidly be determined as a function of the two controls. This formulation presents a simple problem with more than one degree of optimization freedom; that is, two controls and one payoff. An additional model has been defined through the introduction of a second payoff quantity to represent a constraint. This model presents a problem with one degree of optimization freedom; that is, two controls, one payoff, one constraint.

The original plan was to permit arbitrary fourth order polynomial representations of the payoff and constraint surfaces. The hills were to be defined through an input grid of payoff and constraint values. A least squares fit was then to be designed to define the coefficients of the fourth order polynomial that most nearly approximated the payoff and constraint hill shapes desired. An automatic contour routine was to be added to prepare contour derivatives of the hills so that their shape could be verified before problems were run.

In practice, it was determined that it was possible to simulate the convergence difficulties associated with the system optimization program without resorting to complicated hill shapes. Simple second order hills of the correct proportion proved adequate. Consequently, the fourth order polynomial and least squares fit routines were developed but were not used for the problems considered. These routines will be available for future studies should the need arise. The automatic contour routine development was not completed and additional work would be required to bring this routine to operational status.

A family of elliptic paraboloids was selected for the payoff hill shapes for the convergence studies to take advantage of their simple analytic formulations. Three aspect ratios, 1:1, 2:1 and 5:1, have been used to demonstrate the variation in behavior of various optimization procedures with changes in the symmetry of the payoff hill. The 5:1 paraboloids are sufficiently extended to produce typical ridge behavior with the normal gradient routine that is used in the optimization program. On this type of elongated hill the path tends to oscillate back and forth across the ridge while creeping towards the top of the hill. This characteristic proved to be a vexing problem that has yet to be consistently solved.

The paraboloid shape was also used as a constraint for problems where both a payoff and constraint were considered. The 1:1 aspect ratio was used for most constraint situations; however, isolated cases were run with a 5:1 aspect ratio on the constraint hill. It was important to keep the constraint non linear because the gradient procedure can follow any surface with a constant slope exactly and such motion would appear as a straight line on a simplified model.

In the following sections the linear optimization routine, automatic gain selection routines and some non-linear techniques are demonstrated first for payoff only problems. The behavior of some of the routines is also shown for the more difficult payoff hills with a constraint imposed.

4.1.1 Linear Optimization Routine

The operation of the standard linear optimization routine on the 1:1 aspect ratio paraboloid is shown in Figure 4-1. This case is included to demonstrate the behavior of the step size selection procedure since the routine naturally follows a constant direction ascent on this hill. The process begins at point 1 in the figure and proceeds with a succession of payoff improvements at constant step size to point 4. Since the optimum

FIG 4-1

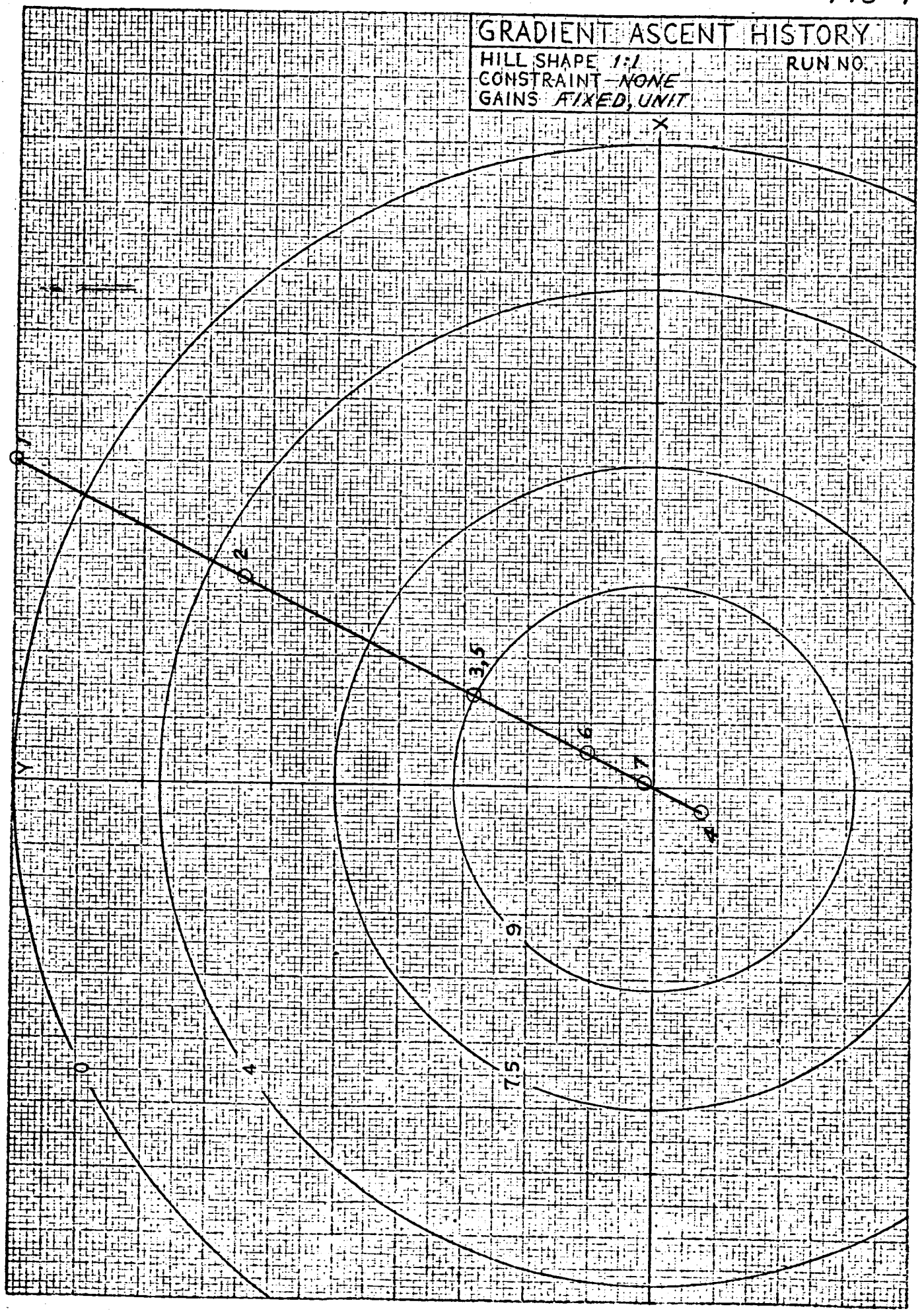

has been passed at this point the direction reverses and the routine experiences a succession of payoff losses beginning with point 5. After each loss the step size is halved by halving the parameter N used in the equation for payoff improvements. The process was terminated at point 7.

Figure 4-2 shows the behavior of the linear routine on the 2:1 aspect ratio paraboloid. Again the constant step size operation is evident until the path recrosses the ridge at point 5. Here the halving process begins and a minor oscillation develops before the calculation approaches the optimum at point 12.

When the same routine is operated on the 5:1 paraboloid the situation deteriorates markedly as shown in Figure 4-3. On this path we were fortunate in experiencing a failure at point 7 and the halving process resulted in a position almost exactly on the ridge at point 8. This good fortune was not sufficient, however, to prevent the oscillation from resuming and the routine continued to oscillate until the run was terminated still some distance from the optimum. Figures 4-4 and 4-5 show that the same oscillatory situation develops regardless of the starting condition used.

The orientation of the hill with respect to the control axes has little effect on the behavior of the linear optimization routine. Figure 4-6 shows that the behavior of the routine is essentially the same on the 5:1 paraboloid when the direction of the elongated axis is skewed at an angle of 45 degrees to each control axis.

Having established as a reference the behavior of a routine identical to that used for the full optimization program we will now proceed with the investigation of modifications designed to circumvent the problems demonstrated in this section.

4.P.2 Optimization Gain Section

Since our experience with the more general system optimization problem

Figure 4-2

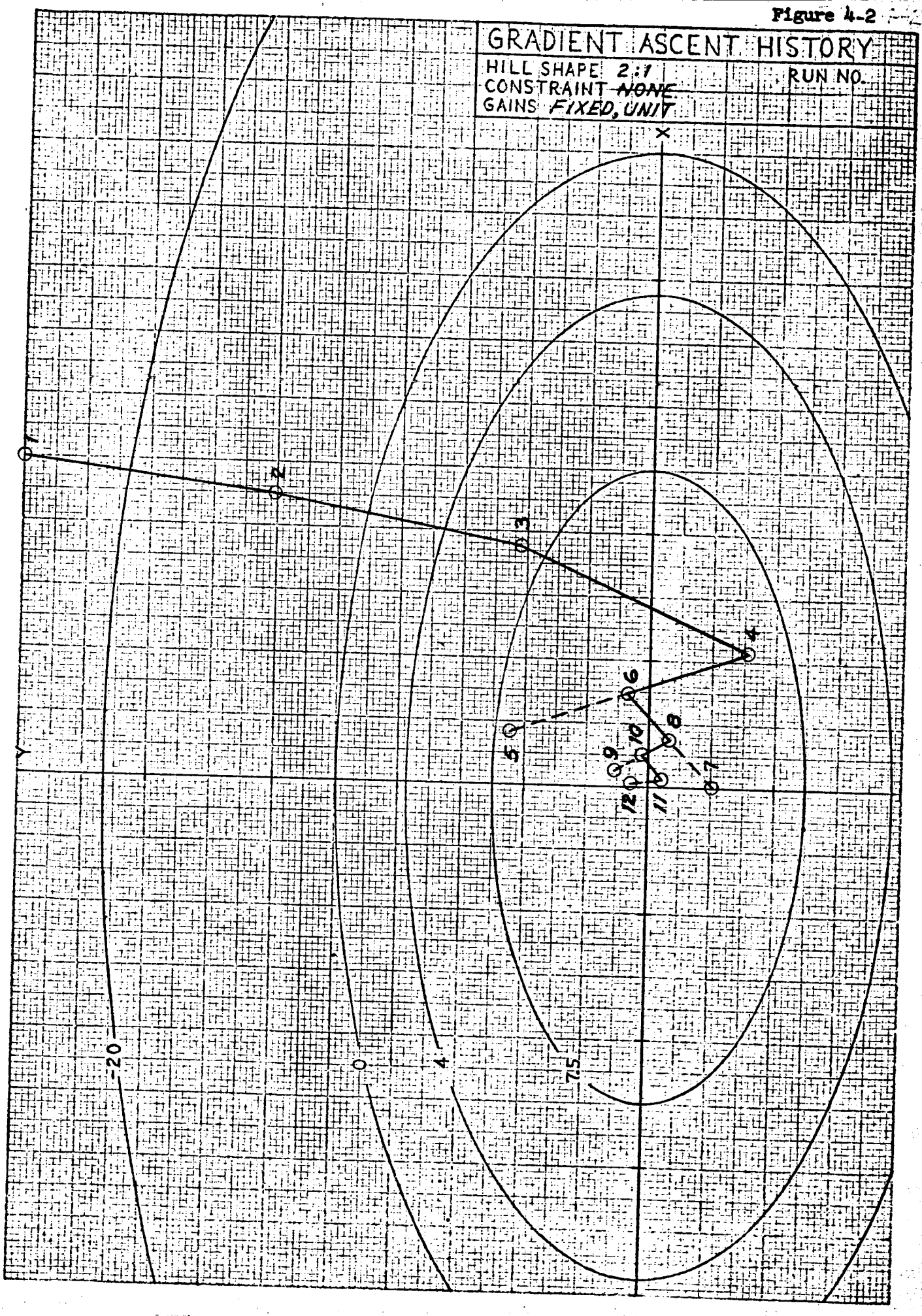
GRADIENT ASCENT HISTORY
HILL SHAPE 2:1
CONSTRAINT NONE
GAINS FIXED, UNIT
RUN NO.
X
Y
1
2
3
4
5
6
7
8
9
10
11
12
-20
0
4
75

Figure 4-3

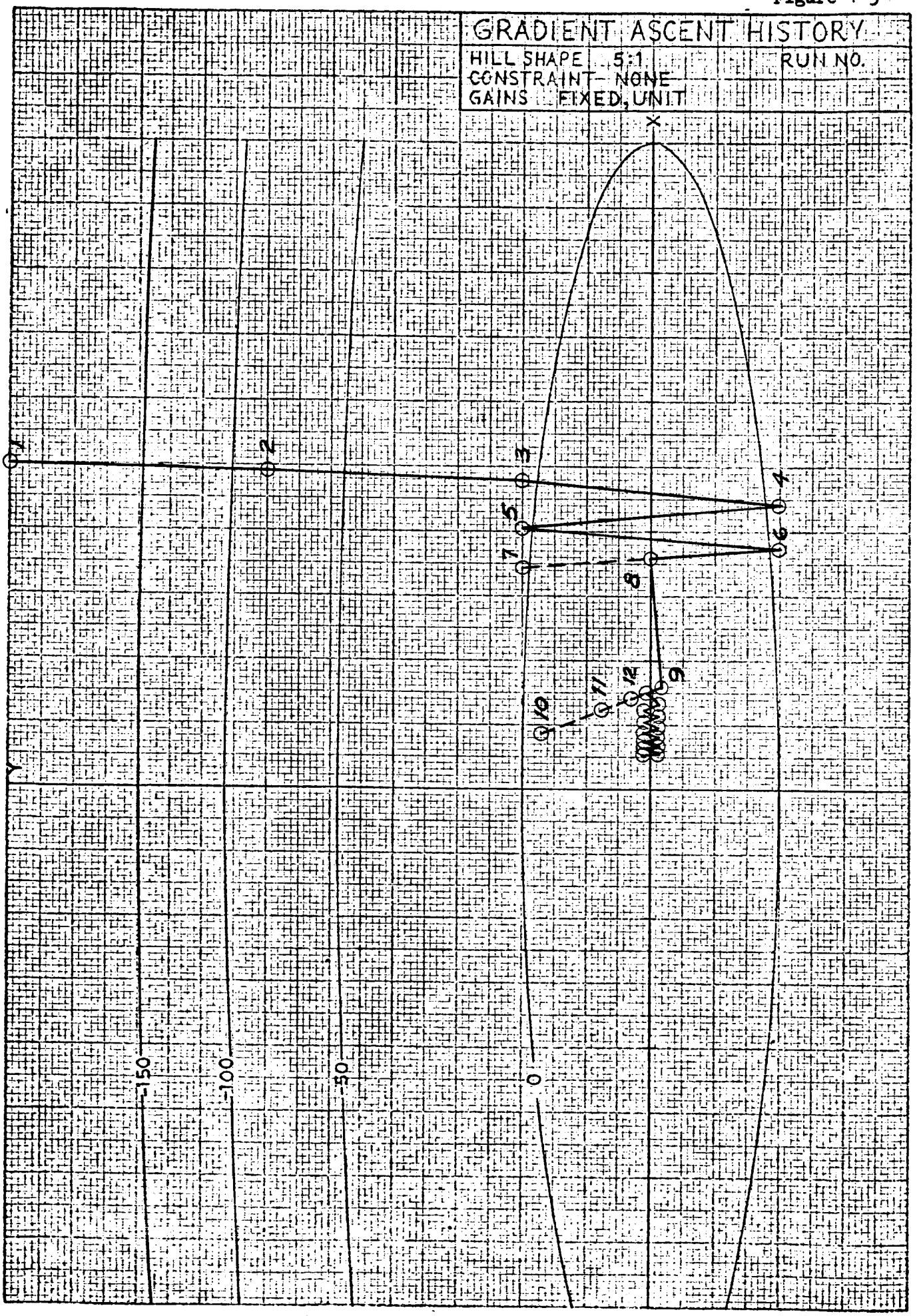

Figure 4-4

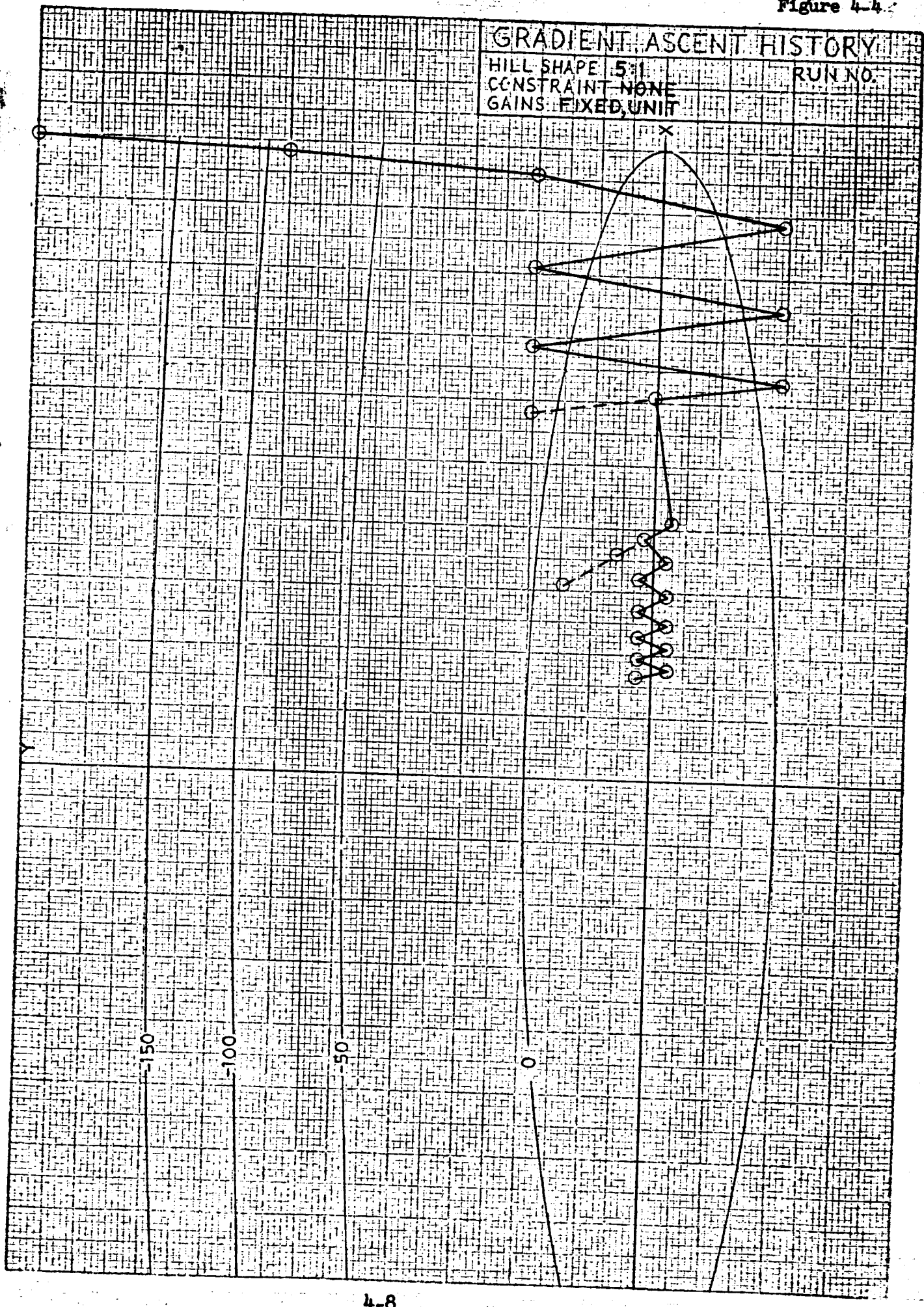

Figure 4-5

Figure 4-6

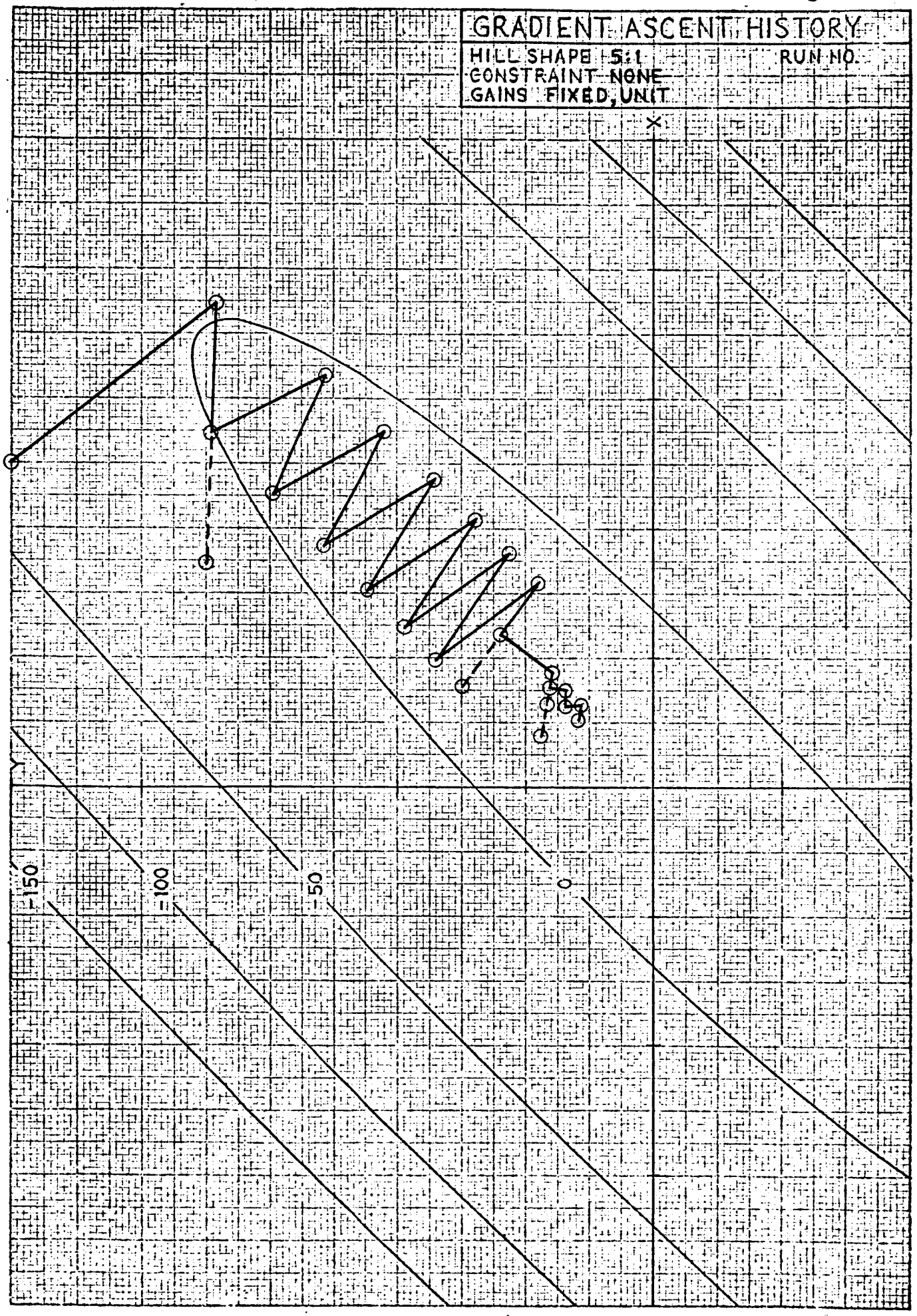
GRADIENT ASCENT HISTORY
HILL SHAPE 5:1
CONSTRAINT NONE
GAINS FIXED, UNIT
RUN NO.
X
Y
-150
-100
-50
0

developed some feel for the influence of the optimization gain constants (η_i), it was natural to investigate improved convergence routines that automatically adjust those constants during the run. Two automatic gain selection techniques were evaluated with the simplified hill climber routine. Both techniques used the history of the payoff derivatives to determine the gains for the next step. Figure 4-7 shows the logic for these two approaches. It is evident that the only difference between the two techniques is that the second technique modifies the gains on both failures and successes, whereas the first technique continues with the same gains following a failure. Both routines halve the step size using the parameter, N, which represents the square root of the sum of the squares of the control changes.

The behavior of the Mod 1 gain selection routine on the 5:1 paraboloid is shown in Figure 4-8. This concept proved extremely effective with this type of payoff hill, reaching the cutoff condition at the maximum value of the payoff parameter in ten steps. Recall that the standard optimization routine discussed above required a large number of steps, exhibited a creeping oscillation, and did not reach the optimum before the run was terminated.

Tracing the operation of the gain selection procedure, at point 2 in Figure 4-8, both gains were doubled. At point 3 the X control gain was doubled and at point 7 the X gain was again doubled and the Y gain was halved. The X gain was doubled for a third time at point 8 and the Y gain was halved at point 9. At points 4, 5, and 6 and at point 10 the gains remained fixed but the step size was halved.

The behavior of the Mod 1 routine on this same hill with a different starting condition is shown in Figure 4-9. Again the routine is successful in moving to the optimum in less than ten steps.

After examining the results achieved with this gain selection technique, we decided to extend the same gain selection procedure to the failure loop

GAIN SELECTION LOGIC

Mod 1 Gain Selection Logic

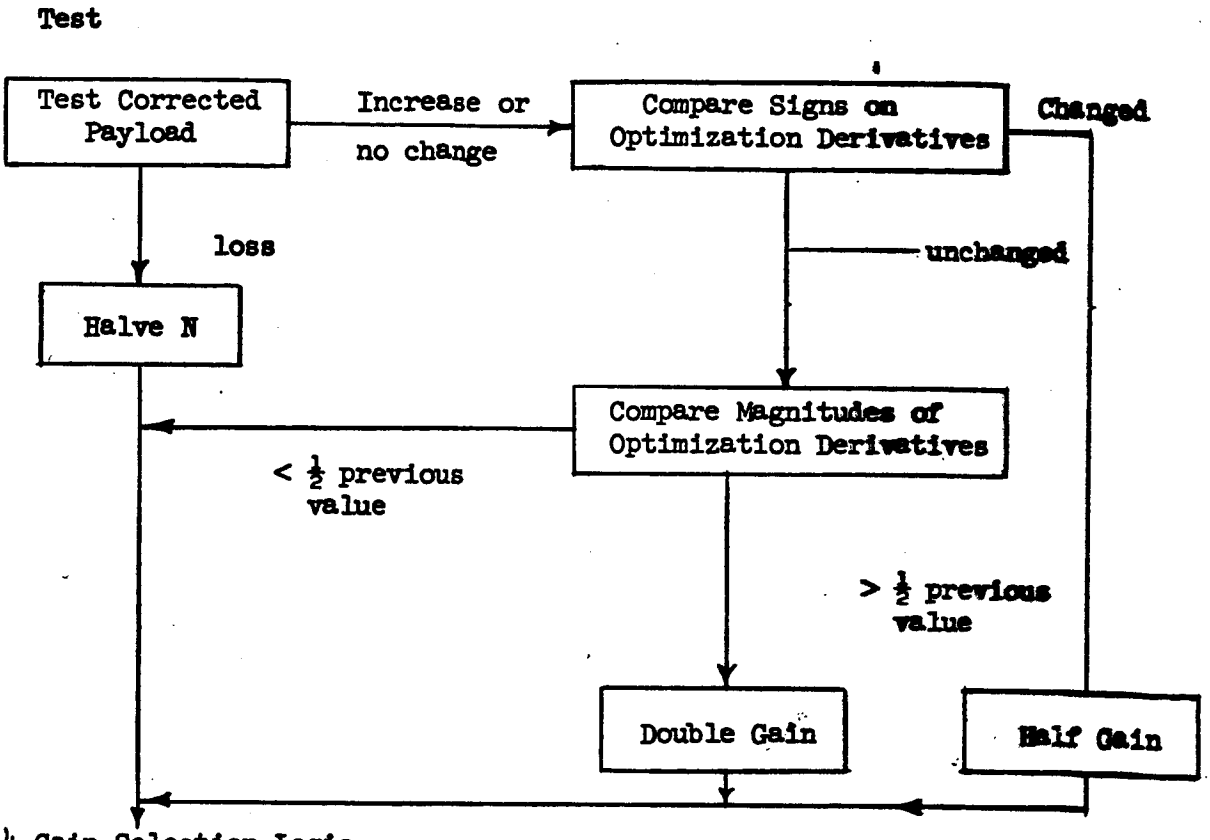

Mod 4 Gain Selection Logic

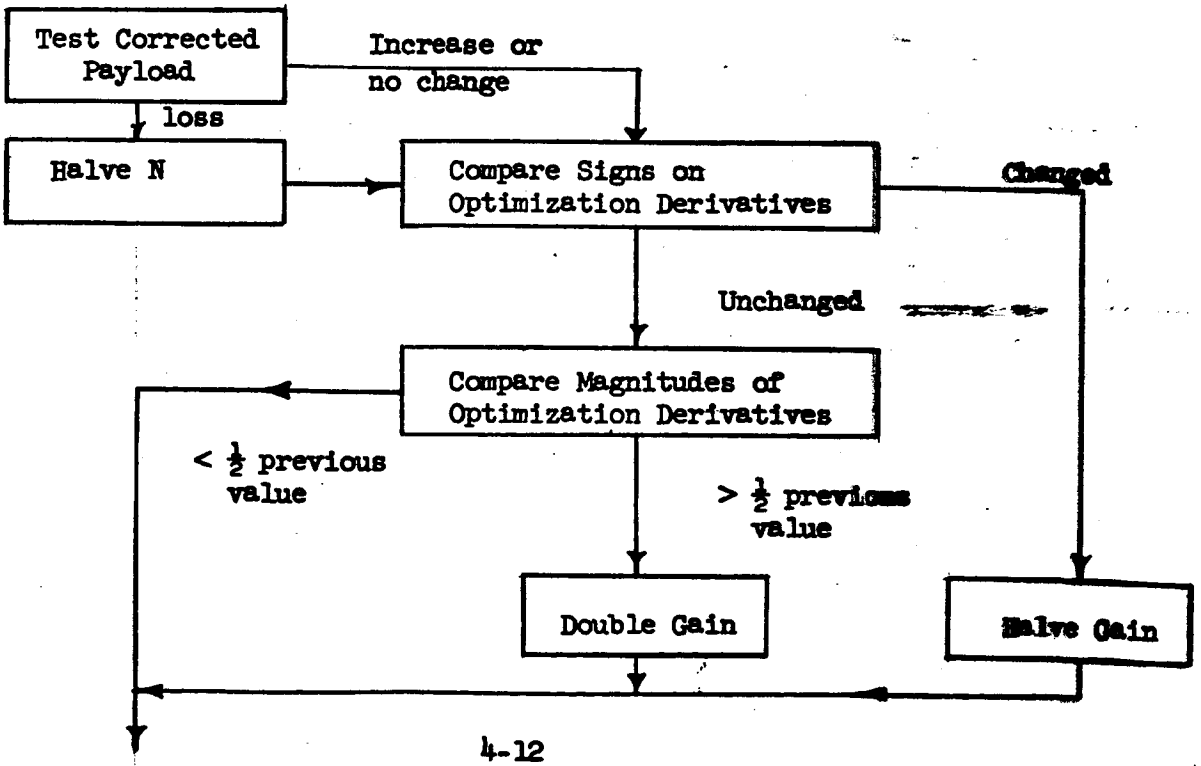

Figure 4-8

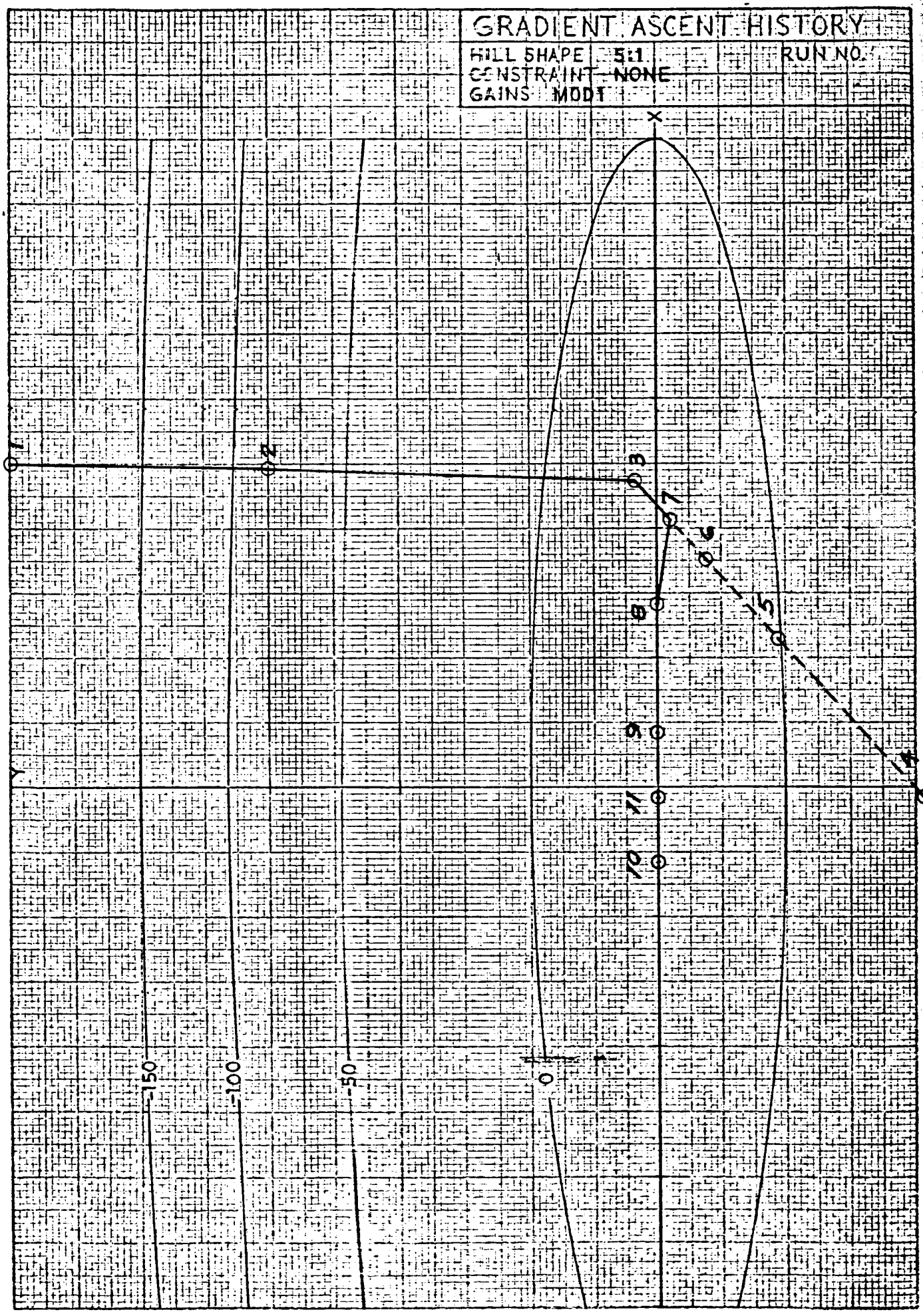
GRADIENT ASCENT HISTORY
HILL SHAPE 5:1
CONSTRAINT NONE
GAINS MOD1
RUN NO.
X
Y
1
2
3
4
5
6
7
8
9
10
11
-150
-100
-50
0

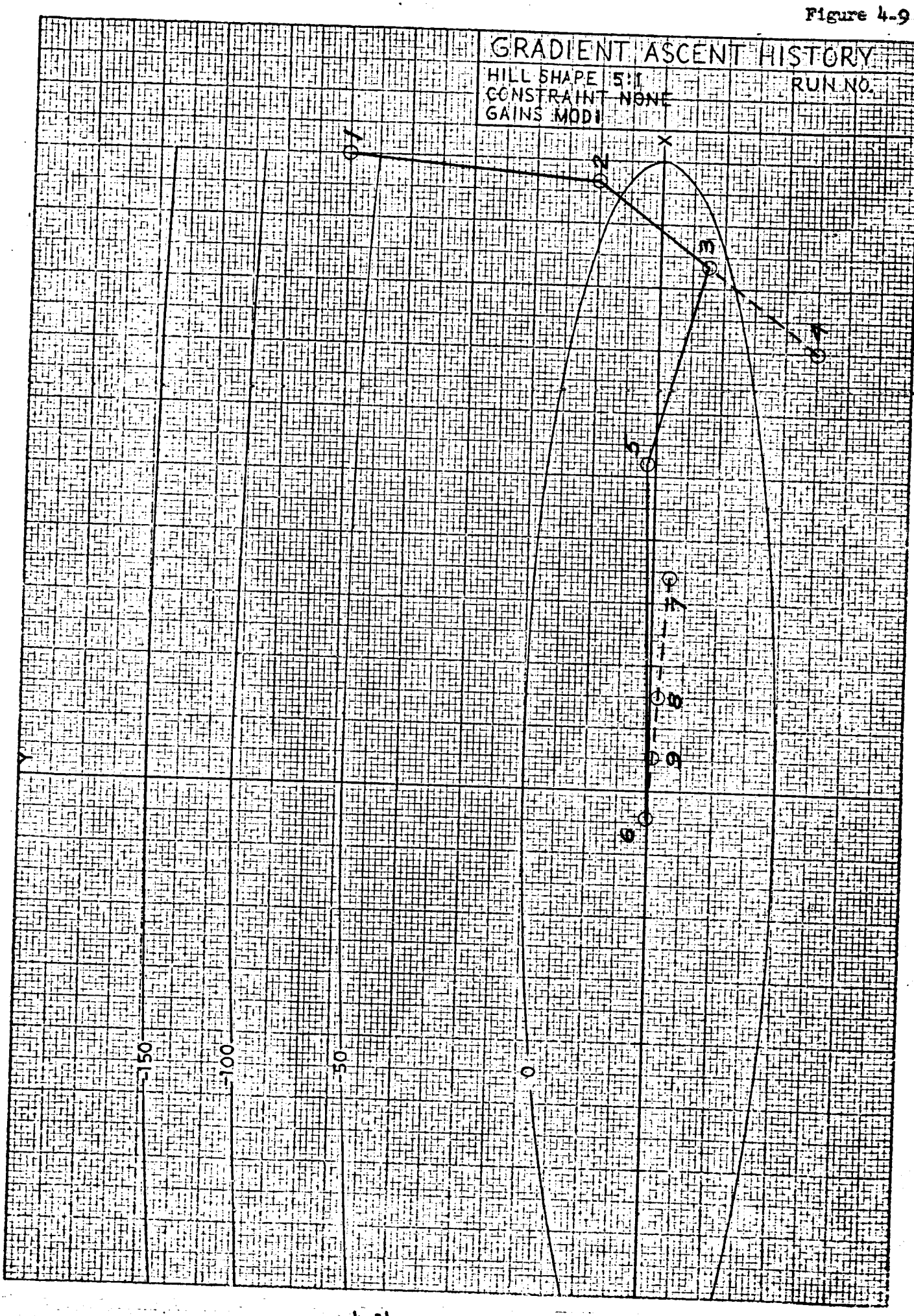
GRADIENT ASCENT HISTORY
HILL SHAPE 5:1
CONSTRAINT NONE
GAINS MOD1
RUN NO.
X
Y
-150
-100
-50
0
1
2
3
4
5
6
7
8
9

as shown in Figure 4-7. The operation of this Mod 4 routine on the 5:1 paraboloid is shown in Figure 4-10. The new routine was even more successful and reached the maximum payoff condition in eight steps.

The Mod 4 routine reaches the maximum more rapidly than the Mod 1 routine because it also takes advantage of information gained from a failure. Tracing the operation of this Mod 4 routine in Figure 4-10, the procedure was identical to the Mod 1 routine to point 3. At point 4 both gains were halved, in addition to the step size parameter, N; and at point 5 the X gain was doubled and the Y gain was halved along with the step size parameter. At point 6 the X gain was again doubled, at point 7 the Y gain was halved, and at point 8 both gains were halved along with the step size parameter.

The results achieved with these simple gain selection techniques were extremely encouraging and indicate that substantial improvements in the behavior of a gradient routine can be achieved with these methods on elongated payoff hills. At first glance they represent a promising solution for the difficulty with the ridge. However, the situation is not quite that simple. If we turn now to the hill with the elongated axis skewed at 45 degrees, to the two control axes and apply the Mod 1 and Mod 4 gain selection routines to this problem, their behavior is not substantially better than that shown for the standard routine in Figure 4-6. The Mod 1 operation is shown in Figure 4-11 and the Mod 4 operation is shown in Figure 4-12. Neither of these routines satisfactorily solves the ridge problem with the skewed hill.

This might be expected because it is not possible to emphasize motion along the ridge by emphasizing one or the other of the control variables. An appropriate gain selection technique for the problem with the skewed ridge must emphasize a combined motion in the controls X and Y, in the direction along the ridge, and de-emphasize combinations of X and Y motion perpendicular to the ridge. To date, we have been unable to synthesize techniques for this

Figure 4-10

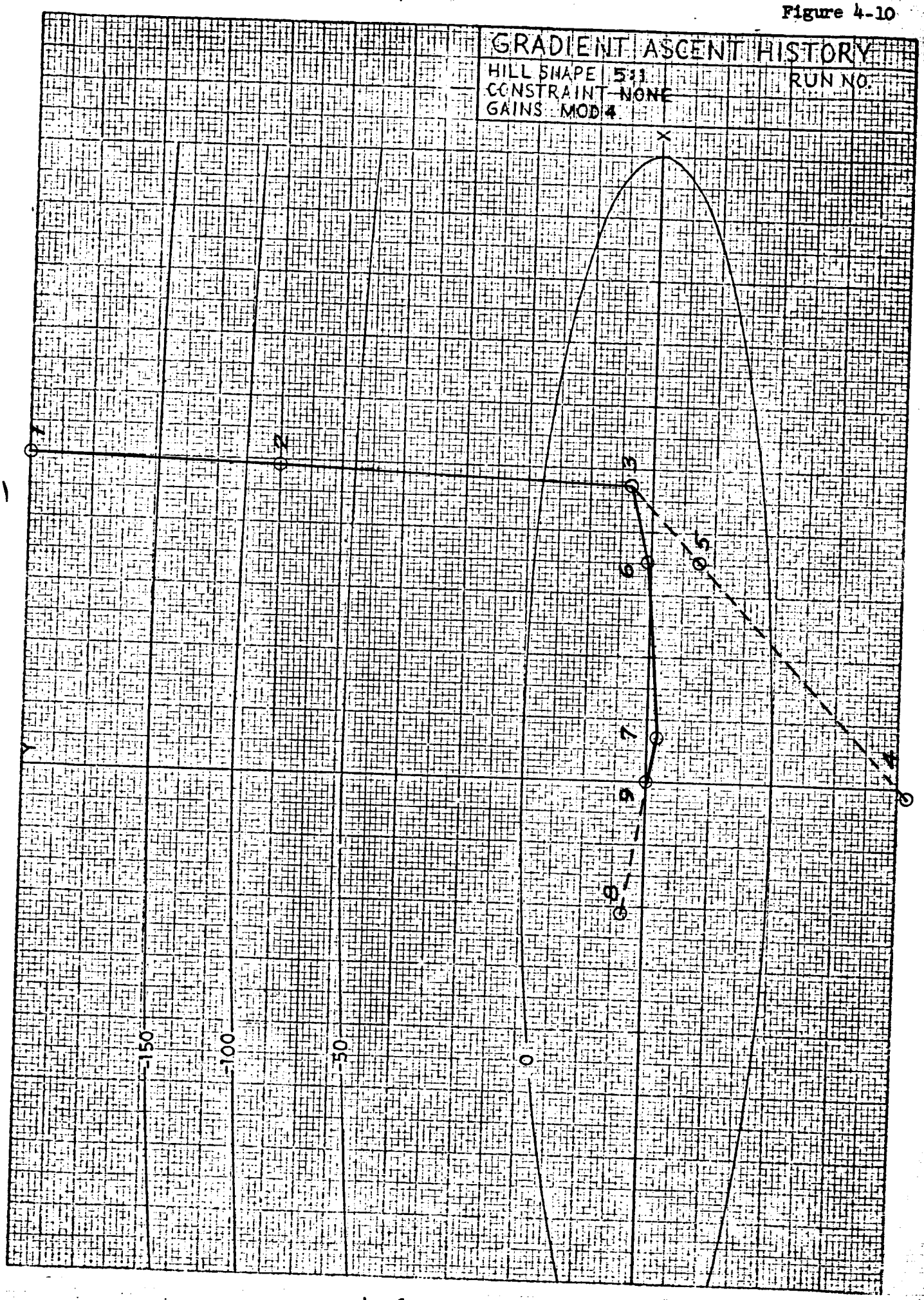
GRADIENT ASCENT HISTORY
HILL SHAPE 5:1
CONSTRAINT NONE
GAINS MOD 4
RUN NO.
X
Y
Z
1
2
3
4
5
6
7
8
9
-150
-100
-50
0

Figure 4-11

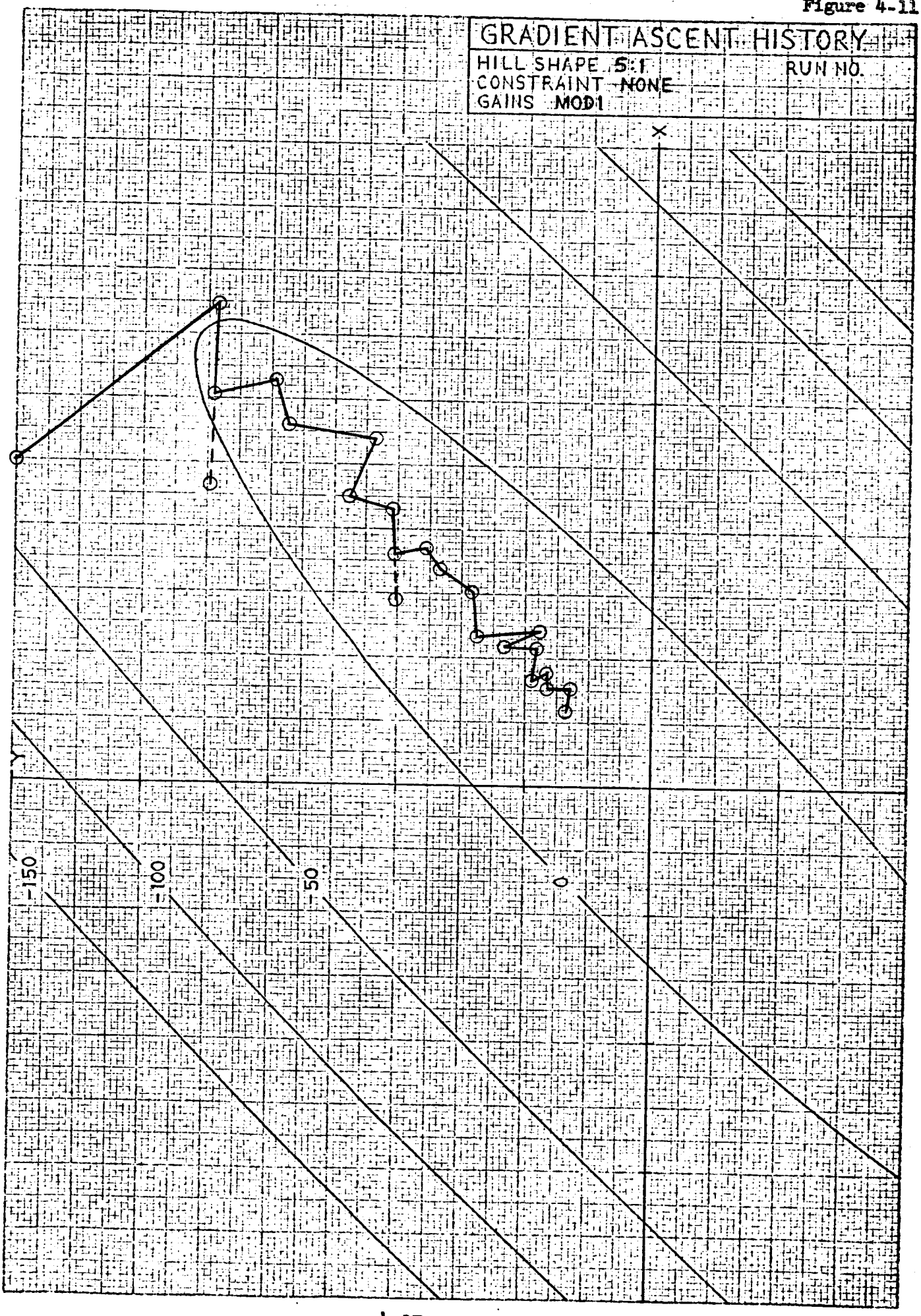
GRADIENT ASCENT HISTORY
HILL SHAPE 5:1
RUN NO.
CONSTRAINT NONE
GAINS MOD1
X
Y
-150
-100
-50
0

Figure 4-12

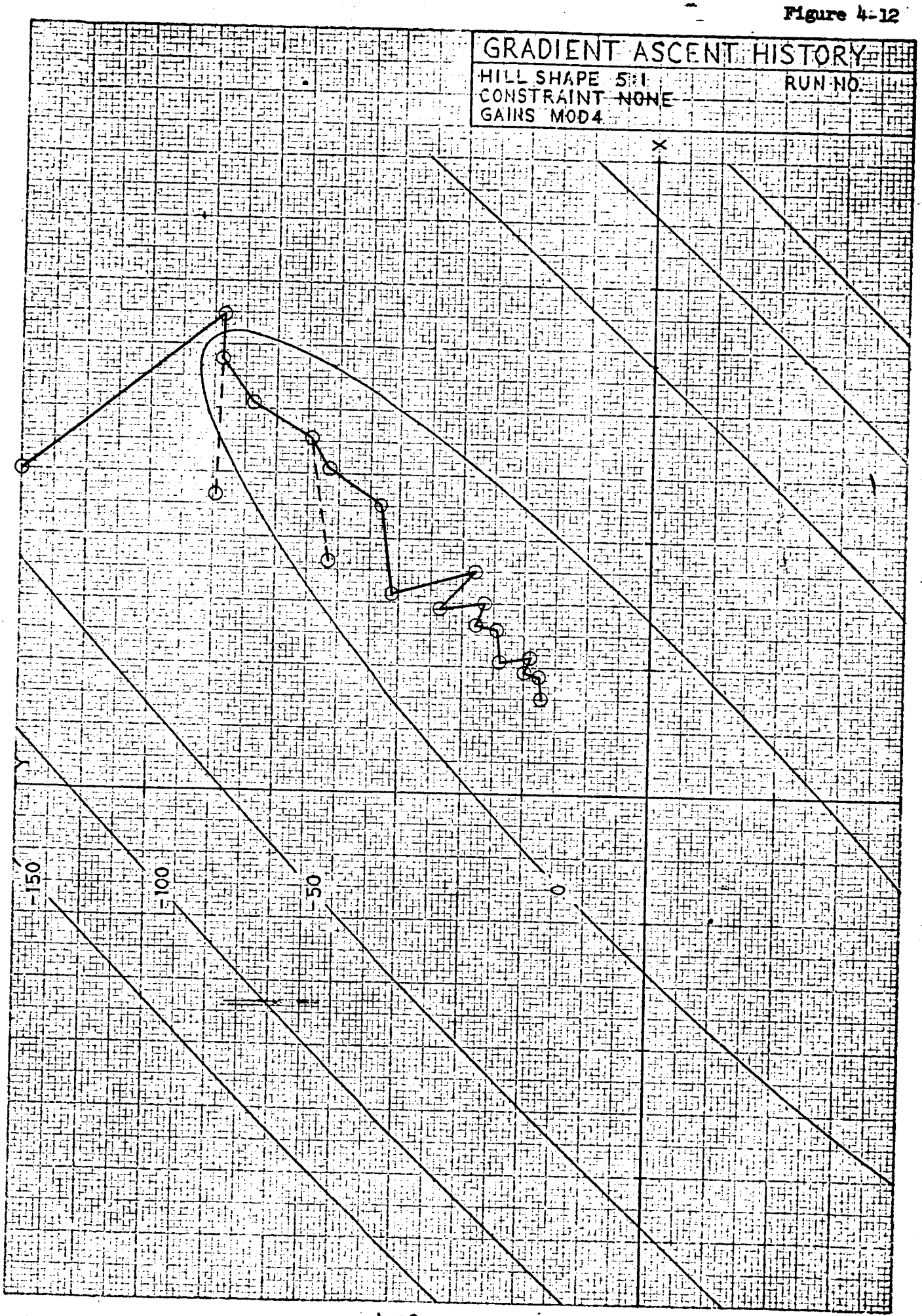
GRADIENT ASCENT HISTORY
HILL SHAPE 5:1
CONSTRAINT NONE
GAINS MOD4
RUN NO.
X
Y
-150
-100
-50
0

type of gain selection that are sufficiently general for application to the complete system optimization problem. Unfortunately, this problem is not fictitious and the type of operation where more than one control oscillated, indicating skewed-ridge type behavior, was frequently encountered during the system optimization study discussed in the previous section.

4.1.3 Non-linear Techniques

Since we were unable to achieve satisfactory solutions to the problem of the skewed elongated ridge with automatic gain selection procedures, it was decided that it might be appropriate to examine some higher order procedures. Two non-linear techniques were investigated with the simplified hill climber routine.

The first was what might be called a uni-directional approach. The idea is to move in the direction determined initially by the local gradient until a maximum payoff is reached. A new gradient calculation is then performed and the routine moves in that direction until the payoff again maximizes, etc.

The second technique is a derivative averaging process. In this procedure the gradient step is first computed using the derivatives at the current point. That step is taken and then the derivatives at the new point are averaged with those from the previous point and the step is re-computed. The procedure is repeated until the average derivatives determined agree within some specified tolerance with those used for the step itself.

Both of these techniques show promise for future application to the full system optimization problem and their behavior with the simple hill climber routine will be discussed in the following paragraphs.

In Figure 4-13, the parabolic fit routine is applied to the 5:1 paraboloid hill. The points shown represent the maximums determined for

Figure 4-13

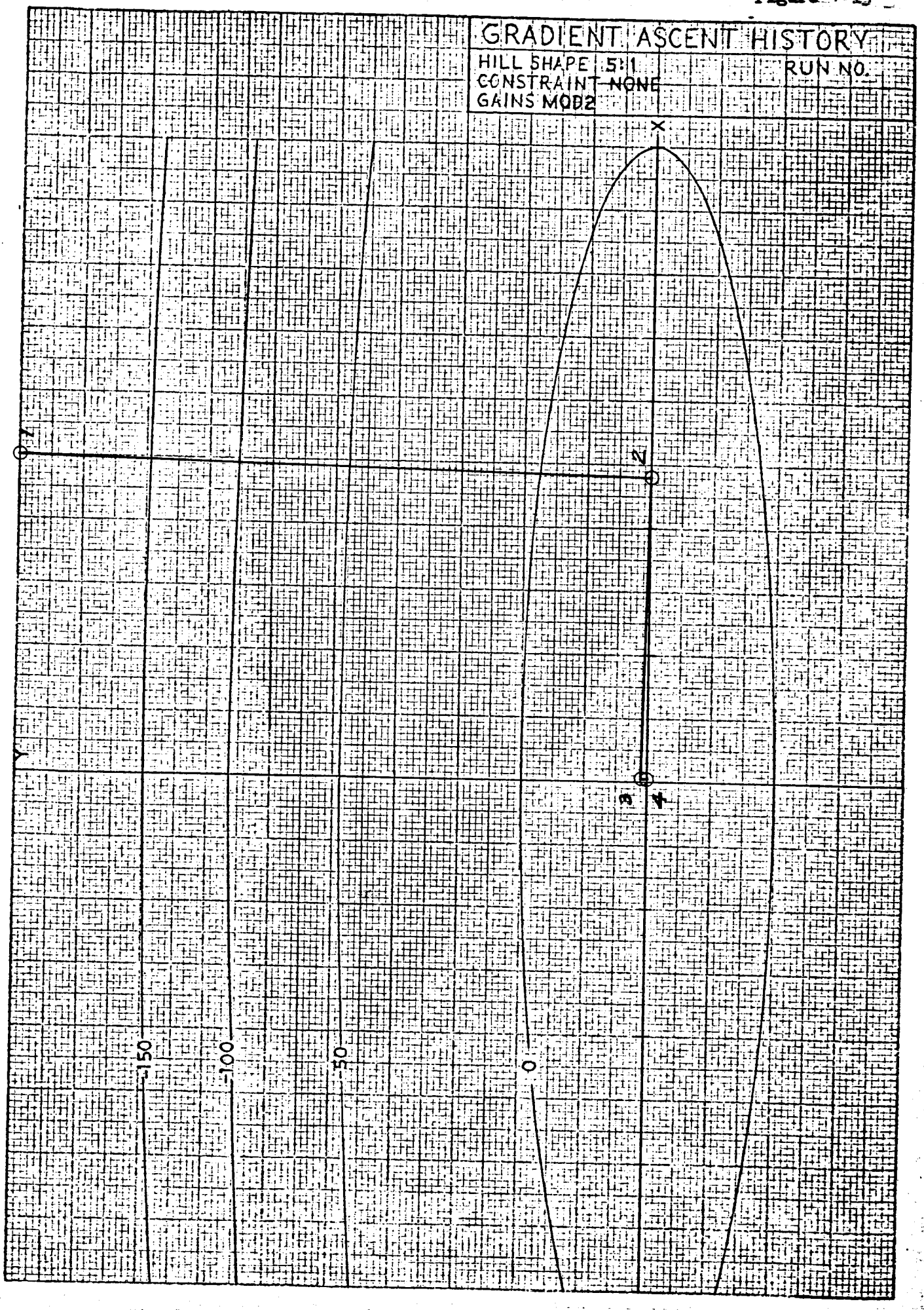

each fit. Uni-directional motion is achieved by keeping the control changes in the proportions computed for the first gradient step until the maximum payoff is passed. A parabola is then computed which fits the points that bracket the maximum value of the payoff using the following expression to define the step length, δS.

$$\delta S = \sum_i \delta X_i^2 = N$$

As would be expected, each succeeding fit is in a direction approximately 90 degrees to that of the previous fit, since the routine sees no gradient in the direction of the previous parabola. Figure 4-13 shows that three fits were required to reach the optimum on the 5:1 payoff hill.

When this same routine was applied to the skewed hill, we obtained the results shown in Figure 4-14. In this instance, the number of fits required to reach the peak of the hill was approximately double that of the previous case. Since there is no reason why the introduction of a skewed ridge should produce different behavior with this routine, we must assume that the variation shown between Figures 4-13 and 4-14 is simply the result of the relative difference in starting conditions used (i.e., the starting condition with respect to the ridge was different for these two cases).

Figures 4-13 and 4-14 are somewhat deceptive in that each step taken by the parabolic fit routine is not shown. In general, a minimum of three steps is required for each fit so that the path shown in Figure 4-14, for example, actually used twenty-four steps to reach the top of the hill. Nevertheless, even this represents some improvement over the standard routine and from other sets of initial conditions a much greater improvement would be anticipated.

The derivative averaging routine was not too successful on the payoff-only hill. A routine of this type must incorporate some safeguards

Figure 4-14

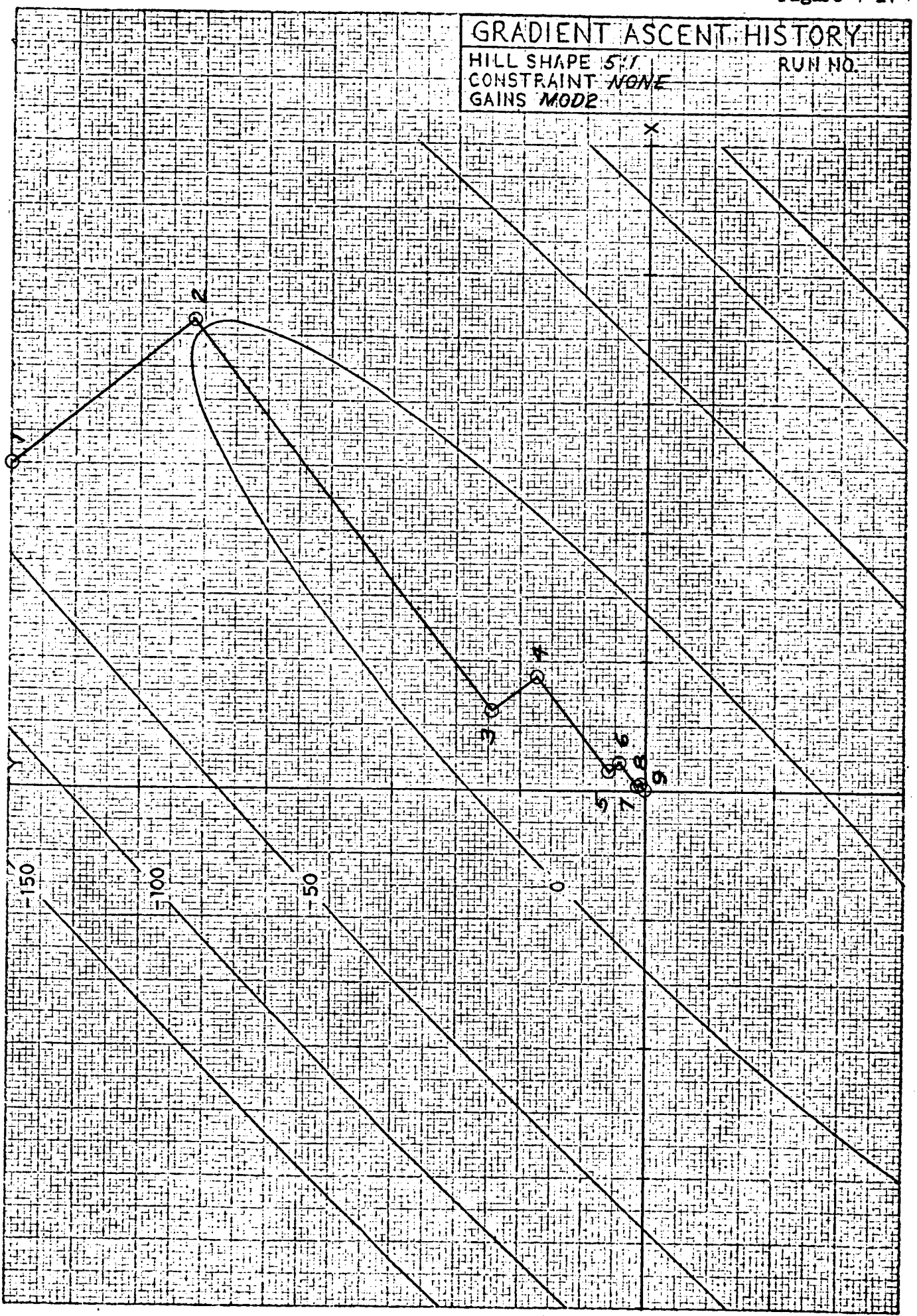
GRADIENT ASCENT HISTORY
HILL SHAPE 5:1
CONSTRAINT NONE
GAINS MOD2
RUN NO.
X
Y
-150
-100
-50
0
1
2
3
4
5
6
7
8
9

to prevent the process from becoming divergent when the step crosses over a ridge, and one or more of the control derivatives changes sign. In this particular case, the safeguard used was a test on the sign of the control derivative that automatically reduced the step size when a sign change was encountered. Unfortunately, the step size reduction in the case shown in Figure 4-15 was sufficient to stop the routine well out on the ridge. In the present study we had insufficient time to explore this derivative averaging technique further. However, we feel that this procedure still holds great promise and that a variety of effective techniques can be developed that will circumvent the step size problem. It will be shown in Section 4.1.4 that the derivative averaging process behaved very well on the elongated payoff hill for the problem that included a constraint.

The derivative averaging process would, of course, be of very little benefit if the complete system optimization cycle, including the trajectory optimization, had to be completed for each trial step. The idea behind this routine, however, is that the major non-linearities in the system optimization problem appear to be traceable to the propulsion equations defined in Section 2. These propulsion derivatives appear in the expressions for the payoff and constraint partials and multiply certain elements of the exchange ratios. It would be possible to rapidly determine the influence of the non-linearities in these terms by introducing a third iteration loop in the system optimization program that operated in the same fashion as the derivative averaging routine described above.

Before leaving the discussion of non-linear routines, it is worthwhile to mention one interesting possibility that was not covered by the present study but which deserves further exploration. Of course, the ultimate approach to the hill climbing problem would be some type of routine that continuously added information on the history of the hill shape to the direction and step size formulations. A first step in this direction might be a routine that formed a continually updated solution for the coefficients of a higher order polynomial representation

Figure 4-15

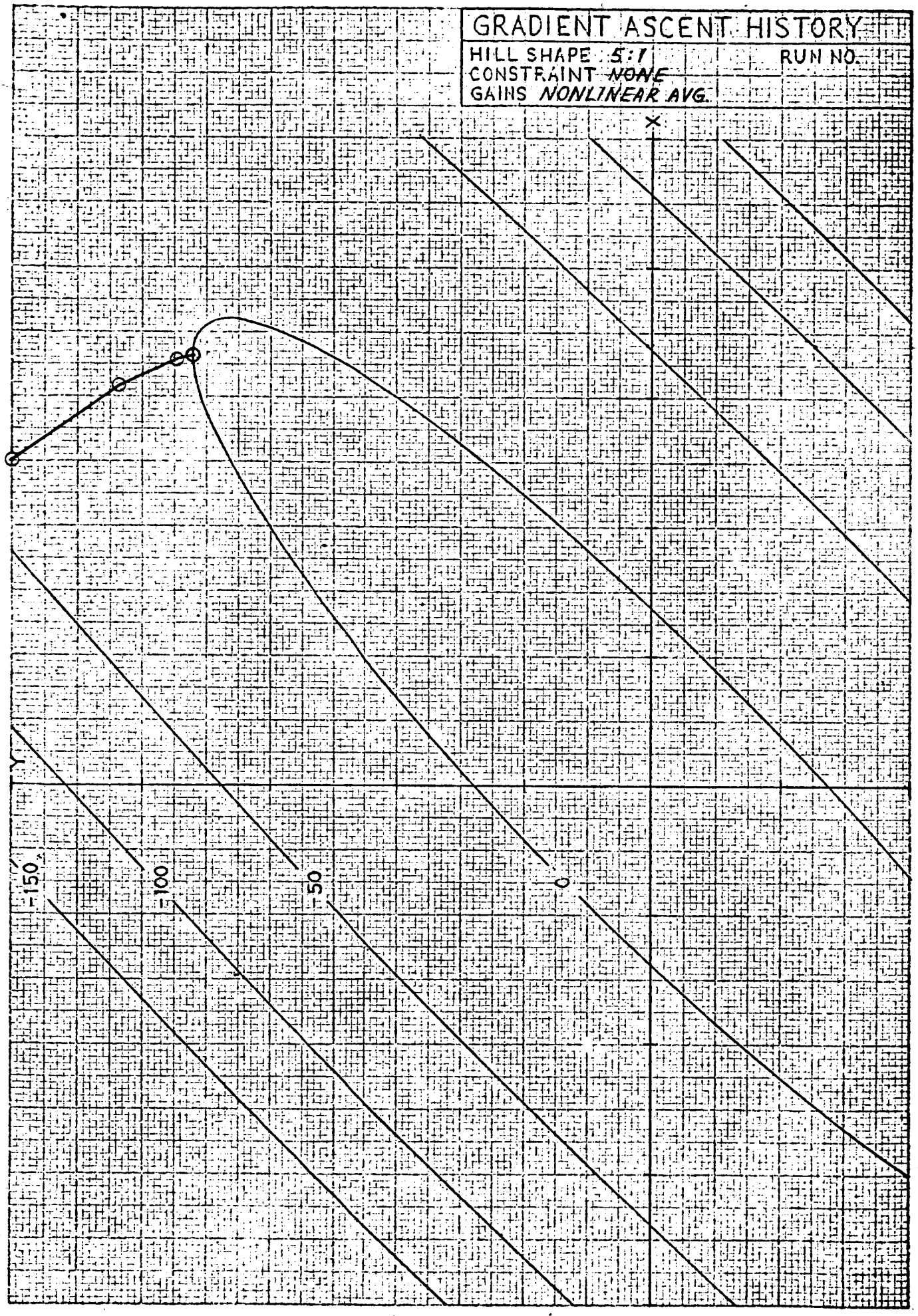
GRADIENT ASCENT HISTORY
HILL SHAPE 5:1
RUN NO.
CONSTRAINT NONE
GAINS NONLINEAR AVG.
X
Y
-150
-100
-50
0

of the payoff hill. A normal gradient path could be pursued until sufficient steps had been taken to determine the necessary coefficients. The routine would then attempt to move to the maximum defined by the polynomial in a single step and from that point the process would continuously update the estimated polynomial coefficients as new information became available. This procedure then would involve a series of normal gradient steps followed by a series of second order steps. The technique should properly recognize higher order relationships between the payoffs and the controls and the significant cross-relationships between the controls and the control derivatives.

4.1.4 The Effect of Constraints

The optimization program modifications discussed above have also been tested on problems involving both a payoff and a constraint. Figures 4-16 and 4-17 show the behavior of the linear optimization routine on this type of problem. In these figures the constraint is shown as a circle in the X, Y plane (the constraint hill shape is a 1:1 paraboloid). The maximum possible payoff with this constraint imposed lies at the intersection of the constraint circle and the ridge line. The cases shown immediately point out several problems with the success criterion.

First the success criterion used in the standard routine corrects each payload obtained for the current constraint miss before comparing it with the payload from the previous case. The procedure is analagous to that used by the PRESTO trajectory program and is designed to take advantage of iterations that would normally be rejected because the constraint miss was not within tolerance. The second term in the equation for payoff improvement (Eq. 2-6) is used to correct the payload for the constraint miss. This assumes that the correction is obtained with a minimum sum square change in the controls (i.e., moving on the maximum constraint gradient). When this expression was used to define the slope $\frac{\delta f}{\delta w}$, at the last successful iteration

Figure 4-16

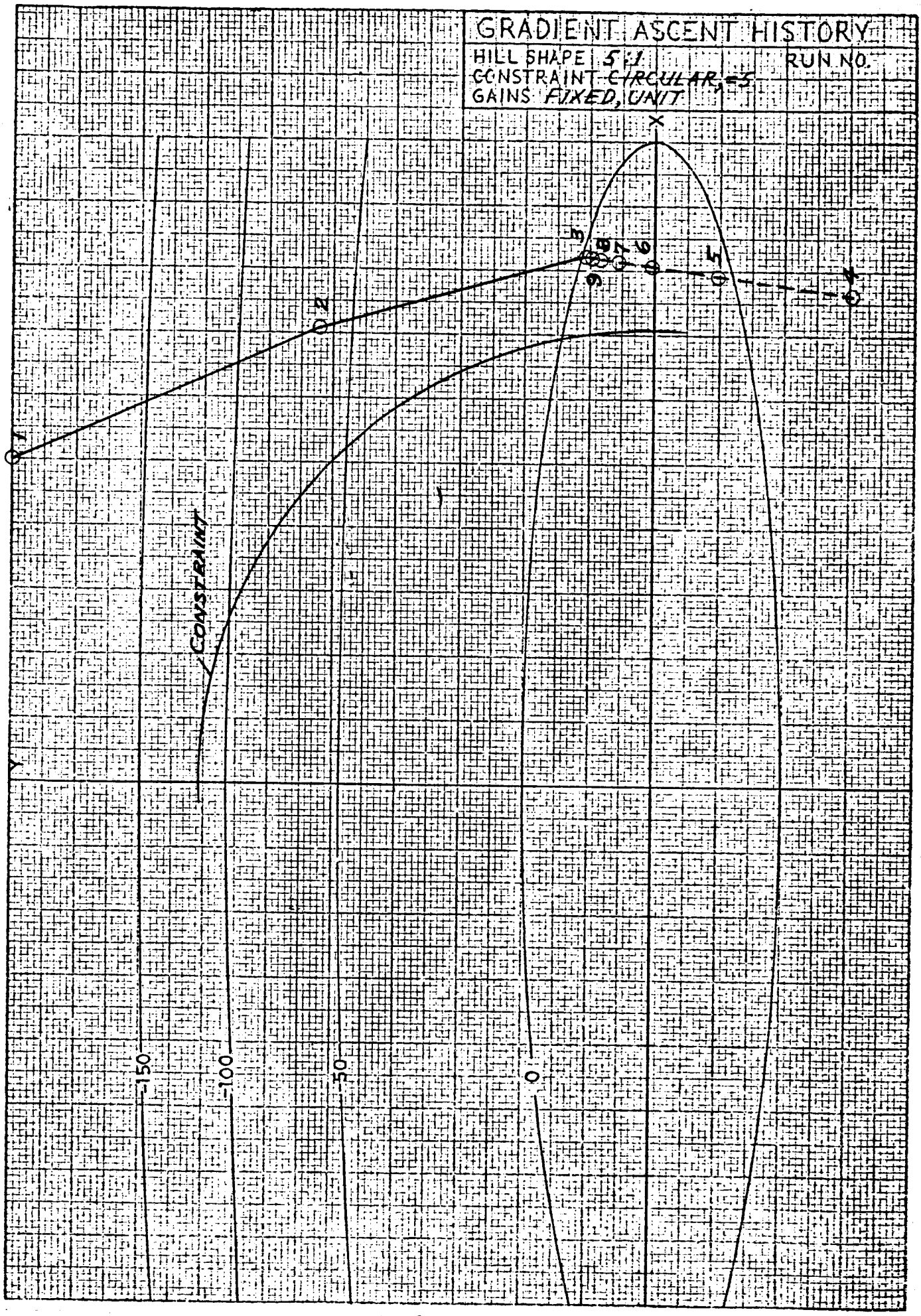

Figure 4-17

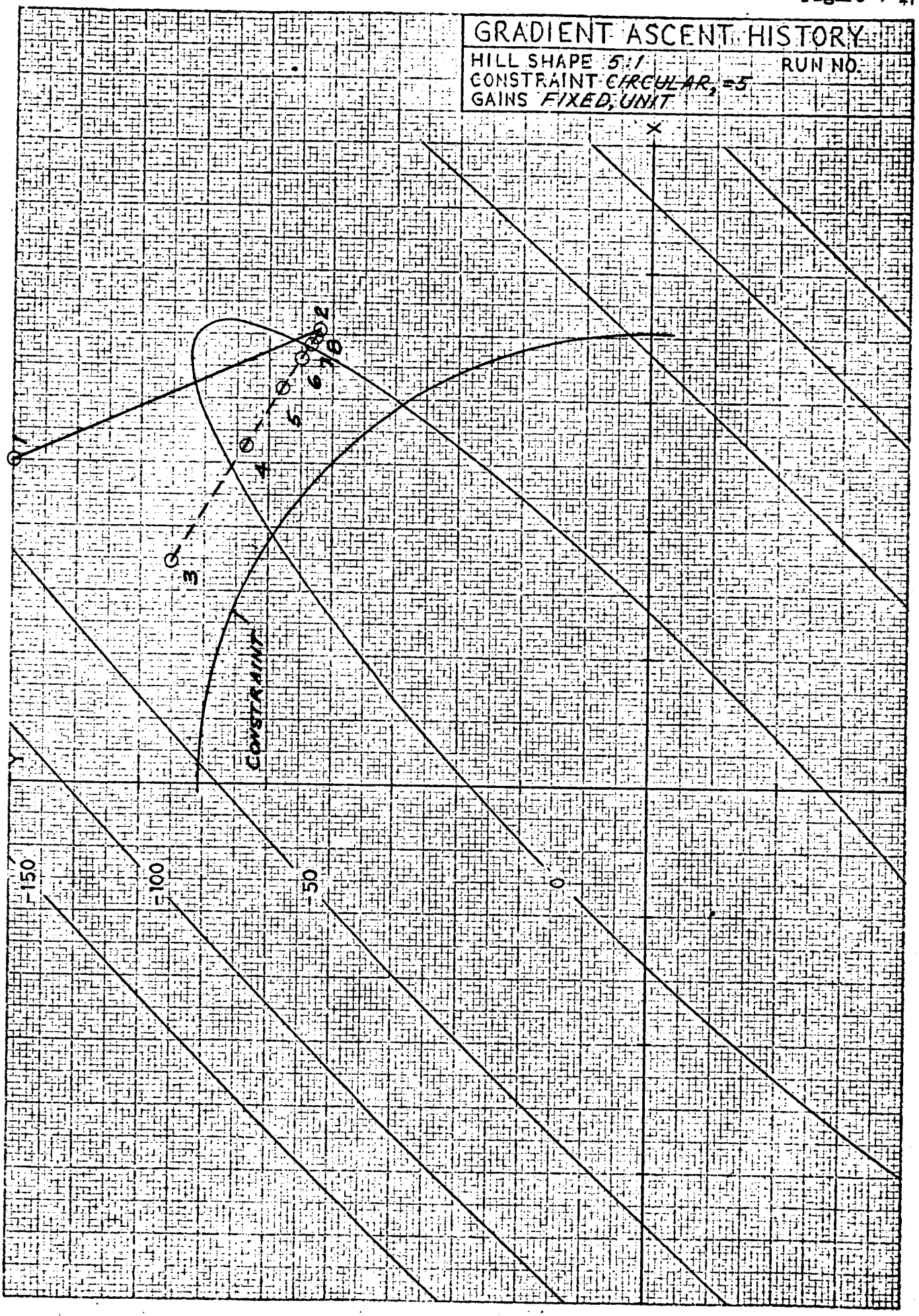
GRADIENT ASCENT HISTORY
HILL SHAPE 5:1
RUN NO.
CONSTRAINT CIRCULAR, =5
GAINS FIXED, UNIT
X
Y
CONSTRAINT
-150
-100
-50
0

in Figures 4-16 and 4-17, the resulting payload adjustment for the constraint miss was too high. Consequently, the routine over-estimated the payload at those points and was unable to improve on that estimate on further iterations. In fact, this will usually be the result of this type of payoff correction procedure because the second derivative on the payoff hill is usually negative and the payoff correction therefore predicts a payload that is too high. With the full optimization program we attempt to avoid this problem by limiting the permissible constraint miss that is acceptable for a successful iteration.

Figures 4-16 and 4-17 also show that the halving procedure used when the corrected payloads showed a loss introduced difficulty. Previous experience with the full optimization program led us to believe that it was appropriate to halve both the payoff improvement asked and the constraint correction asked in the event of a failure. As shown, this results in a constant direction of motion in the X, Y plane during the halving process and prevents the run from moving closer to the constraint. It is obvious that the constraint adjustment should not be reduced in this situation.

To improve the performance of the basic routine on the constraint problem a rather extensive modification was made in the success criterion. Figure 4-18 shows the logic for this modification, which is designed to accomplish several improvements. First the magnitude of the payload correction for a constraint miss that will be accepted is limited. Second, the sign of the constraint miss correction is examined to determine whether the possibility exists that the routine has over-estimated the payload. Third, the proximity to the constraint is compared with that on the previous iteration to determine whether it might be appropriate to accept a gain in the uncorrected payload. Depending upon the circumstances detected by the routine, several courses of action are possible.

Figure 4-18

MODIFIED SUCCESS CRITERION LOGIC

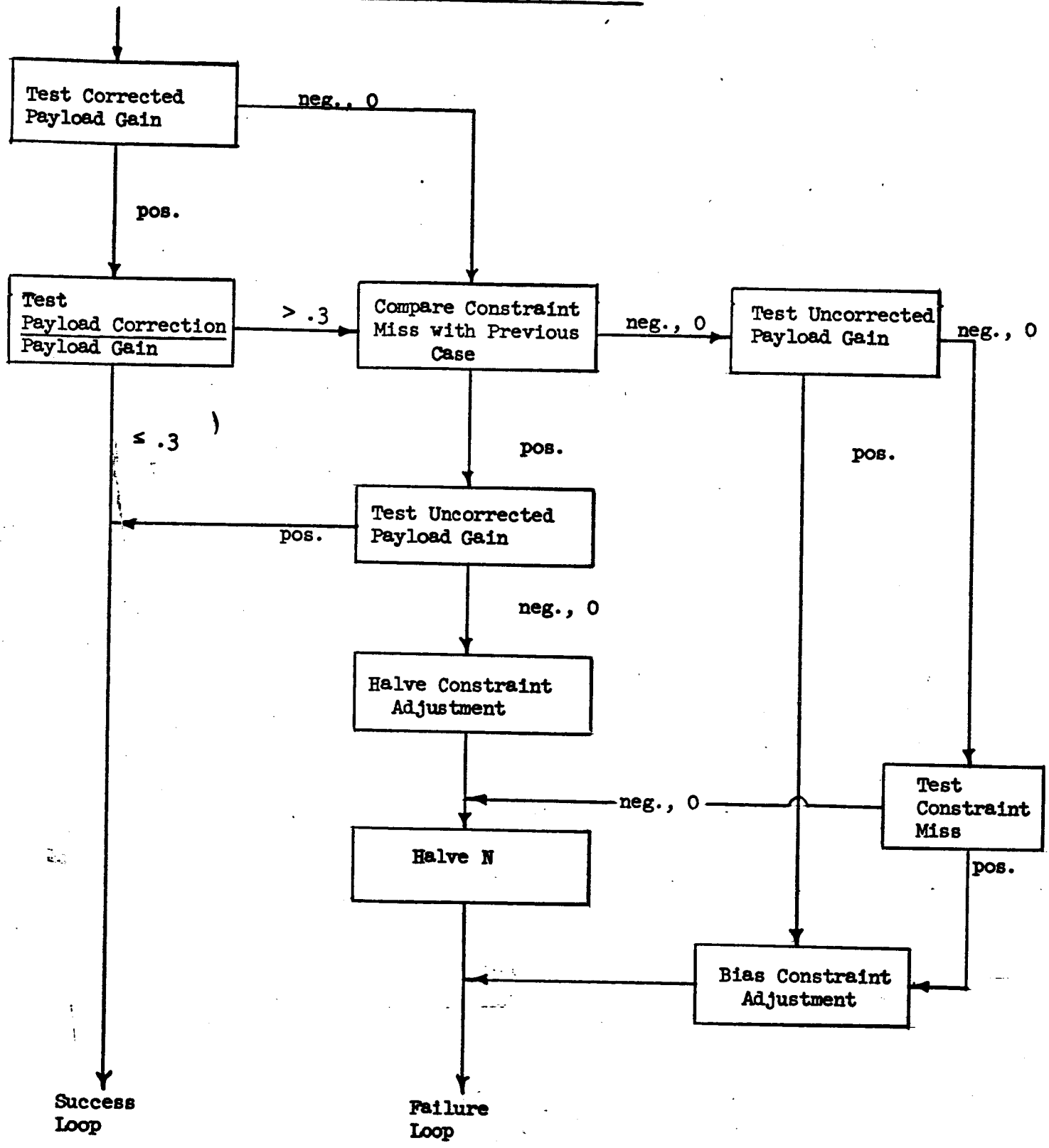

The operation with this revised success criterion is shown in Figures 4-19 and 4-20 for the parabolic constraint surface. It is apparent that this modified routine has little difficulty in approaching the optimum for both cases considered. The action of the constraint biasing procedure is demonstrated nicely in each of these figures. Figure 4-21 shows the operation of the same routine for a problem where the shape of the constraint surface has been changed to a 5:1 paraboloid. Again the routine has little difficulty in approaching the optimum although the route followed is somewhat circuitous.

The non-linear techniques described above were also applied to the problem that includes the constraint. Figure 4-22 shows the behavior of the uni-directional parabolic fit routine on the constraint problem. We found it was helpful also to fit with a parabola the constraint miss that occurred during the generation of the points necessary for the parabolic payoff fit. When the step was taken to move to the top of a given parabola the constraint miss was biased in accordance with this fit. As indicated in Figure 4-22 the procedure encountered some difficulty and an oscillation developed along the constraint surface about the ridge on the 5:1 paraboloid. Further work will be required to establish the correct approach for handling constraints when the parabolic fit routine is used. However, we feel that this should present no particular difficulty.

The operation of the derivative averaging routine on the constraint problem is shown in Figure 4-23. This routine behaved very well, reaching the optimum in seven steps.

The results achieved for the hill climber simulations that included a constraint must be carefully interpreted. We are caught in somewhat of a dilemma here because our simple hill climber model was not sufficiently general to demonstrate a case that includes a constraint and exhibits the severe oscillations typical of those experienced with the payoff-only problem.

Figure 4-19

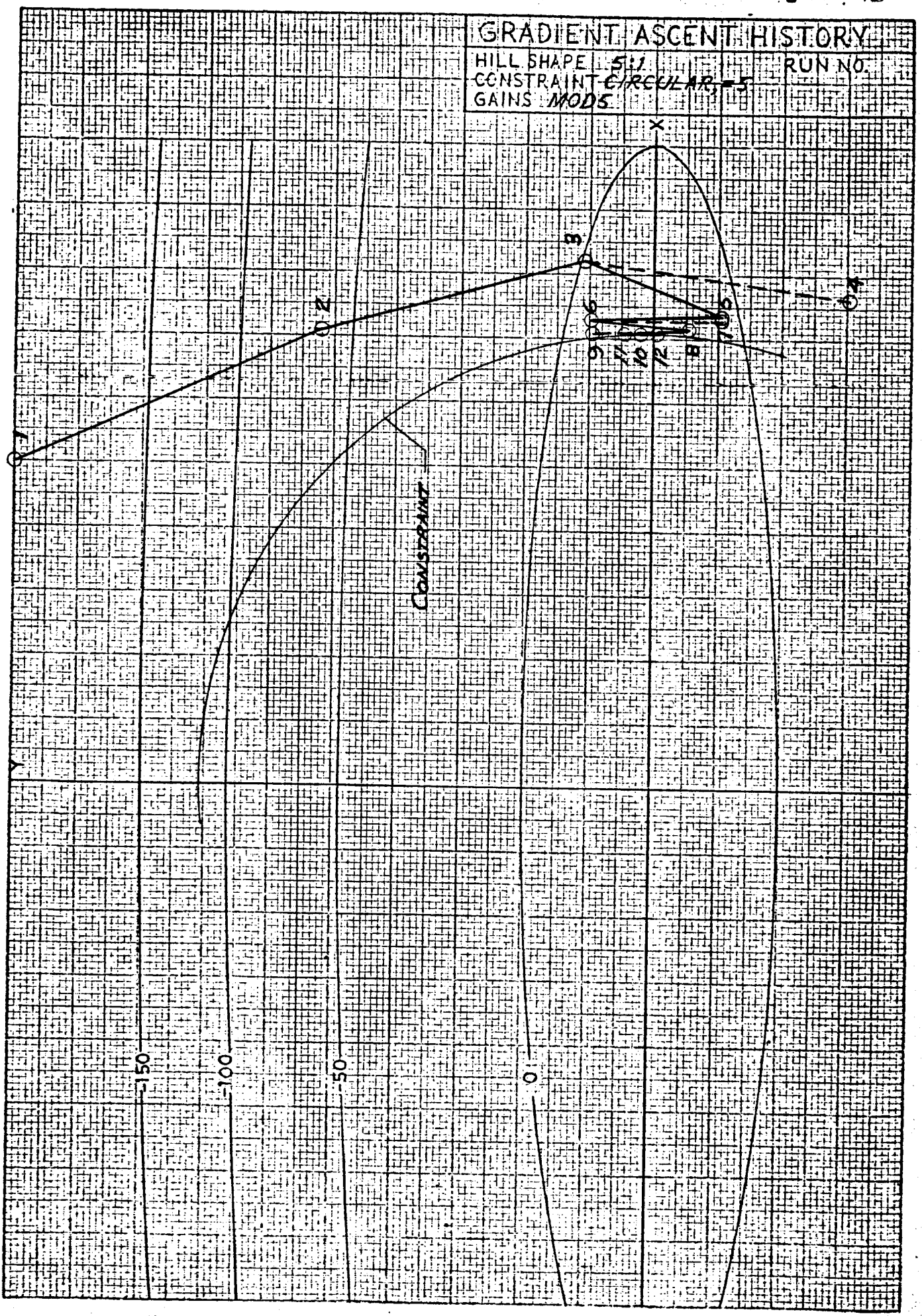

Figure 4-20

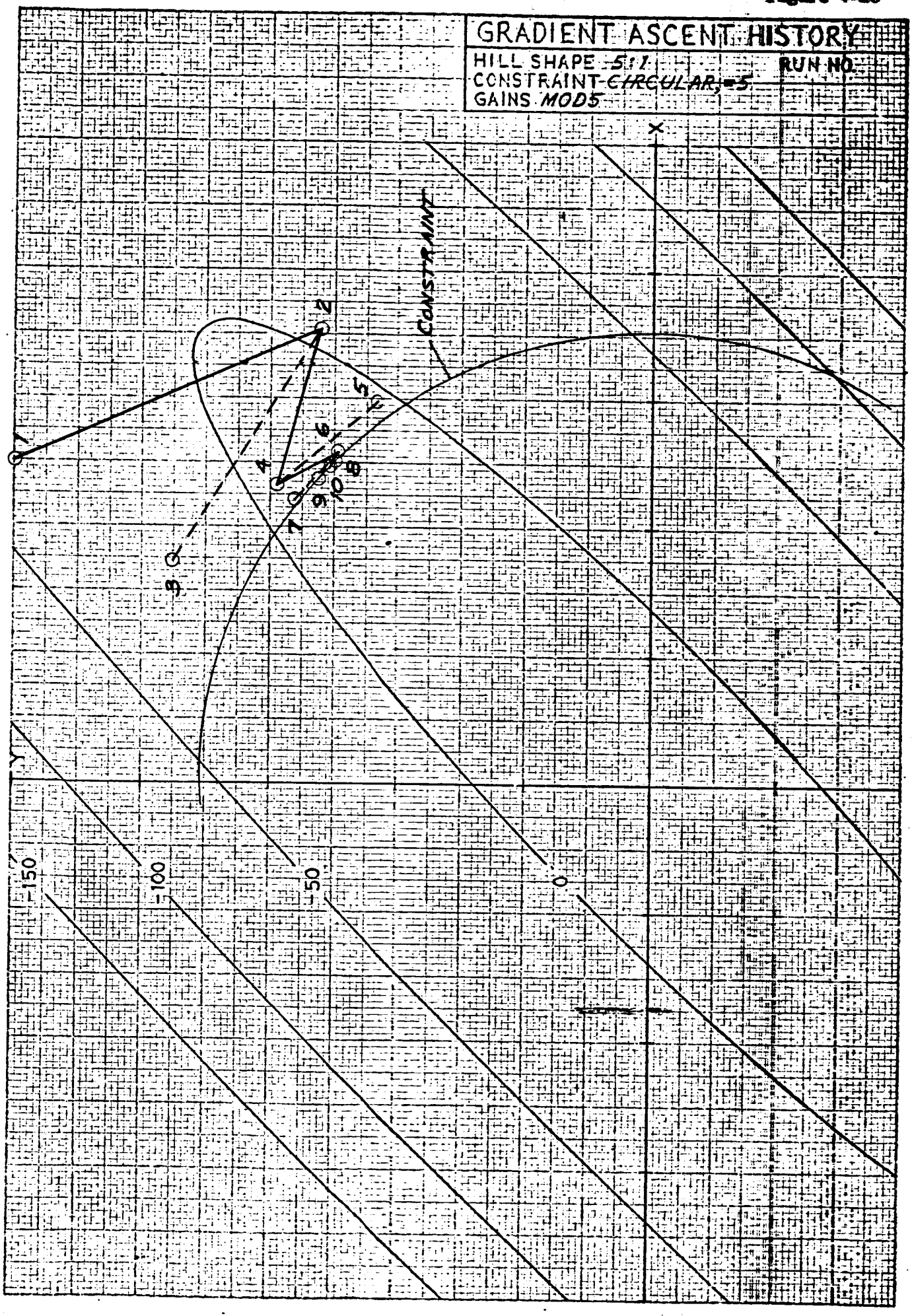
GRADIENT ASCENT HISTORY
HILL SHAPE 5:1
RUN NO.
CONSTRAINT-CIRCULAR, r=5
GAINS MOD5
CONSTRAINT
X
Y
-150
-100
-50
0
1
2
3
4
5
6
7
8
9

Figure 4-21

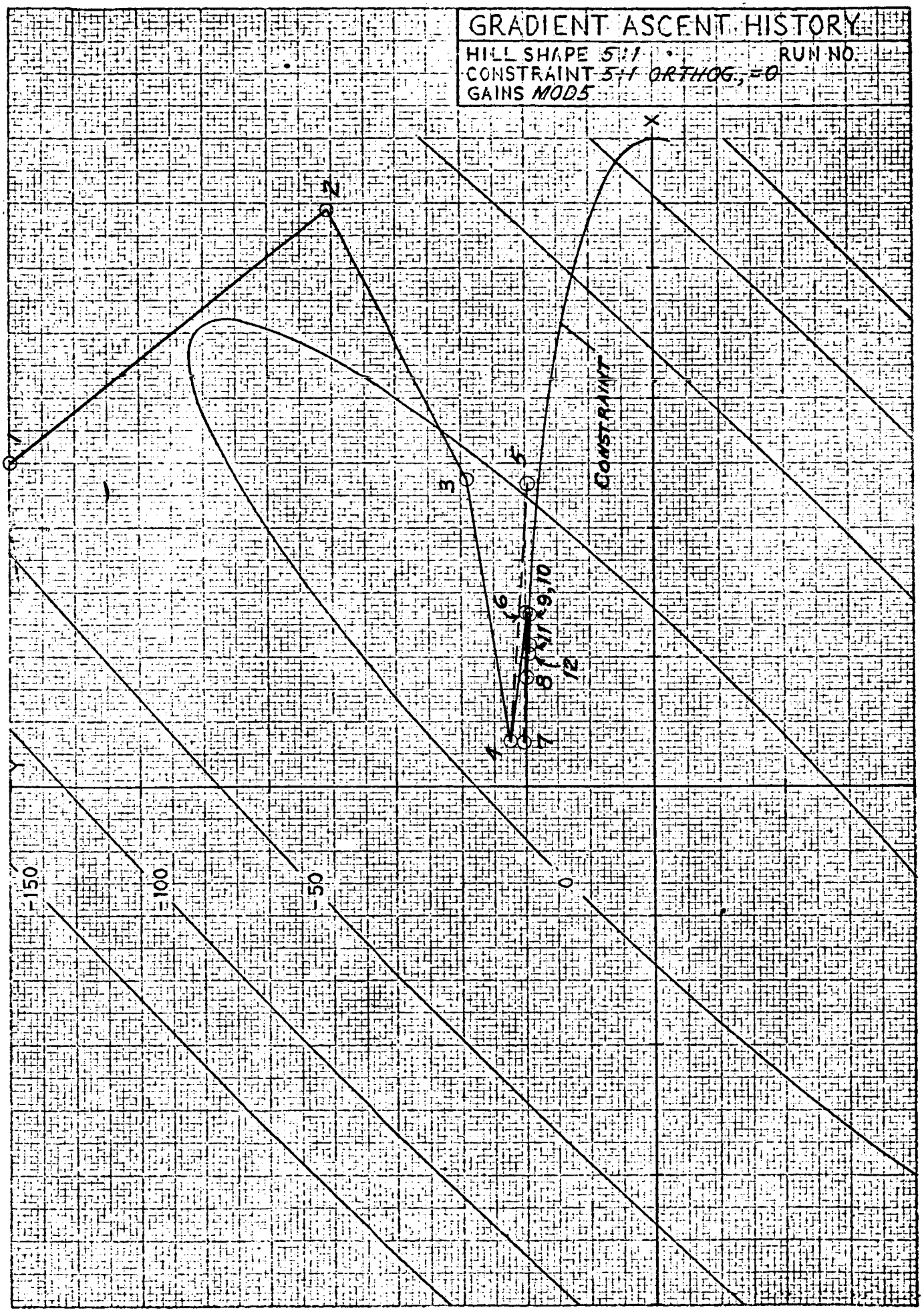
GRADIENT ASCENT HISTORY
HILL SHAPE 5:1
RUN NO.
CONSTRAINT 5:1 ORTHOG., =0
GAINS MOD5
X
Y
CONSTRAINT
1
2
3
4
5
6
7
8
9,10
11
12
-150
-100
-50
0

Figure 4-22

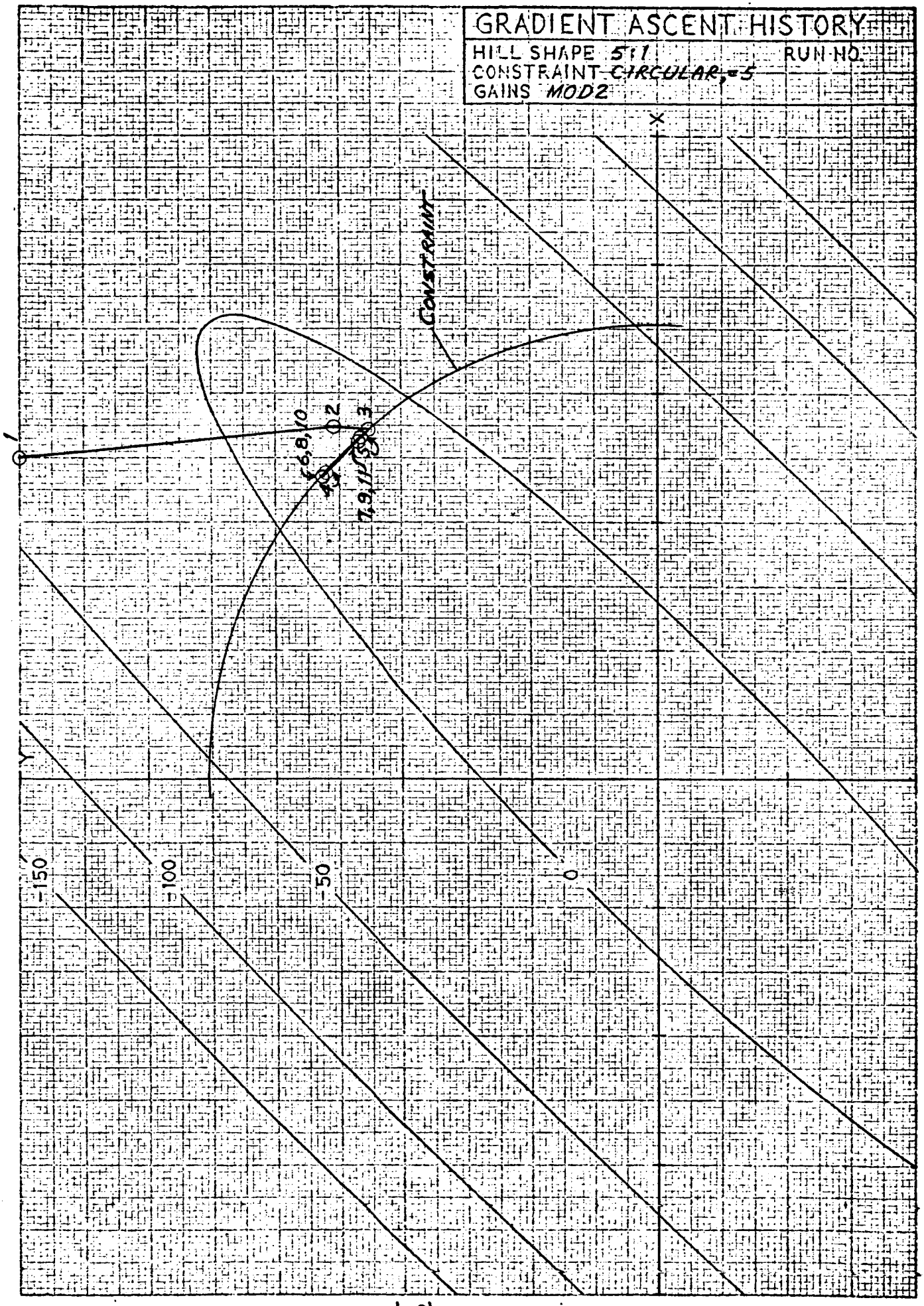
GRADIENT ASCENT HISTORY
HILL SHAPE 5:1
RUN NO.
CONSTRAINT-CIRCULAR,-5
GAINS MOD2
X
Y
CONSTRAINT
1
2
3
4,6,8,10
7,9,11
-150
-100
-50
0

Figure 4-23

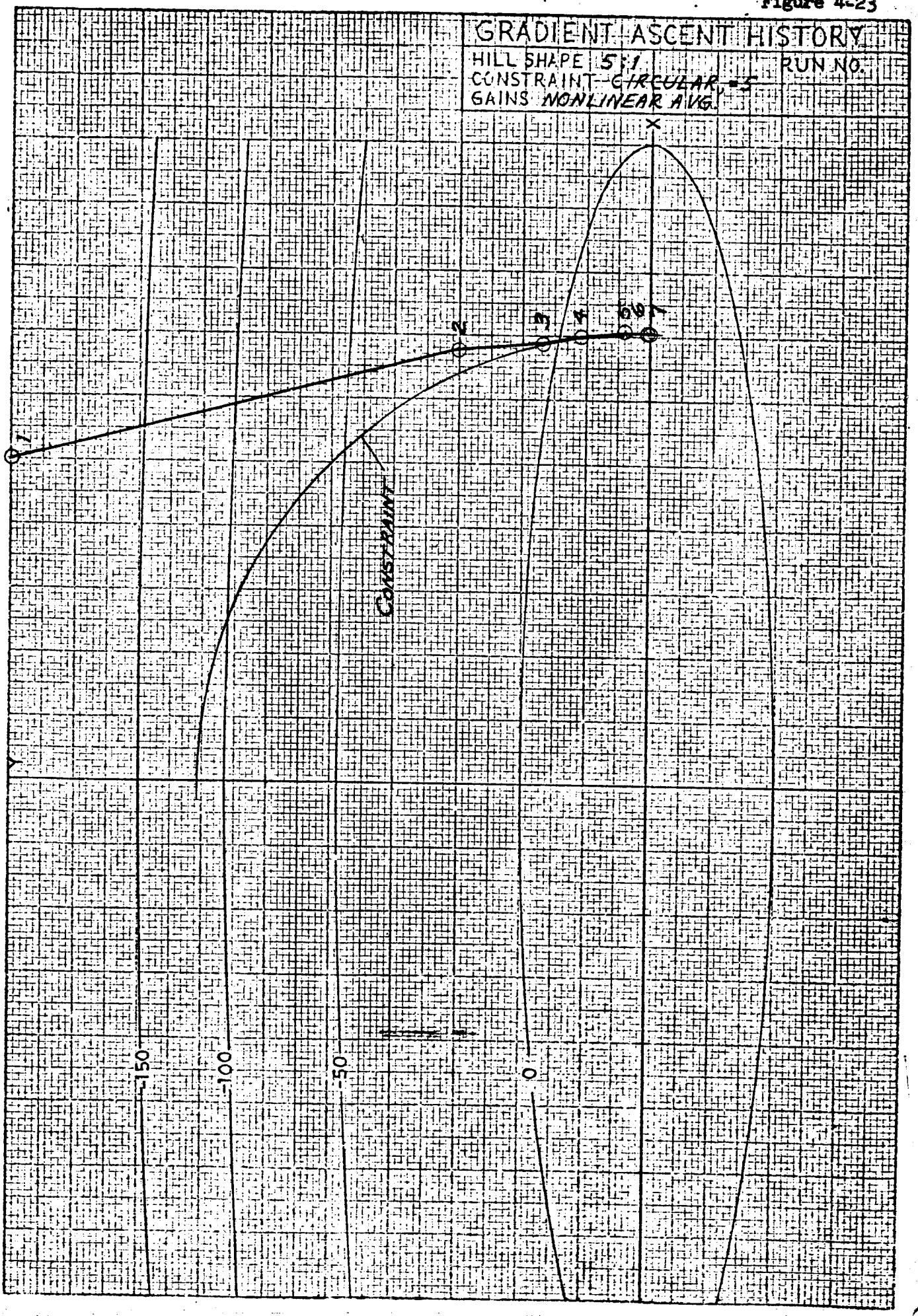

If more controls were available the model would permit oscillations while following the constraint but we have been unable to develop a simple concept that includes more than two controls and at the same time permits reasonable visualization of the behavior. Unfortunately, with only two controls we have but one degree of optimization freedom remaining and the constraint surface acts as a guide that the routine can follow on the way to the maximum payload.

In conclusion, about all that can be said about the constraint simulations on the hill climber routine is that they provide a useful basis for testing routines that we are experimenting with on the payoff-only problem. The oscillation problem must first be solved for the hill with no constraint and that solution must work when a constraint is introduced.

4.2 Convergence Gains Study

A brief study was conducted to determine whether a set of optimization gains could be defined that would significantly improve the behavior of the full system optimization program. The sixth case from the vehicle mission matrix described in Section 3 was selected for this study because the oscillation problems simulated by the skewed ridges considered with the hill climber were readily apparent during the original passes on this case. In addition, since only two stages were involved it was possible to complete a systematic variation in the optimization gains without a very large number of cases.

The problem was initiated at the beginning of the third pass for Case 6 which is shown in Table 3-7. Notice that we required four passes involving several gain adjustments to complete the original case from that point. If one control is selected as a reference parameter it then becomes necessary to complete a systematic variation of each of the three remaining

controls to properly establish the variation in program behavior that can be achieved with changes in the optimization gains. Table 4-1 summarizes the matrix of eight optimization runs that were used for this study.

The results are summarized in Figures 4-23 through 4-26. these figures show the variation in each of the system controls at each iteration for the gain combination considered. It is immediately apparent that for most cases significant oscillations are encountered although the behavior of the program with the nominal set of gains was quite acceptable. In this case the only problem evident was that associated with the creeping second stage burn time although an oscillation did begin to develop in the first stage burn time and second stage propellant loads towards the end of the run. Some of the gain adjustments considered produced violent oscillations and made little progress towards the optimum. One case from the matrix behaved very well and the program converged smoothly in all parameters in ten iterations. This was a considerable improvement from the original solution which required nearly forty iterations from the same point.

After studying the results we were unable to develop any technique for predicting a priori the most satisfactory gain combination. It is likely that the proper combination is not only a function of the system being evaluated but is also sensitive to the particular set of initial conditions (i.e., nominal system controls selected).

4.3 Launch System Optimization with a Second Order Routine

The results achieved with the parabolic fit routine on the model problems considered with the high speed hill climber formulation were sufficiently encouraging to entice us to experiment with this technique on the complete system optimization problem. A major revision was introduced in the launch system optimization program to accommodate this technique. The

Table 4-1

OPTIMIZATION GAIN MATRIX

Case No.	Gain Multipliers			
	Stage 1		Stage 2	
	Propellant	Burn Time	Propellant	Burn Time
1	1	Nominal	Nominal	Nominal
2	1	x 10	Nominal	Nominal
3	1	Nominal	x 10	Nominal
4	1	Nominal	Nominal	x 10
5	1	x 10	x 10	Nominal
6	1	x 10	Nominal	x 10
7	1	Nominal	x 10	x 10
8	1	x 10	x 10	x 10

Figure 4-23

OPTIMIZATION GAINS STUDY

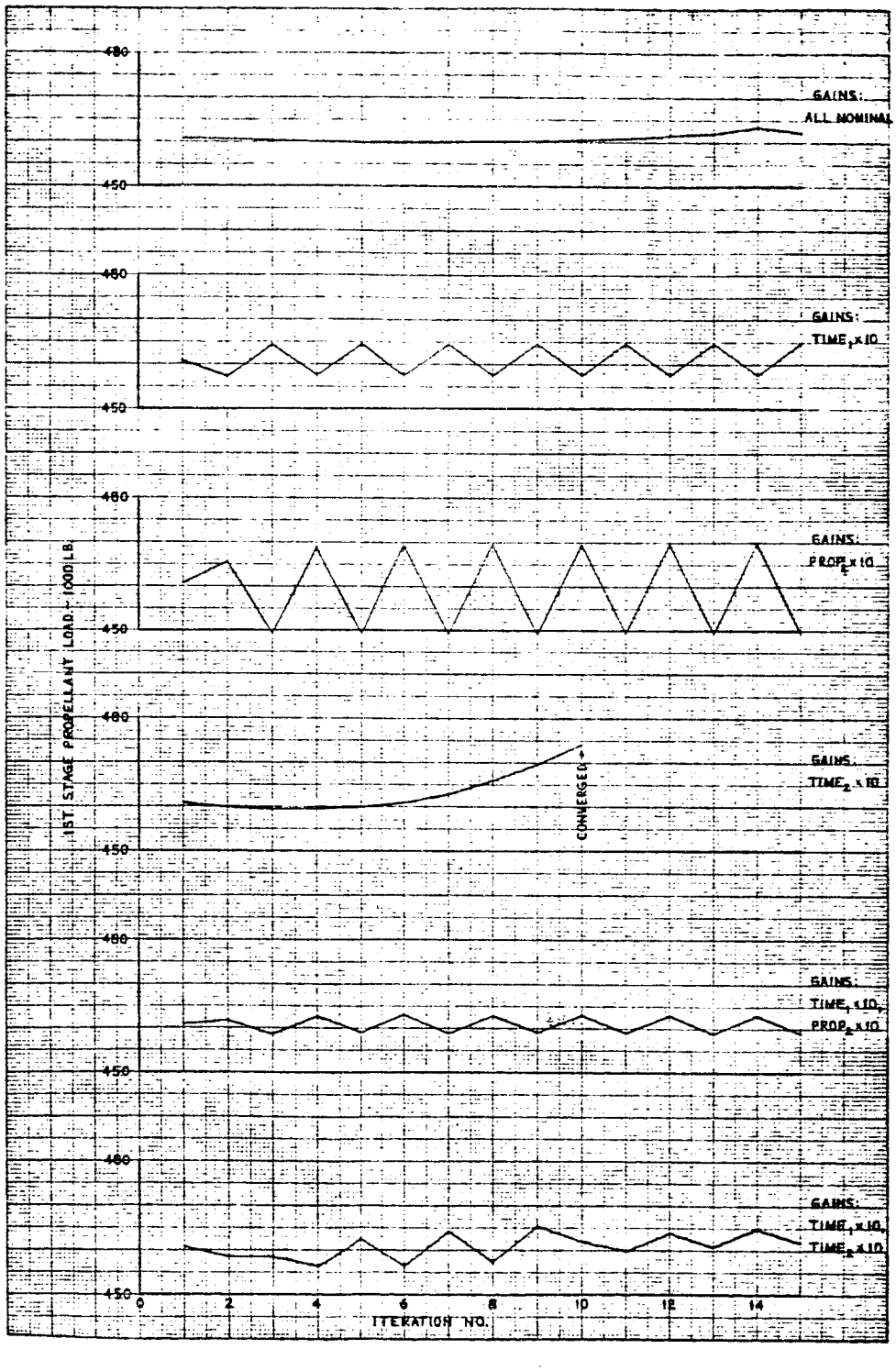

FIG 4-23

4-39

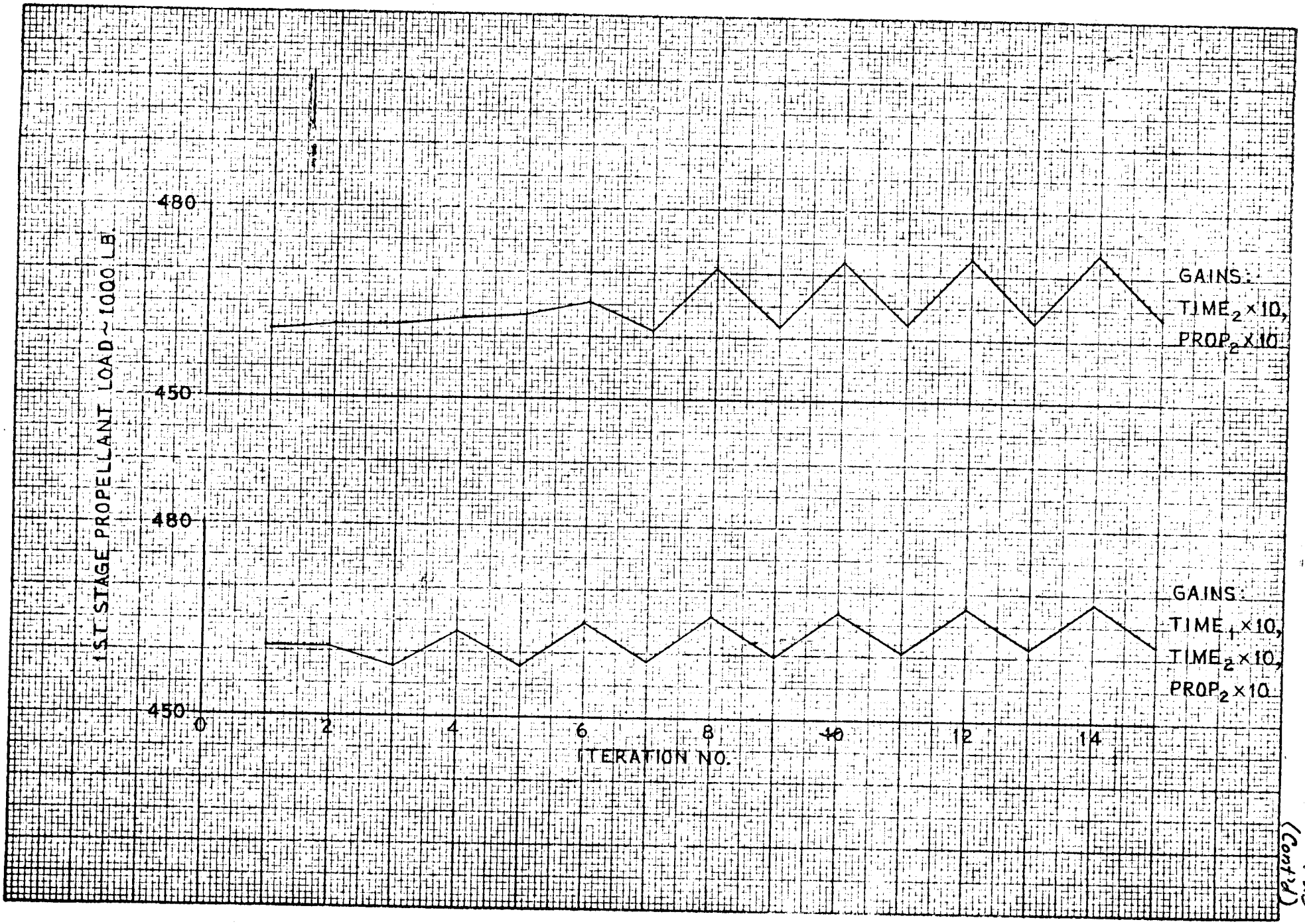

FIG 4-23 (Cont'd)

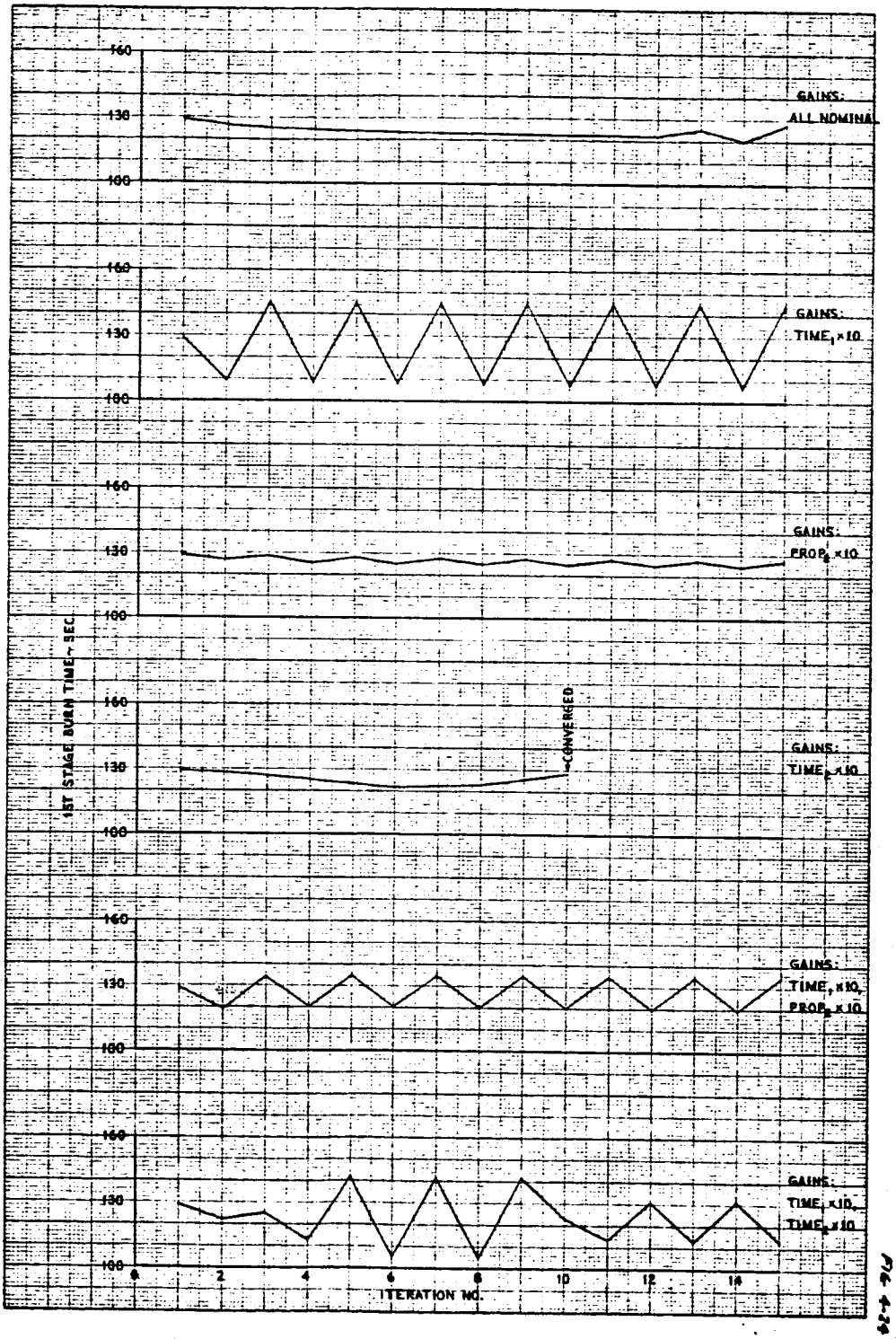
OPTIMIZATION GAINS STUDY
1ST STAGE BURN TIME - SEC.
160
130
100
GAINS: ALL NOMINAL
GAINS: TIME$_1$ ×10
GAINS: PROP$_2$ ×10
CONVERGED
GAINS: TIME$_1$ ×10
GAINS: TIME$_1$ ×10, PROP$_2$ ×10
GAINS: TIME$_1$ ×10, TIME$_2$ ×10
0
2
4
6
8
10
12
14
ITERATION NO.
4-41
FIG 4-24

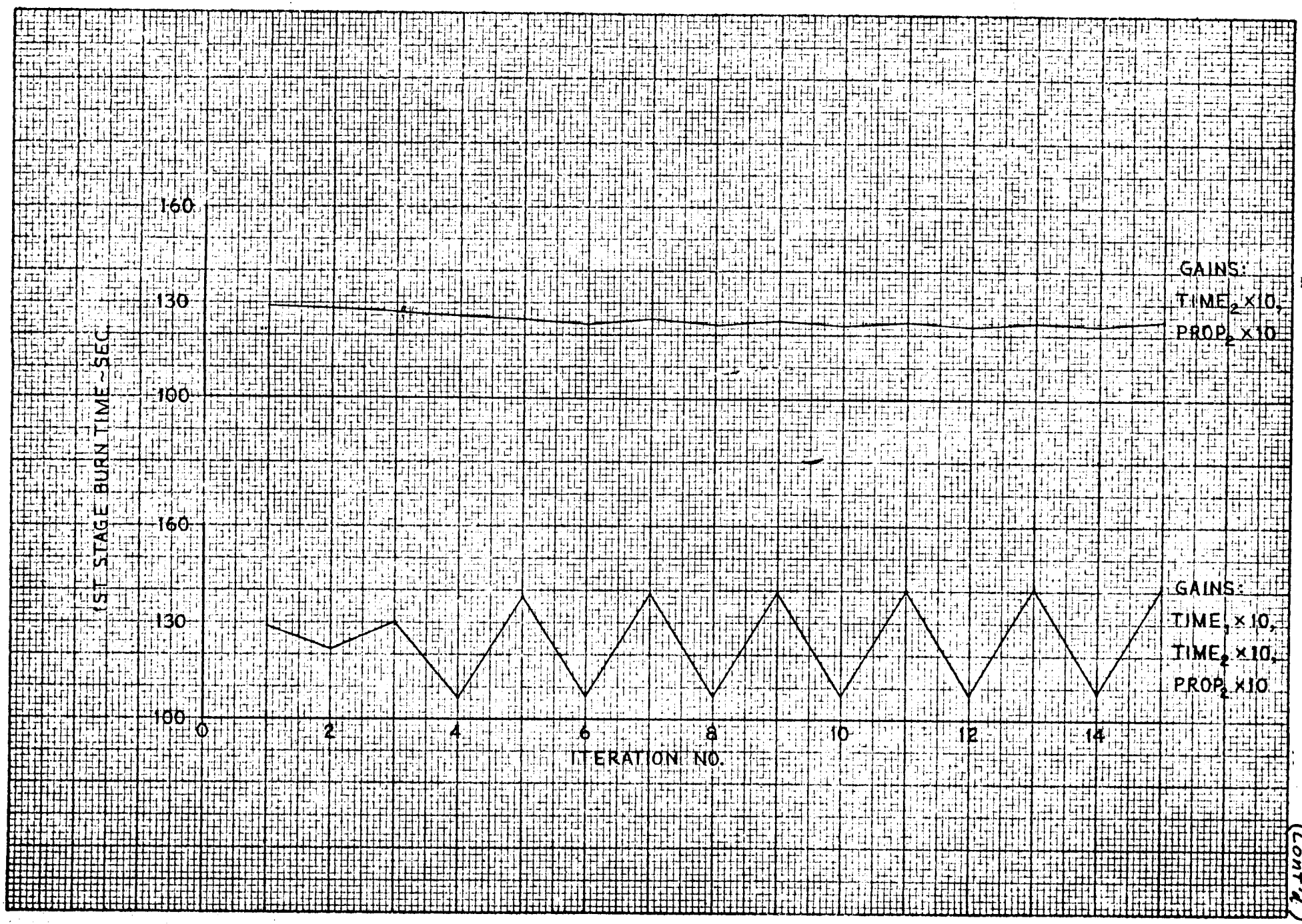

FIG 4-24 (Cont'd)

OPTIMIZATION GAINS STUDY

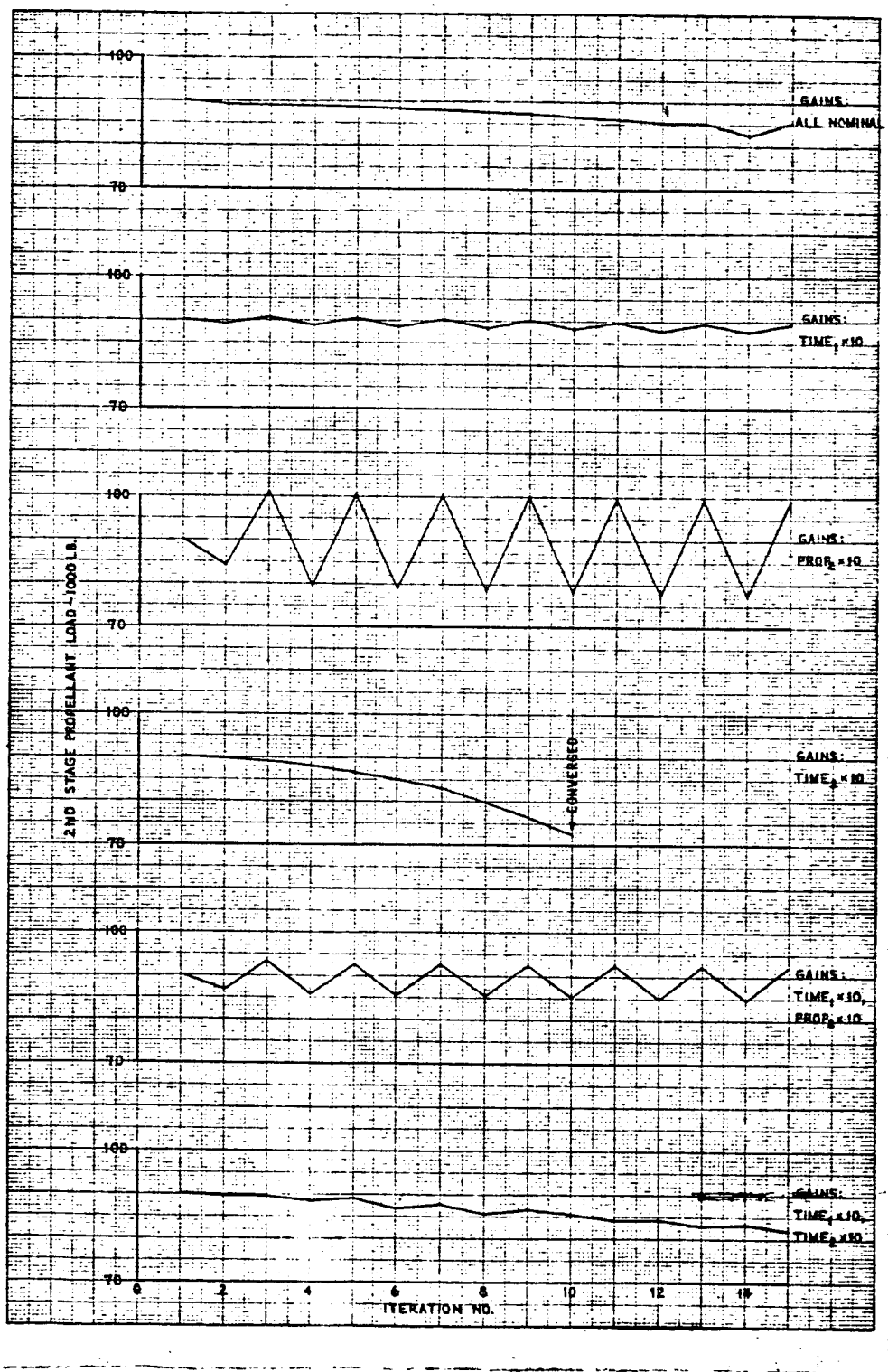

Fig 4-25

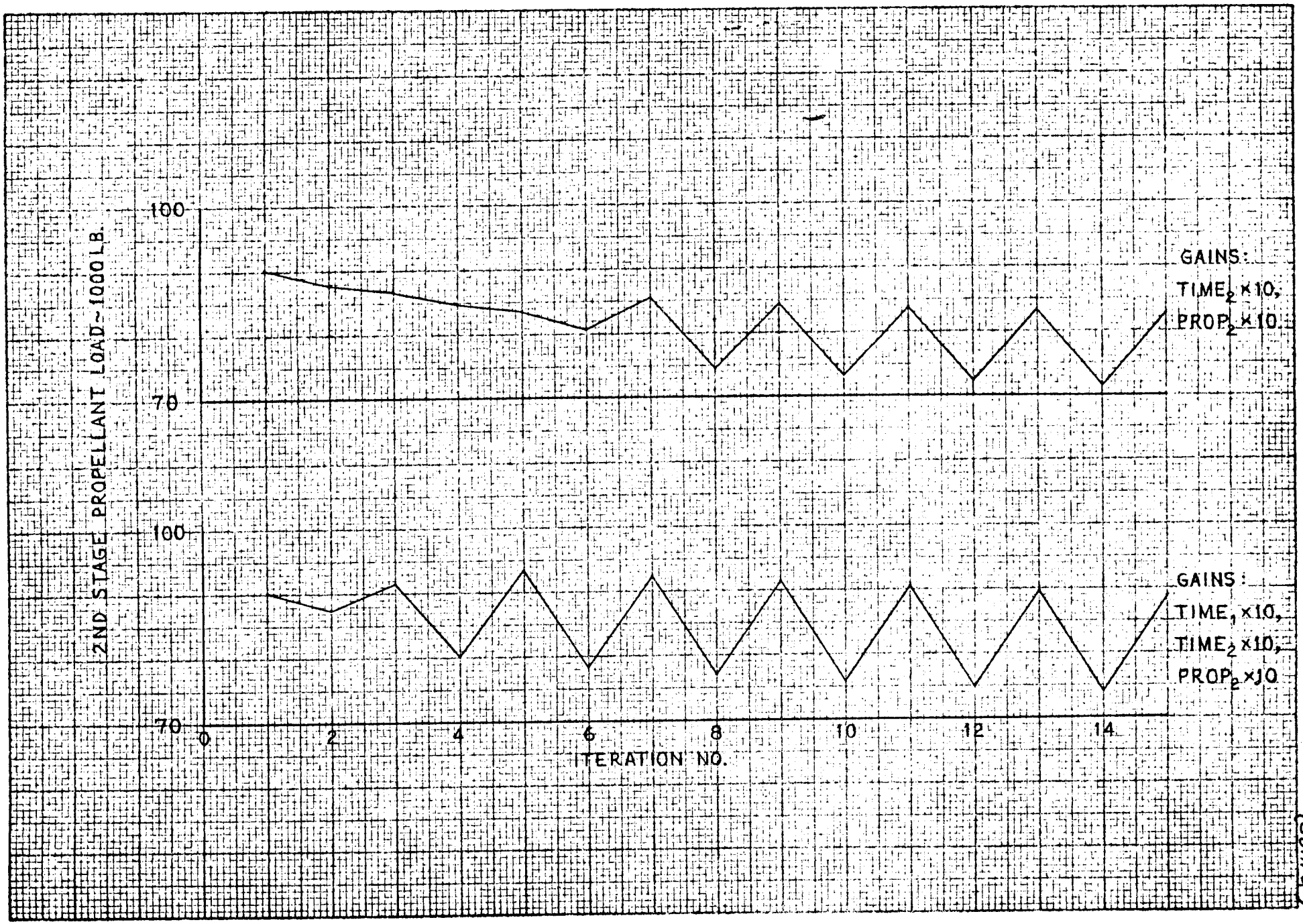

FIG 4-25 (Contd)

Figure 4-26

OPTIMIZATION GAINS STUDY

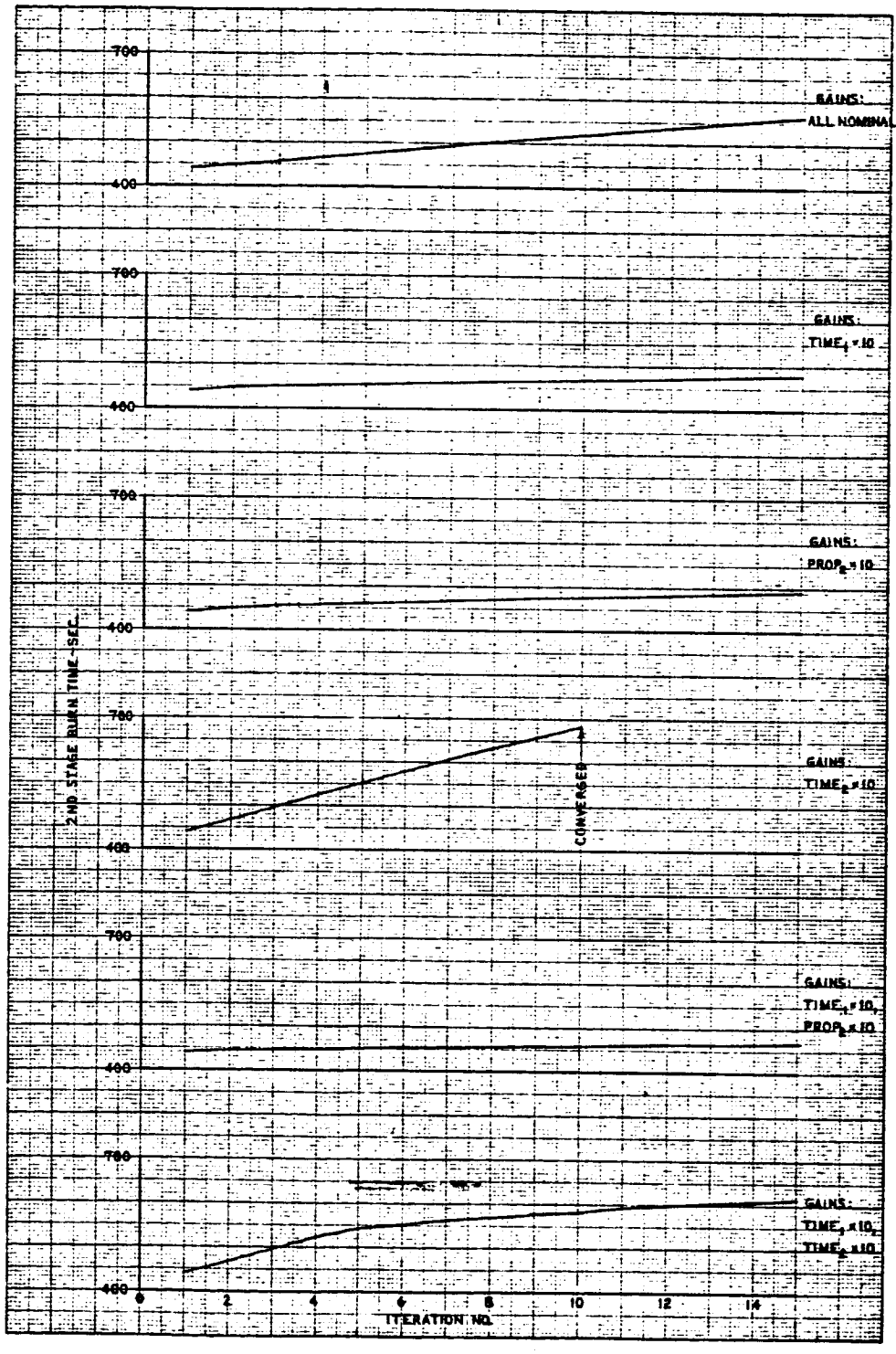

FIG 4-26

4-45

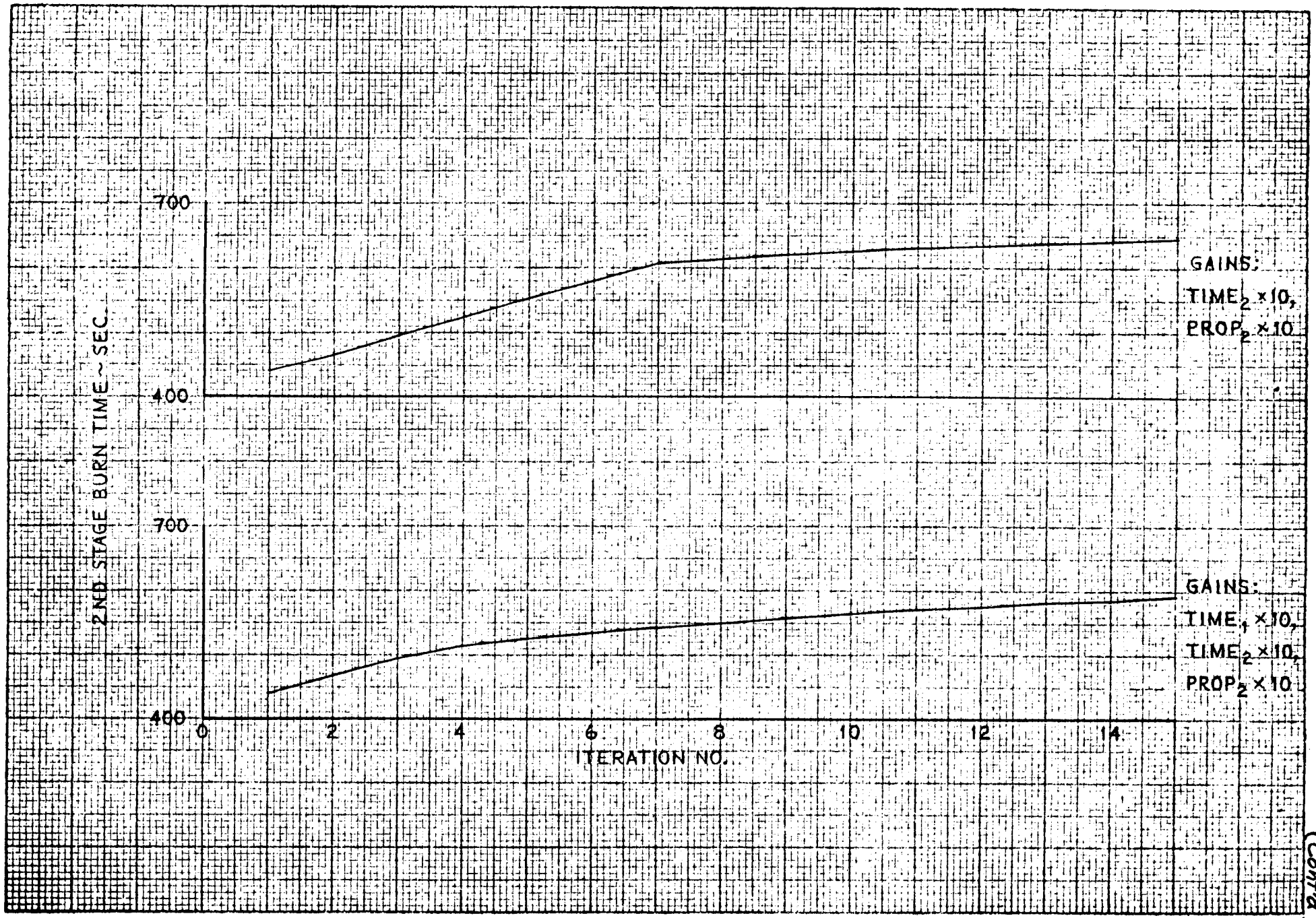

FIG 4-26 (Cont'd)

approach used is similar to that outlined in Section 4.1. Cases 3 and 6 from the original vehicle-mission matrix described in Section 3 were selected as examples and launch system optimization runs were completed using the parabolic fit procedure.

The new routine behaved fairly well on Case 3. Figure 4-27 shows the variation in system controls produced. Each iteration in this figure represents the values determined for the peak of each parabola and at least three complete iterations are required per step. The symbols shown at the right-hand side of this figure define the values computed by the original linear optimization routine. The program seemed to have some difficulty with the non-linearity of the constraint. The parabolic fit was not applied to the constraint error in this case although provision was included to accomplish a constraint adjustment if the constraint deviation at any hill peak exceeded the input tolerance. This situation did not develop since the constraint tolerance input was $\pm$400 lb in launch weight.

It is interesting to examine the direction changes occurring at each peak. Recall that the parabolic fit routine changed direction approximately 90 degrees at each peak on the payoff-only cases considered with the hill climber routine. When a constraint is introduced the behavior changes and the operation approaches the condition where each step is tangent to the constraint surface. The angle between adjacent fits will therefore approach zero and this is demonstrated by the hill climber solution shown in Figure 4-22. The actual angle between adjacent parabolic fits used by the full optimization program may be computed using the dot product of vectors defining the direction of motion for successive parabolas. The history of that angle for Case 3 is shown below.

PARABOLIC FIT RUN ~ CASE 3

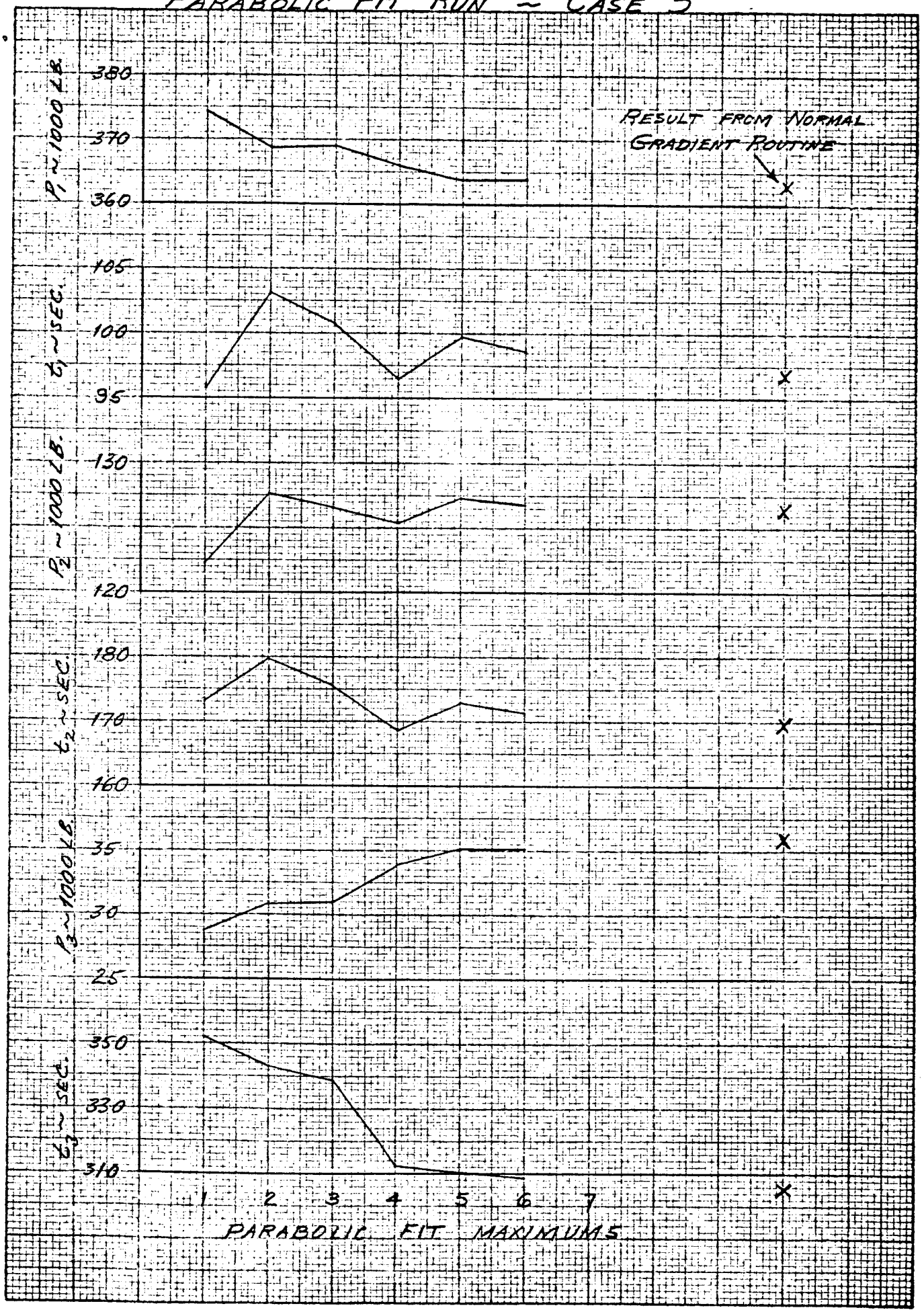

Fit No.	Direction Change ~ deg
1	± 147.7
2	± 161.7
3	± 20.5
4	± 144.9
5	± 170.8
6	± 5.2

From these figures and from the corresponding payload and launch weight histories shown in Figure 4-28, it can be seen that the routine is oscillating across the constraint surface as it approaches the maximum payload. Some form of constraint correction technique such as the bias procedure used with the hill climber routine might improve the operation on this case.

The operation on Case 6 was not very satisfactory. Figure 4-29 shows that oscillations in the system controls occurred during the run and that the second stage burn time was creeping. The values determined by the original gradient routine are shown at the right-hand side of this figure. The computation apparently has still some distance to go and this can be confirmed by comparing the final payload shown in Figure 4-30 with that shown for Case 6 in Table 3-14. The parabolic routine is about 450 lb low in payload.

From this brief experiment it appears that the parabolic fit routine as it is presently formulated is not very satisfactory for the full optimization problem. Oscillations were still encountered during the optimization test runs and optimization gain manipulations would be required to achieve satisfactory convergence. Apparently the system control interactions must be recognized by the formulation before second order routines will offer an advantage.

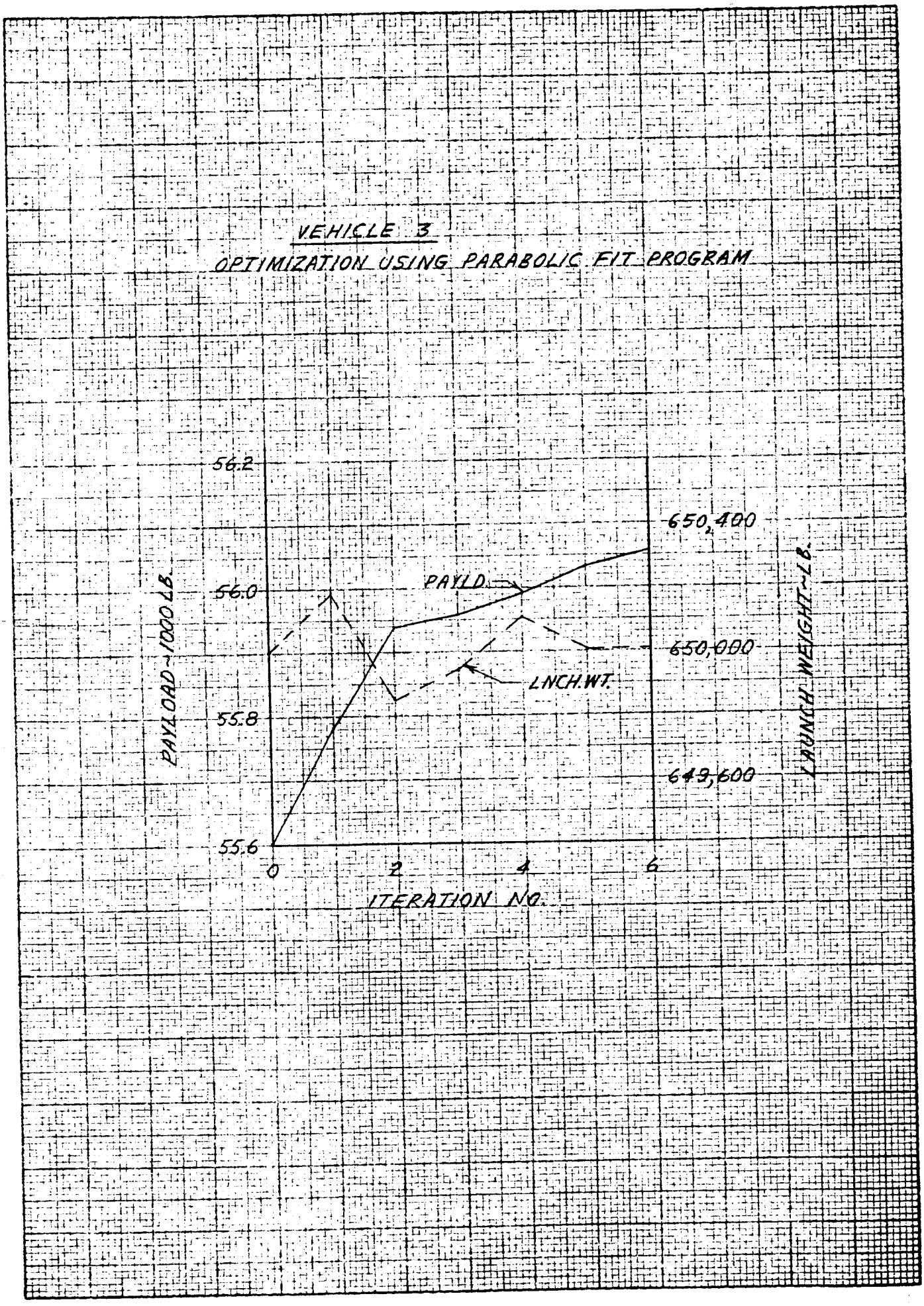
VEHICLE 3
OPTIMIZATION USING PARABOLIC FIT PROGRAM
56.2
56.0
55.8
55.6
PAYLOAD-1000 LB.
650,400
650,000
649,600
LAUNCH WEIGHT-LB.
PAYLD.
LNCH.WT.
0
2
4
6
ITERATION NO.

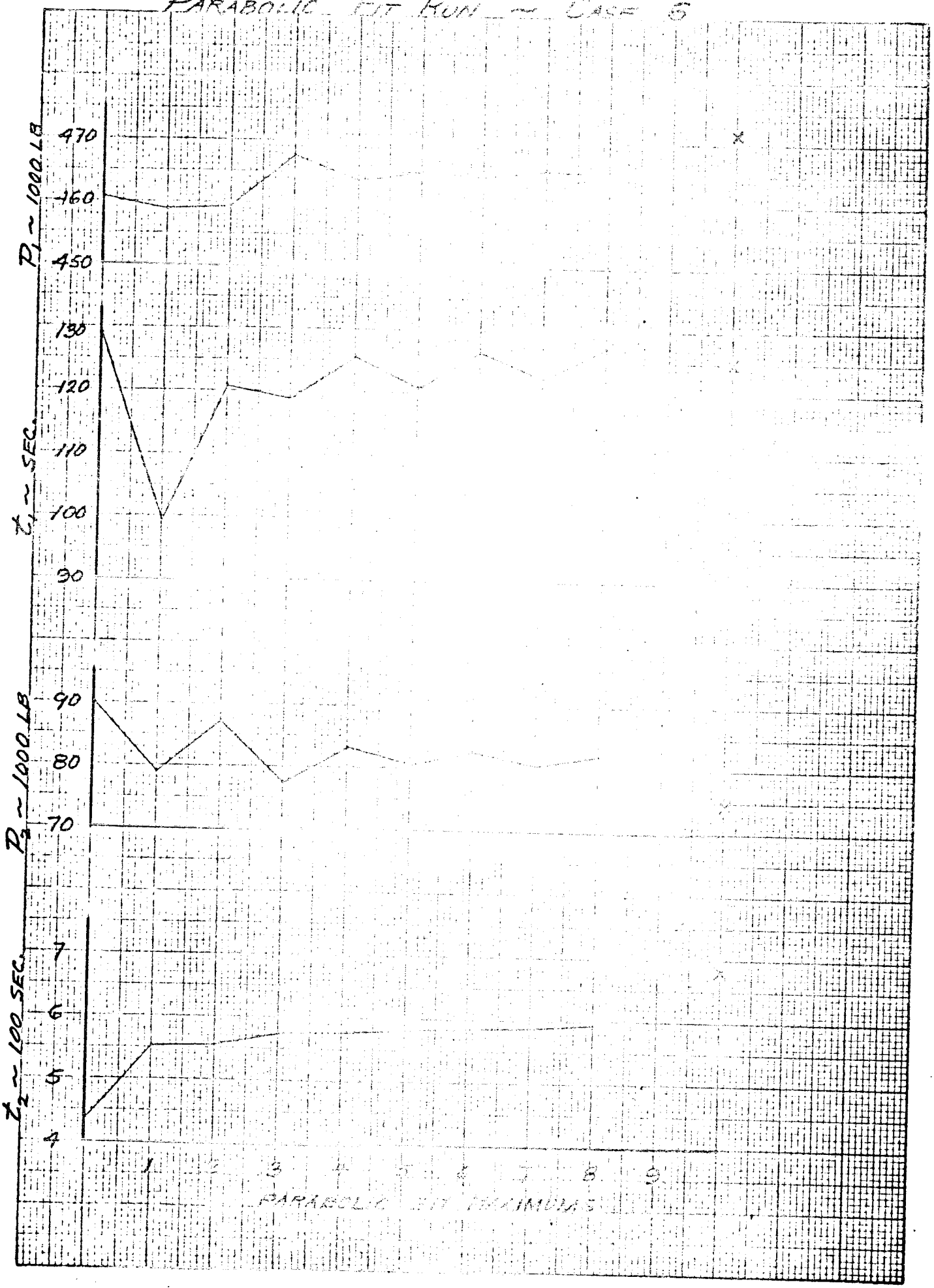
PARABOLIC FIT RUN ~ CASE 5
P_1 ~ 1000 LB
T_1 ~ SEC.
P_3 ~ 1000 LB
T_2 ~ 100 SEC.
470
460
450
130
120
110
100
90
80
70
7
6
5
4
1
2
3
4
5
6
7
8
9
PARABOLIC FIT MINIMUMS

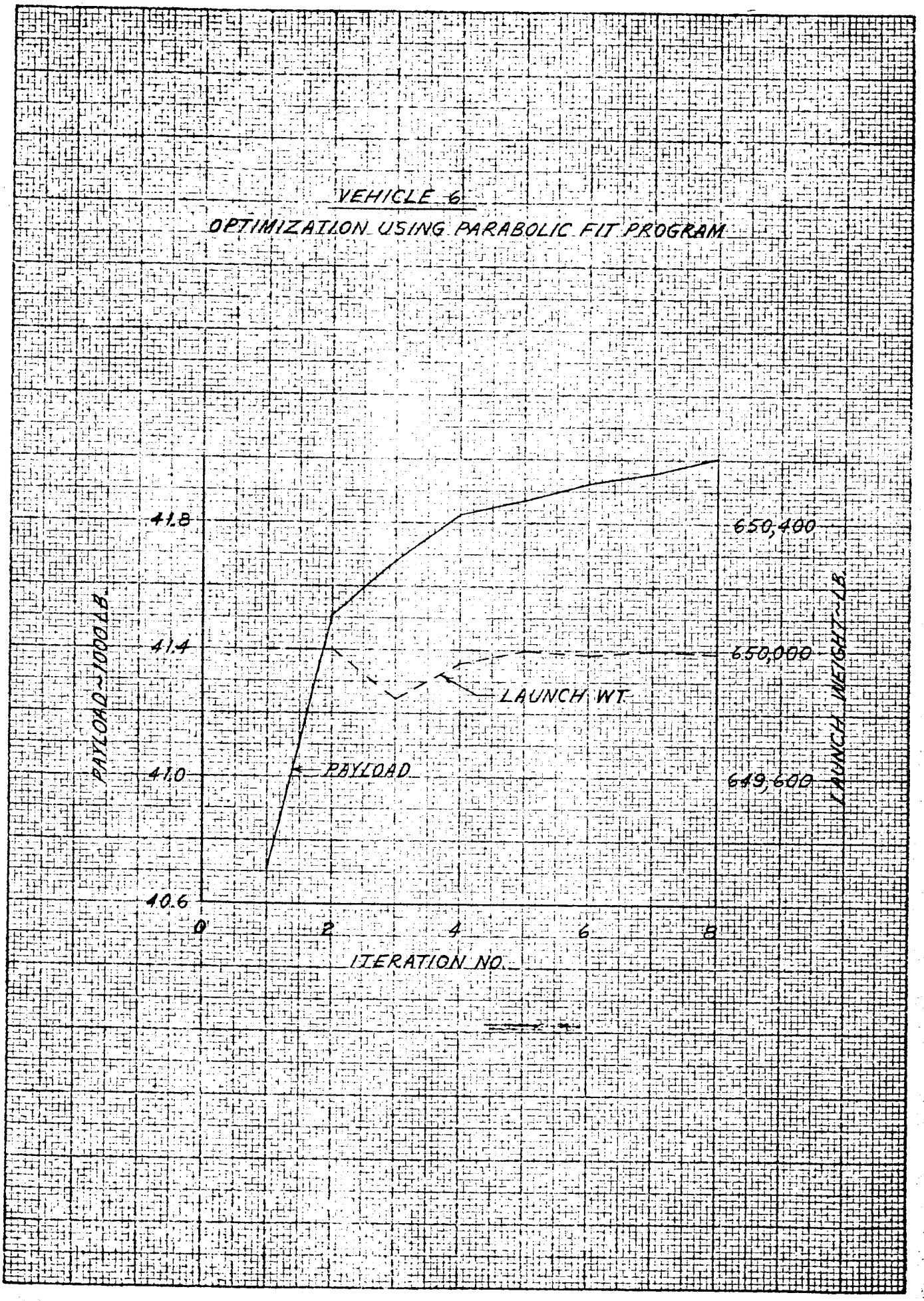
VEHICLE 6
OPTIMIZATION USING PARABOLIC FIT PROGRAM
41.8
41.4
41.0
40.6
PAYLOAD-1000 LB.
650,400
650,000
649,600
LAUNCH WEIGHT-LB.
LAUNCH WT.
PAYLOAD
0
2
4
6
8
ITERATION NO.

Section 5.0
CONCLUSIONS

It is difficult at this point to reach final conclusions. The gradient approach offers a major improvement for the future on launch system synthesis problems. While practical reliable routines have eluded us to date, they are certainly on the horizon. It is fair to say that we are closer to these routines today than we were to the modern trajectory routine four years ago. Within the next two years we can expect that a major portion of the design synthesis activity presently concerned with determining optimums can be redirected toward the more difficult problem of the basic concept, and high speed computer routines can assume much of the previous activity.

The work described covers a range of topics on the subject of applied gradient optimization techniques. The emphasis has been on the experience gained through the application of these techniques to representative design optimization problems for multi-stage liquid propellant launch systems. Their mission was to deliver payloads from the Earth's surface to low altitude circular Earth orbits. The material presented has covered the complete spectrum from the detailed problem formulation to a thorough review of the results obtained on specific problems. The approach used and the results obtained from a convergence study concerned with the problems introduced by major non-linearities have been described. Some of the techniques investigated were applied to the launch vehicle problem and their behavior was reviewed.

In conclusion, the following comments are offered on the subjects considered during this study.

Approach and Formulation

1. The dual-loop gradient optimization routine described in this report can produce acceptable solutions to the design synthesis problem for liquid propellant launch vehicles when the problem is formulated so that the influences of the trajectory environment on the design are removed.

2. The dual-loop technique represents an intermediate position between trial and error methods with trajectory optimization programs and a complete gradient system optimization routine that includes the trajectory controls.

3. It offers the advantage of a series of intermediate design outputs with the corresponding optimum launch trajectories.

4. Sufficient flexibility is retained to accept any form of design equation by simply replacing the simple relationships presently in use.

5. The routine may be attractive in situations where the non-linearities in the system cause problems, because second order steps can be computed by re-solving the high speed vehicle loop without re-entering the trajectory loop.

6. The routine is slower than a complete gradient solution since the number of trajectory optimizations required is equal to the product of the number of system iterations and trajectory iterations rather than to the number of system iterations. The trajectory computation requires a high percentage of the total computing time.

7. The same approach can be used when the environmental influences are known by adding environmental constraints on such parameters as dynamic pressure and heating, for example, and then treating those quantities as system controls during the optimization process.

Optimization Study Results

1. The major performance changes for continuous burn ascents were those associated with changes in mission altitude and specific impulse.

2. Fifty percent changes in the stage weight factors produced payload changes of less than 6%; however, when the system was re-optimized, radical changes in the optimized design of the final stage occurred.

3. Three-stage configurations did not perform significantly better than two-stage configurations.

4. The total burn time roughly doubled when the mission altitude was increased from 100 to 400 nm.

5. Direct ascent to 400 nm is impractical because the payload loss from the 100 nm case could be halved by introducing a coast during ascent. The total system burn time would also be about halved by this change in the mission mode.

6. The net payload loss associated with changes in the system design can be significantly reduced by re-optimizing the system; however, in general, rather large changes in the design parameters can be accepted with relatively small effects on payload. The major sensitivity is to the final stage.

Convergence Study

1. Significant convergence problems were encountered with the gradient routine. Solutions for sample problems encountered during the study usually required multiple computer passes with intermediate gain adjustments.

2. The current routine can be used to determine adequate solutions to the system optimization problem but does not exhibit the rapid reliable convergence of modern trajectory optimization programs.

3. Severe non-linearities in the form of strong inter-relationships between the system controls were the source of the convergence difficulty.

4. Simple automated gain selection routines and crude non-linear techniques radically improved performance on some problems. None of these

techniques produced consistently superior behavior on all problems.

5. The most effective solutions will recognize the control interactions in the formulation.